NACA RM L56H06

NACA

RESEARCH MEMORANDUM

LONGITUDINAL AND LATERAL STABILITY CHARACTERISTICS OF A LOW-ASPECT-RATIO UNSWEPT-WING AIRPLANE MODEL AT MACH NUMBERS OF 1.82 AND 2.01

By M. Leroy Spearman and Cornelius Driver

Langley Aeronautical Laboratory
Langley Field, Va.

NATIONAL ADVISORY COMMITTEE FOR AERONAUTICS

WASHINGTON

January 28, 1957
Declassified October 16, 1961

NATIONAL ADVISORY COMMITTEE FOR AERONAUTICS

RESEARCH MEMORANDUM

LONGITUDINAL AND LATERAL STABILITY CHARACTERISTICS OF A LOW-ASPECT-RATIO UNSWEPT-WING AIRPLANE MODEL AT MACH NUMBERS OF 1.82 AND 2.01[1]

By M. Leroy Spearman and Cornelius Driver

SUMMARY

An investigation has been made in the Langley 4- by 4-foot supersonic pressure tunnel at Mach numbers of 1.82 and 2.01 to determine the longitudinal and lateral stability characteristics of a fighter-type airplane model having a low-aspect-ratio unswept wing and a high horizontal tail. The complete model and various combinations of component parts were tested, as well as various configuration changes including a modified vertical tail, several ventral fins, and several external store arrangements.

The results for the basic clean configuration indicated a region of reduced longitudinal stability at low lifts at a Mach number of 2.01 that was apparently caused by fuselage flow fields or vertical-tail effects on the horizontal tail.

A considerable portion of the vertical-tail contribution to directional stability was required to overcome the large unstable yawing moment of the body. The directional stability decreased rapidly at high angles of attack, primarily because of increased instability of the wing-body combination. The directional stability was increased considerably through the use of an enlarged swept vertical tail and was increased to some extent through the use of ventral fins.

The addition of tip-mounted stores had little effect on the longitudinal stability but did result in an increase in the minimum-drag level and caused a reduction in directional stability at high angles of attack. The addition of a body-mounted store reduced the directional stability throughout the angle-of-attack range.

---

[1]The information presented herein was previously made available to the U. S. military air services.

INTRODUCTION

An investigation has been made in the Langley 4- by 4-foot supersonic pressure tunnel at Mach numbers of 1.82 and 2.01 to determine the static longitudinal and lateral stability characteristics of a model of a fighter-type airplane having low-aspect-ratio unswept wings. The complete model and various combinations of its components, including a modified vertical tail and several ventral-fin arrangements, were tested through an angle-of-attack and sideslip range. In addition, the effects of a pylon-mounted fuselage store, two wing-tip-mounted missile configurations, and wing-tip fuel tanks were determined.

The tests were made at Reynolds numbers of 1.38×10^6 and 1.02×10^6 (based on the wing mean geometric chord) for Mach numbers of 1.82 and 2.01, respectively.

COEFFICIENTS AND SYMBOLS

The lift, drag, and pitching-moment coefficients are referred to the stability-axis system (fig. 1(a)) and the lateral-force, rolling-moment, and yawing-moment coefficients are referred to the body-axis system (fig. 1(b)) with the reference center of moments at 25 percent of the wing mean geometric chord. The coefficients and symbols are defined as follows:

b	wing span
C_L	lift coefficient, L/qS
C_l	rolling-moment coefficient, M_X/qSb
C_m	pitching-moment coefficient, $M_Y/qS\bar{c}$
C_n	yawing-moment coefficient, M_Z/qSb
C_X	longitudinal-force coefficient, X/qS
C_Y	lateral-force coefficient, Y/qS
C_{l_β}	effective-dihedral parameter measured at $\beta \approx 0^\circ$
$C_{m_{C_L}}$	longitudinal-stability parameter

C_{n_β}	directional-stability parameter measured at $\beta \approx 0^\circ$
C_{Y_β}	side-force parameter measured at $\beta \approx 0^\circ$
c	wing chord
$\bar{c}$	wing mean geometric chord
i_t	horizontal-tail incidence angle, deg
L	lift
M	Mach number
M_X	moment about X-axis
M_Y	moment about Y-axis
M_Z	moment about Z-axis
q	free-stream dynamic pressure
S	total wing plan-form area, including body intercept
X	longitudinal force, equal and opposite to drag at zero sideslip
Y	lateral force
α	angle of attack of fuselage reference line, deg
β	angle of sideslip of fuselage reference line, deg

Configuration symbols:

B	body
H	horizontal tail
W	wing
V_1	basic tail with thickened trailing edges
V_2	basic tail

V_3	enlarged vertical tail
U_1, U_2, U_3, U_4	ventral fins (see fig. 2(c))
T_1	wing-tip tanks
A_1	body-mounted store
M_1	four tip-mounted Falcon missiles
M_9	two tip-mounted Sidewinder missiles

MODEL AND APPARATUS

Drawings of the model are shown in figure 2. Details of the various store configurations are shown in figure 3. Photographs of several of the configurations are shown in figure 4. The geometric characteristics of the model and various external store arrangements are given in table I.

The model was equipped with a wing having 18.1° sweep of the quarter-chord line, an aspect ratio of 2.45, a taper ratio of 0.377, and 3.36 percent modified circular-arc sections. The wing was set at zero incidence to the fuselage reference line and had 10° negative geometric dihedral. The test model was not equipped with internal ducting and the side inlets were faired into the contour of the body.

A modified vertical tail having a larger area and increased sweep (fig. 2(b)) was tested to determine its effectiveness in improving the directional characteristics at angles of attack. Several ventral-fin configurations were also investigated. The ventral fins were thin aluminum plates with beveled edges and were fitted to the bottom of the body. (See fig. 2(c).)

The model was equipped with a horizontal tail fixed at zero incidence only. The external store arrangements tested were as follows: (a) a pylon mounted fuselage store (fig. 3(a)), (b) two fuel tanks, one on each wing tip (fig. 3(b)), two Sidewinder missiles, one on each wing tip (fig. 3(c)), and four Falcon missiles, two on each wing tip (fig. 3(d)).

Forces and moments were measured through the use of a six-component internal strain-gage balance and indicating system.

CORRECTIONS AND ACCURACY

The angles of attack and sideslip were corrected for the deflection of the balance and sting under load. The drag data were adjusted to a base pressure equal to free-stream static pressure. The maximum probable errors in the data are as follows:

	M = 1.82	M = 2.01
C_L	±0.0065	±0.0049
C_X	±0.0050	±0.0037
C_m	±0.0014	±0.0011
C_l	±0.00022	±0.00016
C_n	±0.00021	±0.00015
C_Y	±0.0016	±0.0012
α, deg	±0.1	±0.1
β, deg	±0.1	±0.1

It should be pointed out that the maximum probable error in the drag coefficient is large because of random zero shifts caused by temperature variations that affected the drag strain-gage link only. For most of the tests, the C_X errors are believed to be within ±0.0010.

TEST CONDITIONS AND PROCEDURE

The conditions for the tests were as follows:

	M = 1.82	M = 2.01
Reynolds number based on mean geometric chord	1.02×10^6	1.38×10^6
Stagnation dewpoint, °F	< -20	< -20
Stagnation pressure, lb/sq in. abs	10	15
Stagnation temperature, °F	100	110
Mach number variation	±0.01	±0.01
Flow angle in the horizontal or vertical plane, deg	±0.1	±0.1

Tests were made through an angle-of-attack and sideslip range up to about 20°. A figure index containing the test configurations and angle ranges is presented in table II.

RESULTS AND DISCUSSION

As seen in table II, the basic longitudinal data are presented in figures 5 to 7; the basic lateral data, in figures 8 to 16; the external store data, in figures 17 to 19; and the summary data, in figures 20 to 24.

Longitudinal Characteristics for Clean Configuration

The aerodynamic characteristics in pitch for various combinations of model components are presented in figure 5 for $M = 1.82$ and in figure 6 for $M = 2.01$. The addition of the horizontal tail to the body—wing—vertical-tail configuration provides rather large increases in lift with increasing angle of attack and, of course, increases the pitching-moment slope C_{m_α} for both Mach numbers. The addition of the vertical tail (fig. 5) had little effect other than to cause an increase in drag and a slight positive increment of pitching moment.

The longitudinal stability characteristics for the complete model for Mach numbers of 1.82 and 2.01 are compared in figure 7. The pitching-moment variation for the complete configuration at $M = 2.01$ is considerably less linear than that for $M = 1.82$, the primary difference being a reduction in $C_{m_{C_L}}$ in the low lift range at $M = 2.01$. The same trend was observed from tests of a similar model (ref. 1). Although the moment variation with the horizontal tail removed (BWV_2, fig. 6) is reasonably linear at low lifts, the moment variation with the wing removed but with the horizontal tail installed (BV_2H) is very nonlinear and indicates the same reduction in $C_{m_{C_L}}$ at low angles as does the complete model. Hence, it appears that the nonlinear pitching-moment variation at low lifts may result from fuselage flow fields or vertical-tail effects on the horizontal tail.

An unstable break in pitching moment for the complete model (figs. 5 and 6) that occurs at the higher angles of attack ($\alpha \approx 18°$) is probably influenced by the large unstable moment of the body—vertical-tail configuration. An abrupt unstable break exists for the wing-off case (BV_2H, fig. 6) as a result of the decrease in lift indicated for the horizontal tail. The break is less abrupt for the body-wing configuration (BWV_2) because of the stabilizing effect of the wing carryover lift.

Some interference effect of the wing on the horizontal tail is indicated (fig. 6) in that the lift and moment increments provided by the tail are decreased in the presence of the wing at the lower angles of attack. Above about $\alpha = 16^{\circ}$ the reverse is true, the tail lift and moment increments being somewhat greater in the presence of the wing.

Lateral and Directional Characteristics for Clean Configuration

Effects of component parts.- The aerodynamic characteristics in sideslip at $M = 1.82$ were obtained for several combinations of model components at angles of attack of 2.4°, 8°, and 12.7° (fig. 8). In addition, results were obtained through the angle-of-attack range for a sideslip angle of about 5.3° (fig. 9) and these results are summarized in figure 20.

The addition of the vertical tail, of course, provides a stabilizing increment of yawing moment (fig. 20) but a considerable portion of the tail contribution (56 percent at $\alpha = 0^{\circ}$) is required to overcome the large unstable moment caused by the long body. The addition of the horizontal tail near the tip of the vertical tail provides an increase in the lateral-force, yawing-moment, and rolling-moment derivatives that becomes more pronounced with increasing angle of attack (fig. 20). These increases result partly from the end-plate effect of the horizontal tail on the vertical tail and partly from the transmittal of positive pressures from the lower surface of the horizontal tail to the windward side of the vertical tail. Apparently it is this transmittal of pressures that provides the more pronounced effect of the horizontal tail with increasing angle of attack since, under such conditions, the positive pressures on the underside of the horizontal tail would increase. As a result of this same interference effect, however, much of the increase in directional stability provided by the horizontal tail at high angles of attack may be lost when the tail is deflected downward for trimming in pitch. This effect is shown in reference 2 for a similar model.

The directional stability C_{n_β} for the complete configuration (fig. 20) decreases rapidly at the higher angles of attack, primarily because of the increased instability of the wing-body combination and not because of any loss in tail contribution. This characteristic may be influenced by sidewash induced at the wing-body juncture. Because of the negative dihedral angle, this sidewash, which should be similar to that for a low-wing circular-body configuration, would be adverse below and favorable above the center of the wing-body disturbance field (see ref. 3). This would result in an increase in the instability of the wing-body configuration with increasing angle of attack as the afterbody moves down through a region of adverse sidewash. The vertical tail, on the other hand, would indicate little change in effectiveness with increasing angle of attack as it moves down through a region of favorable sidewash.

The aerodynamic characteristics in sideslip at $M = 2.01$ for various combinations of model components are presented in figure 10 for several angles of attack. These results are summarized in figure 21.

The results, in general, are similar to those for $M = 1.82$, insofar as the horizontal-tail effects and angle-of-attack effects are concerned. The primary difference for the $M = 2.01$ case, of course, is the more critical level of directional stability that results from the decreased vertical-tail contribution (tail lift-curve slope) at the higher Mach number. This decrease in stability is in agreement with that estimated on the basis of the variation of the lift-curve slope with Mach number for the vertical tail as obtained through the use of reference 4.

Some sideslip tests were made at $M = 2.01$ for angles of attack of about 8° and about 18° for the model with the wing removed and with the horizontal and vertical tails on (fig. 10). A summary of these results (fig. 21) indicates little effect of the wing on C_{Y_β} and C_{n_β} at $\alpha \approx 8^\circ$, but at $\alpha \approx 18^\circ$ with the wing removed there is a considerable decrease in both the side force $\left(C_{Y_\beta}\right.$ is less negative$\left.\right)$ and directional stability $\left(C_{n_\beta}\right.$ is more negative$\left.\right)$. This effect adds credence to the sidewash concept previously mentioned in that the addition of the wing at the high angles of attack apparently provides a favorable sidewash at the vertical tail that results in a substantial increase in the side force and directional stability.

The more negative value of C_{l_β} at $\alpha \approx 8^\circ$ with the wing removed is an indication of the negative dihedral effect provided by the wing. The increment of C_{l_β} provided by the wing for the complete model at $\alpha \approx 8^\circ$ is about the same as that indicated by the addition of the wing to the body - assuming that the body alone causes essentially no rolling moment. The effect of the wing on C_{l_β} is less pronounced at the higher angle of attack and the rolling moment provided by the tail appears to predominate.

Effects of sideslip on longitudinal characteristics.- The variations of C_L, C_X, and C_m with β for various combinations of components at various angles of attack are presented in figures 11 and 12 for Mach numbers of 1.82 and 2.01, respectively. The results show that for the complete model, particularly at low angles of attack, a fairly rapid increase in negative pitching moment occurs with increasing sideslip. This characteristic is apparently a horizontal-tail effect since, in general, the configurations without the horizontal tail indicate an opposite trend. This influence of the horizontal tail is also seen at $\alpha \approx 8^\circ$ when the wing is removed (fig. 12(b)). At $\alpha \approx 18.2^\circ$ (fig. 12(d)), however, the influence of the horizontal tail indicated by the negative variation of

C_m with β for the wing-off results is apparently offset by the positive variation of C_m with β provided by the body and wing. Hence, for the complete model a nearly constant variation of C_m with β results.

Effects of vertical-tail section.- The effects of vertical-tail section on the lateral stability of the complete configuration at $M = 2.01$ is presented in figure 13 for angles of attack of 8° and 18.2°. The modified tail section (V_1) had parallel sides aft of the maximum thickness point and resulted in a blunt-trailing-edge version of the basic tail (V_2). Since the basic tail was relatively thin, this modification had no significant effect, although there was a slight tendency toward increased lateral force, rolling moment, and yawing moment for the flat-sided tail.

Effects of vertical-tail plan form.- The effects of vertical-tail plan form on the sideslip characteristics at $M = 2.01$ were obtained at several angles of attack (fig. 14) for the model without the horizontal tail, and the results are summarized in figure 22. The enlarged vertical tail (V_3) provided a substantial increase in the lateral force, yawing moment and rolling moment over that for the basic vertical tail (V_2). An estimate of the increase in lateral force to be expected from the enlarged tail was made by using lift-curve slopes for the isolated tails obtained by the method of reference 4. This estimate was essentially in agreement with the incremental increase obtained experimentally at $\alpha \approx 2.4^\circ$. Some increase with increasing angle of attack is indicated in the increment of C_{Y_β}, C_{n_β}, and C_{l_β} provided by the enlarged tail (fig. 22). This increase apparently is a result of favorable sidewash in the region above the center of the wing-body wake.

The addition of the enlarged swept vertical tail is sufficient to increase the angle of attack at which $C_{n_\beta} = 0$ from about 10° to about 17.5° (fig. 22). The interference effects of the horizontal tail, of course, are not included in these results so that the incremental contributions to the lateral stability provided by the enlarged tail may be altered when the presence of a horizontal tail is considered.

Effects of ventral fins.- The effects of various ventral fins on the sideslip characteristics at $M = 2.01$ of the complete model with the basic vertical tail (V_2) were determined. These effects are shown through the angle-of-attack range at $\beta = 5.3^\circ$ in figure 15 and the results are summarized in figure 23. The effects of two of the ventral fins are shown through the angle of sideslip range at $\alpha \approx 8^\circ$ in figure 16.

Each of the ventral fins, when added to the basic model, provided some increase in the lateral force and yawing moments and a slight reduction in the rolling moments (fig. 23). With the exception of U_1, the ventral fins provided slightly larger increments of C_{Y_β} per unit area than did the vertical tails. However, all of the ventral fins provided significantly smaller increments in C_{n_β} per unit area than did the vertical tails, probably because of the shorter moment arms available with the ventral fins. The increments provided in C_{Y_β} and C_{n_β} by the ventral fins (fig. 23) were essentially constant with angle of attack and resulted in only a small increase in the angle of attack for which $C_{n_\beta} = 0$.

It is interesting to note that the increments in C_{Y_β} and C_{n_β} provided by ventral fins U_1 and U_2 are essentially the same although U_2 has less area and a shorter moment arm than U_1 (fig. 23). This again may be an indication of the sidewash behind the wing-body juncture, which below the center of the wing-body wake appears to be adverse. As a result, the added area of ventral fin U_1 may be offset by an adverse sidewash. This result is particularly interesting inasmuch as the smaller ventral fin (U_2) would be more desirable in any case since it imposes no ground-clearance restrictions. The lower directional stability provided by the larger ventral fin U_1 relative to U_2 is confined to the lower angles of sideslip (see fig. 16). Beyond a sideslip angle of about 6°, where the influence of sidewash from the wing-body juncture would be diminished, the larger ventral fin does provide greater side force and yawing moments than the smaller ventral fin (U_2).

Aerodynamic Characteristics for External Store Configurations

Longitudinal characteristics.- Various arrangements of external stores were investigated at $M = 2.01$ only. The aerodynamic characteristics in pitch with and without the horizontal tail and with the vertical tail V_2 are presented for the configurations with tip tanks and with two tip-mounted Sidewinder missiles in figures 17 and 18, respectively.

The addition of the tip tanks (fig. 17) caused an increase in minimum drag of about 0.0068. This drag increment decreases with increasing lift, however, because of the decreased induced drag resulting from the end-plate effect of the tip-mounted store installation. An increase in lift-curve slope resulting from this end-plate effect is evident both with and without the horizontal tail (fig. 17).

A considerable increase occurs in the static longitudinal stability when the tanks are added to the model with the horizontal tail off. This

increase in stability may be due in part to moments of the store itself and in part to increased wing lift provided by the end-plate effect of the store installation which results in an increase in the stabilizing wing-lift carryover to the afterbody. However, for the complete model, the relatively little effect of the tanks on the longitudinal stability is an indication of some compensating loss in tail contribution resulting from dynamic-pressure changes or downwash induced by the tank.

The addition of the two tip-mounted Sidewinder missiles (fig. 18) provided an increase in minimum drag of about 0.0031. The changes in drag-due-to-lift, lift-curve slope, and longitudinal stability, although smaller in magnitude, are essentially the same as those just discussed for the tank installation.

Lateral characteristics.- The effects of various store installations on the lateral characteristics were obtained in tests made through the angle-of-attack range at a sideslip angle of about 5.3° (fig. 19). These results are summarized in figure 24 for store arrangements that include two tip-mounted Sidewinders, four tip-mounted Falcons, and a fuselage-mounted store.

Each of the installations caused increases in the side-force parameter C_{Y_β} (fig. 24) that varied with store installation size from a small increase with the two Sidewinders to relatively large increases with the four Falcons and the body store. The tip-mounted missiles caused no change in directional stability of low angles of attack but did cause reductions in C_{n_β} with increasing angle of attack that amounted to a decrease in the angle of attack for $C_{n_\beta} = 0$ from about 12.5° to 9.7° for the four Falcons. The fuselage-mounted store, however, which was located slightly forward of the moment reference point, resulted in a significant decrease in C_{n_β} throughout the angle-of-attack range and reduced the angle for $C_{n_\beta} = 0$ to about 5.6°.

The addition of the tip-mounted stores generally resulted in a reduction in the effective dihedral (C_{l_β} was less negative) since the effect of the tip stores is to increase the lift-curve slope of the wing and thereby increase the positive C_{l_β} provided by the wing.

The addition of the fuselage store, however, results in an increase in the dihedral effect (C_{l_β} is more negative) in spite of the increase in lateral force below the moment reference axis and indicates the possibility that the fuselage-store flow field may cause a loss in lift for the trailing wing panel in sideslip.

CONCLUSIONS

An investigation has been made in the Langley 4- by 4-foot supersonic pressure tunnel at Mach numbers of 1.82 and 2.01 to determine the longitudinal and lateral stability characteristics of various arrangements of a fighter-type airplane model having a low-aspect-ratio, tapered, unswept wing and a high horizontal tail. The results of the investigation indicated the following conclusions:

1. A nonlinear variation of pitching moment with angle of attack that occurred at low lifts at a Mach number of 2.01 was apparently caused by fuselage-flow-field or vertical-tail effects on the horizontal tail.

2. A considerable portion of the vertical-tail contribution to directional stability was required to overcome the large unstable yawing moment caused by the long fuselage. The addition of the horizontal tail (with an incidence angle of 0°) near the tip of the vertical tail provided an increase in the directional stability as well as in the lateral force and rolling moments. This influence of the horizontal tail would be expected to diminish, however, when the tail is deflected for trimming in pitch.

3. The directional stability decreased rapidly at the higher angles of attack, primarily because of increased instability of the wing-body combination and not because of any loss in tail contribution - a characteristic apparently influenced by wing-body induced sidewash.

4. An enlarged swept vertical tail for the configuration having no horizontal tail increased the directional stability at low angles of attack by an amount anticipated from estimates and was sufficient to increase the angle of attack at which the directional stability became zero from about 10° for the basic tail to about 17.5°.

5. Each of various ventral fins, when added to the basic model, provided an increase in the directional stability that was essentially constant with angle of attack but resulted in only a small increase in the angle of attack for which the directional stability became zero.

6. The addition of various tip-mounted stores had little effect on the longitudinal characteristics other than to increase the minimum drag level but did result in a decrease in directional stability at the higher

angles of attack. The addition of a body-mounted store resulted in a decrease in directional stability throughout the angle-of-attack range.

Langley Aeronautical Laboratory,
National Advisory Committee for Aeronautics,
Langley Field, Va., July 20, 1956.

REFERENCES

1. Smith, Willard G.: Wind-Tunnel Investigation at Subsonic and Supersonic Speeds of a Fighter Model Employing a Low-Aspect-Ratio Unswept Wing and a Horizontal Tail Mounted Well Above the Wing Plane - Longitudinal Stability and Control. NACA RM A54D05, 1954.

2. Robinson, Ross B.: Longitudinal Characteristics of an Unswept-Wing Fighter-Type Model With External Stores at a Mach Number of 1.82 and Some Effects of Horizontal-Tail and Yaw-Damper Deflection on the Sideslip Derivatives. NACA RM L55L26, 1956.

3. Spearman, M. Leroy, and Henderson, Arthur, Jr.: Some Effects of Aircraft Configuration on Static Longitudinal and Directional Stability Characteristics at Supersonic Mach Numbers Below 3. NACA RM L55L15a, 1956.

4. Harmon, Sidney M., and Jeffreys, Isabella: Theoretical Lift and Damping in Roll of Thin Wings With Arbitrary Sweep and Taper at Supersonic Speeds - Supersonic Leading and Trailing Edges. NACA TN 2114, 1950.

TABLE I.- GEOMETRIC CHARACTERISTICS OF MODEL

Wing:		
Area, sq ft		0.3137
Span, in.		10.480
Mean geometric chord, in.		4.584
Aspect ratio		2.45
Taper ratio		0.377
Sweep of leading edge, deg		27.1
Sweep of quarter-chord line, deg		18.1
Sweep of 70.4-percent-chord line, deg		0
Incidence, deg		0
Dihedral, deg		-10
Airfoil section		Modified 3.36-percent circular arc
Horizontal tail:		
Area, sq ft		0.0771
Span, in.		5.72
Mean geometric chord, in.		2.116
Aspect ratio		2.95
Taper ratio		0.311
Sweep of leading edge, deg		19.5
Sweep of quarter-chord line, deg		10.1
Sweep of midchord line, deg		0
Incidence (on test model), deg		0
Dihedral, deg		0
Airfoil section, root		4.93-percent circular arc
Airfoil section, tip		2.61-percent circular arc
Vertical tails:	V_2	V_3
Area to theoretical root, sq in.	8.30	11.7
Span from theoretical root, in.	2.66	3.61
Mean geometric chord, in.	3.44	3.48
Aspect ratio (panel)	0.85	1.11
Taper ratio	0.378	0.371
Sweep of leading edge, deg	52.3	44.0
Sweep of quarter-chord line, deg	34.9	47.4
Airfoil section	Modified 4.25-percent circular arc	
Tip chord, in.	1.70	1.76
Theoretical root chord (1.52 in. above fuselage reference line), in.	4.50	4.74
Ventral fins:		
Area of U_1, sq in.		5.8
Area of U_2, sq in.		3.5
Area of U_3, sq in.		2.2
Area of U_4, sq in.		1.6
Section		Modified flat plate, 0.050 in. thickness

TABLE I.- GEOMETRIC CHARACTERISTICS OF MODEL - Concluded

Fuselage:	
Length, in.	24.60
Maximum frontal area, sq ft	0.0368
Base area, sq ft	0.0136
Length-diameter ratio	9.25
Body store (A_1):	
Length, in.	6.20
Diameter (maximum), in.	0.88
Length-diameter ratio	7.05
Frontal area, sq ft	0.00463
Wetted area, sq ft	0.1214
Tip tanks:	
Length, in.	8.46
Diameter (maximum), in.	0.80
Length-diameter ratio	10.58
Frontal area, sq ft	0.0035
Sidewinder missile:	
Length, in.	4.40
Diameter (maximum), in.	0.20
Length-diameter ratio	22
Frontal area, sq ft	0.0004
Falcon missile:	
Length, in.	3.46
Diameter (maximum), in.	0.256
Length-diameter ratio	13.52
Frontal area, sq ft	0.0006

TABLE II.- INDEX OF FIGURES

Figure	M	Wing	Horizontal tail	Vertical tail	Ventral fin	Stores	α, deg	β, deg	Data
5	1.82	On	On	V_2	Off	Off	-4 to 21	0	C_m, C_L, C_X
	1.82	On	Off	V_2	Off	Off	-4 to 21	0	C_m, C_L, C_X
	1.82	On	Off	Off	Off	Off	-4 to 21	0	C_m, C_L, C_X
6	2.01	On	On	V_2	Off	Off	-4 to 21	0	C_m, C_L, C_X
	2.01	On	Off	V_2	Off	Off	-4 to 21	0	C_m, C_L, C_X
	2.01	Off	On	V_2	Off	Off	-4 to 21	0	C_m, C_L, C_X
	2.01	Off	Off	V_2	Off	Off	-4 to 21	0	C_m, C_L, C_X
7	1.82	On	On	V_2	Off	Off	-4 to 21	0	C_m, C_L, C_X
	2.01	On	On	V_2	Off	Off	-4 to 21	0	C_m, C_L, C_X
8	1.82	On	Off	V_2	Off	Off	8	-4 to 14	C_n, C_l, C_Y
	1.82	On	Off	Off	Off	Off	8, 12.7	-4 to 14	C_n, C_l, C_Y
	1.82	On	On	V_2	Off	Off	2.4, 8, 12.7	-4 to 14	C_n, C_l, C_Y
9	1.82	On	On	V_2	Off	Off	-4 to 21	5.2	C_n, C_l, C_Y
	1.82	On	Off	V_2	Off	Off	-4 to 21	5.3	C_n, C_l, C_Y
	1.82	On	Off	Off	Off	Off	-4 to 21	5.4	C_n, C_l, C_Y
10	2.01	On	On	V_2	Off	Off	2.4, 8, 12.8, 18.2	-4 to 14	C_n, C_l, C_Y
	2.01	On	Off	V_2	Off	Off	2.4, 8, 12.8, 18.2	-4 to 14	C_n, C_l, C_Y
	2.01	On	Off	Off	Off	Off	2.4, 8, 12.8, 18.2	-4 to 14	C_n, C_l, C_Y
	2.01	Off	On	V_2	Off	Off	8, 18.2	-4 to 14	C_n, C_l, C_Y
11	1.82	On	On	V_2	Off	Off	2.4, 8, 12.7	-4 to 14	C_m, C_L, C_X
	1.82	On	Off	Off	Off	Off	8, 12.7	-4 to 14	C_m, C_L, C_X
	1.82	On	Off	V_2	Off	Off	8	-4 to 14	C_m, C_L, C_X
12	2.01	On	On	V_2	Off	Off	2.4, 8, 12.8, 18.2	-4 to 14	C_m, C_L, C_X
	2.01	On	Off	V_2	Off	Off	2.4, 8, 12.8, 18.2	-4 to 14	C_m, C_L, C_X
	2.01	On	Off	Off	Off	Off	2.4, 8, 12.8, 18.2	-4 to 14	C_m, C_L, C_X
	2.01	Off	On	V_2	Off	Off	8, 18.2	-4 to 14	C_m, C_L, C_X

TABLE II.- INDEX OF FIGURES - Concluded

Figure	M	Wing	Horizontal tail	Vertical tail	Ventral fin	Stores	α, deg	β, deg	Data
13	2.01	On	On	V_1, V_2	Off	Off	8, 18.2	-4 to 14	C_n, C_l, C_Y
14	2.01	On	Off	V_2, V_3	Off	Off	2.4, 8, 12.8, 18.3	-4 to 14	C_n, C_l, C_Y
15	2.01	On	On	V_2	Off	Off	-4 to 21	5.3	C_n, C_l, C_Y
	2.01	On	On	V_2	U_1	Off	-4 to 21	5.3	C_n, C_l, C_Y
	2.01	On	On	V_2	U_2	Off	-4 to 21	5.3	C_n, C_l, C_Y
	2.01	On	On	V_2	U_3	Off	-4 to 21	5.3	C_n, C_l, C_Y
	2.01	On	On	V_2	U_4	Off	-4 to 21	5.3	C_n, C_l, C_Y
16	2.01	On	On	V_2	U_1	Off	8	-4 to 14	C_n, C_l, C_Y
	2.01	On	On	V_2	U_2	Off	8	-4 to 14	C_n, C_l, C_Y
17	2.01	On	On	V_2	Off	T_1	-4 to 21	0	C_m, C_L, C_X
	2.01	On	Off	V_2	Off	T_1	-4 to 21	0	C_m, C_L, C_X
18	2.01	On	On	V_2	Off	M_9	-4 to 21	0	C_m, C_L, C_X
	2.01	On	Off	V_2	Off	M_9	-4 to 21	0	C_m, C_L, C_X
19	2.01	On	On	V_2	Off	M_9	-4 to 21	0	C_n, C_l, C_Y
	2.01	On	On	V_2	Off	M_9	-4 to 21	5.2	C_n, C_l, C_Y
	2.01	On	On	V_2	Off	M_1	-4 to 21	5.2	C_n, C_l, C_Y
	2.01	On	On	V_2	Off	A_1	-4 to 21	5.3	C_n, C_l, C_Y
Summary Figures									
20	Effects of component parts on sideslip derivatives. M = 1.82.								
21	Effects of component parts on sideslip derivatives. M = 2.01.								
22	Effects of vertical-tail plan form on sideslip derivatives. M = 2.01.								
23	Effects of ventral fins on sideslip derivatives. M = 2.01.								
24	Effects of external stores on sideslip derivatives. M = 2.01.								

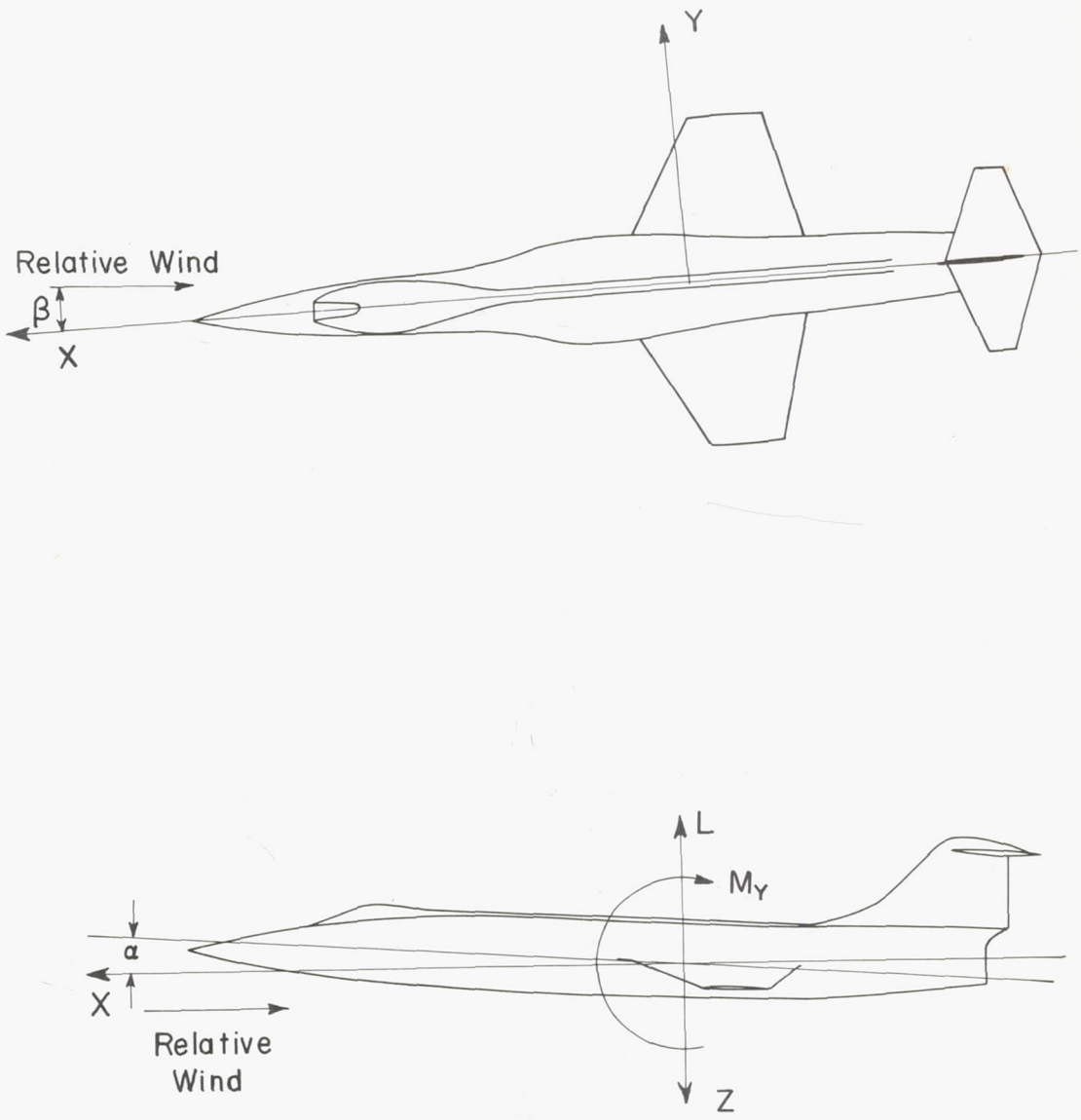

(a) System of stability axes.

Figure 1.- Systems of axes and notation.

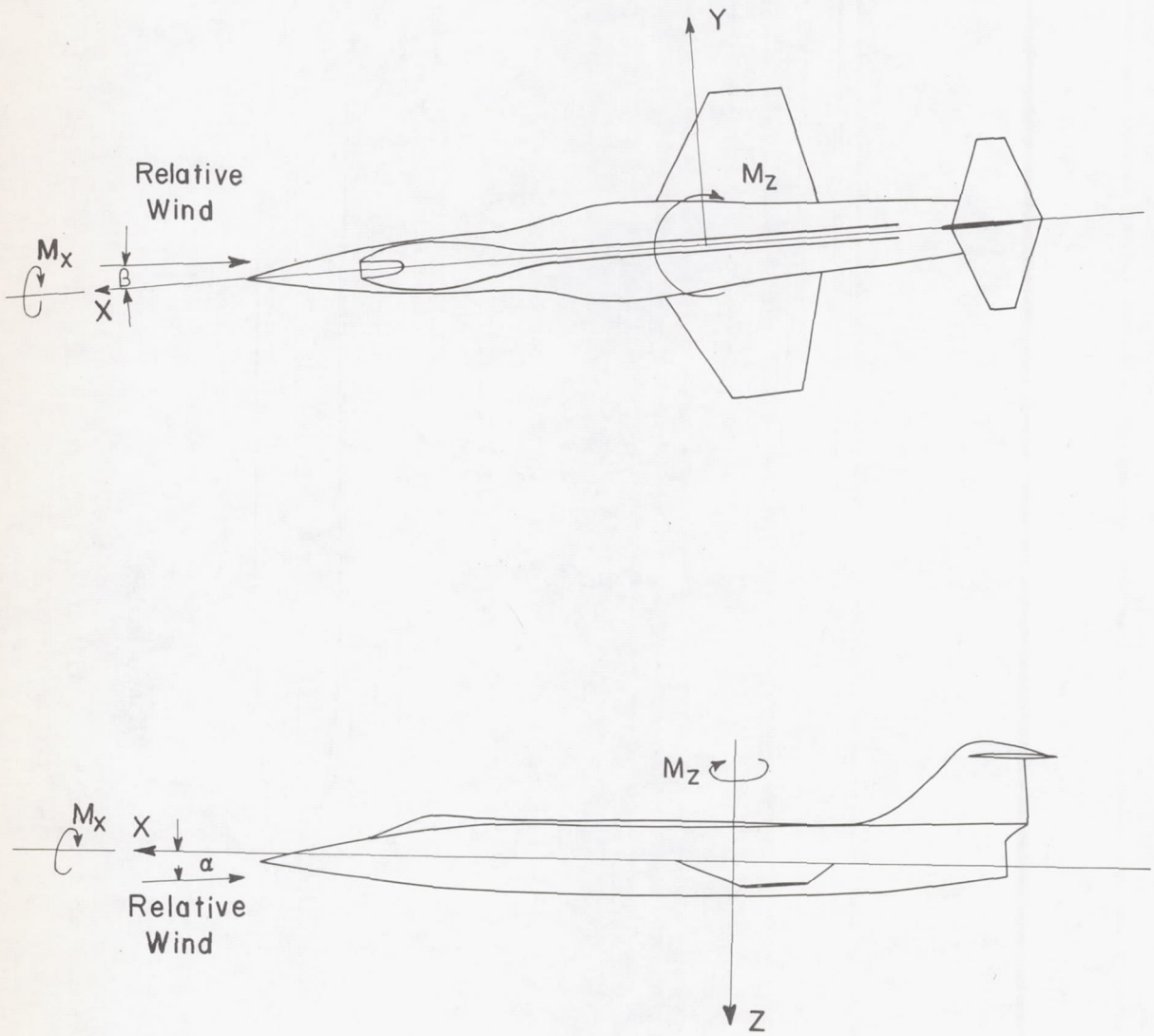

(b) System of body axes.

Figure 1.- Concluded.

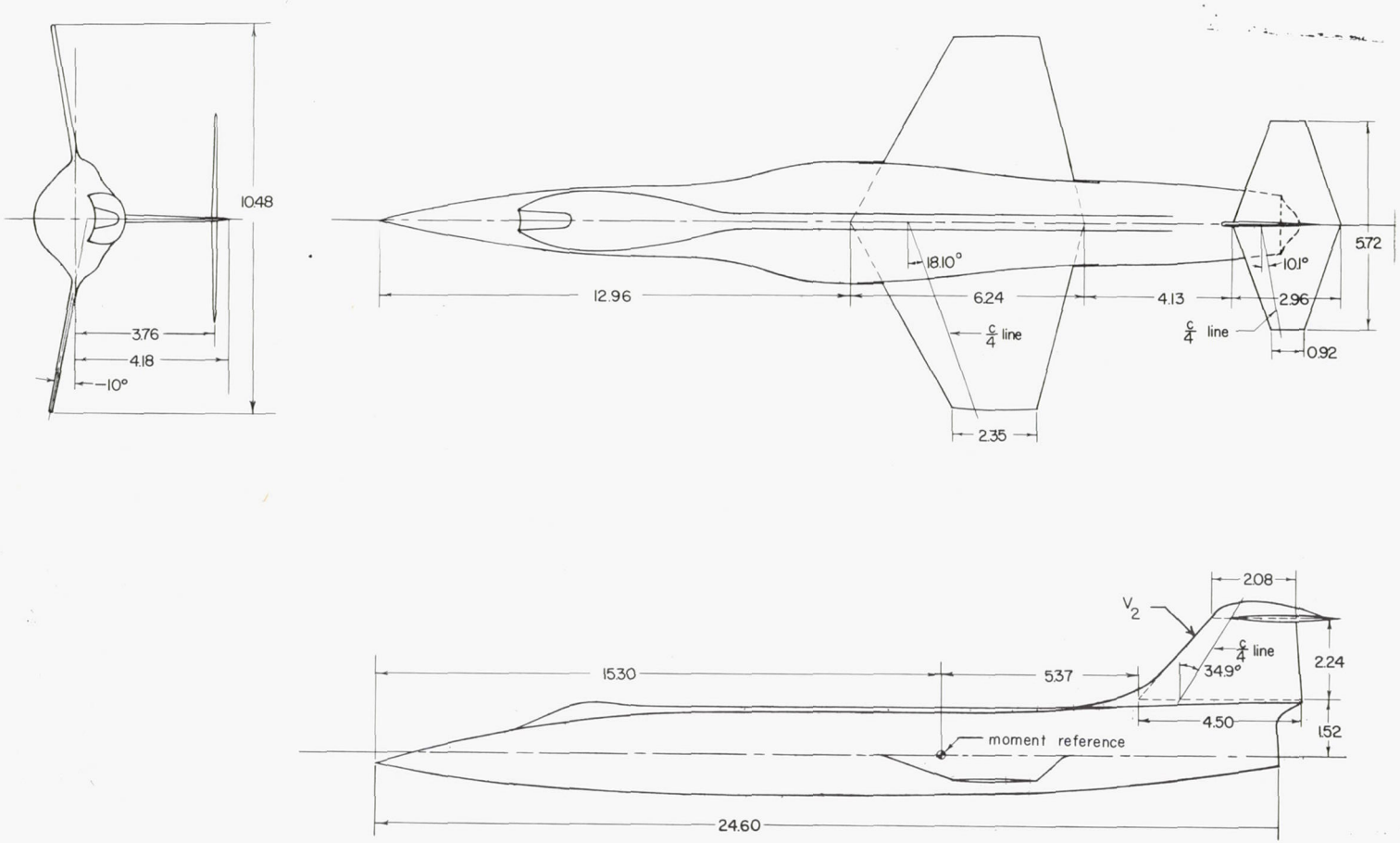

(a) Basic model.

Figure 2.- Details of test model. All dimensions in inches unless otherwise noted.

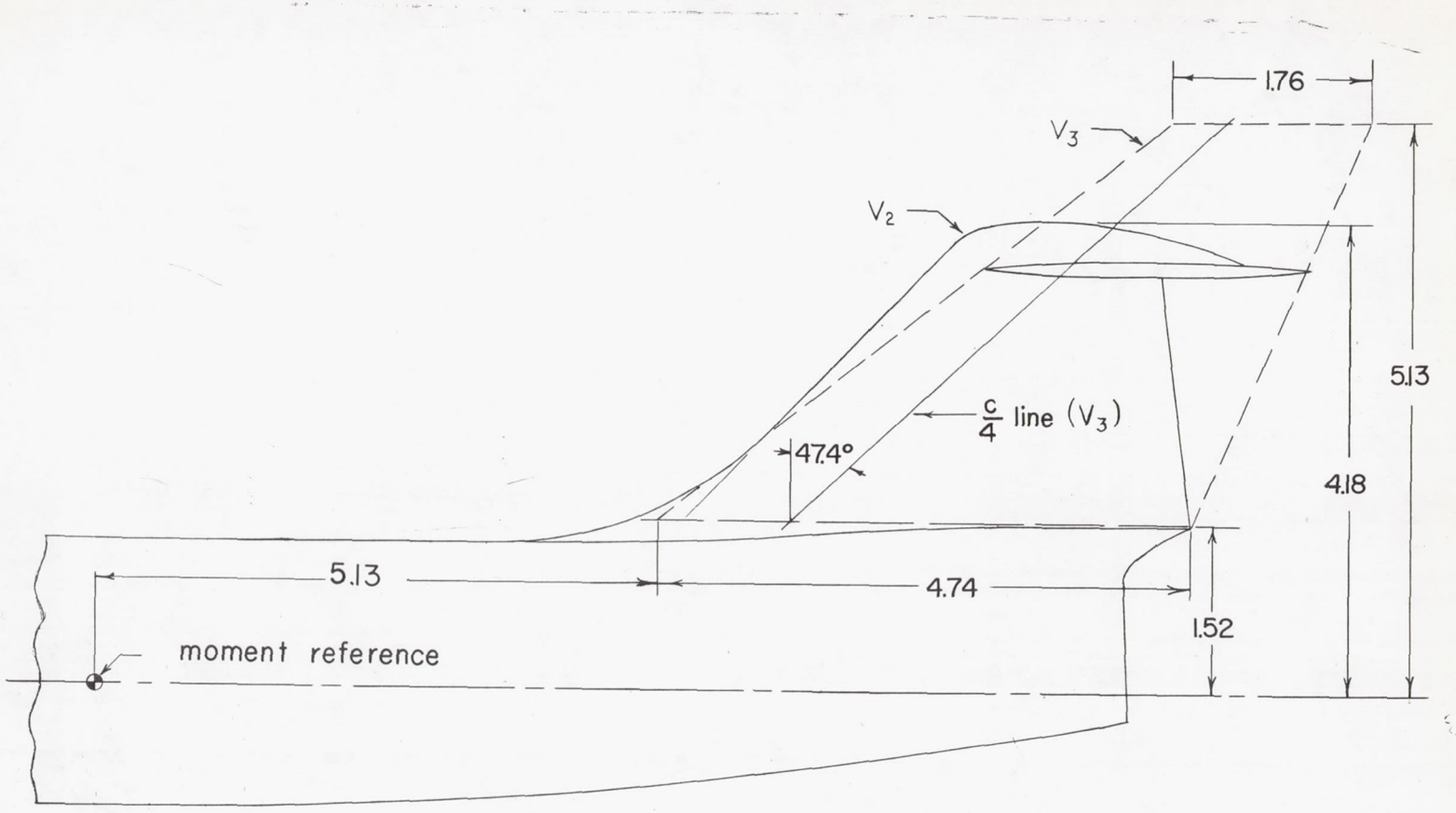

(b) Vertical-tail details.

Figure 2.- Continued.

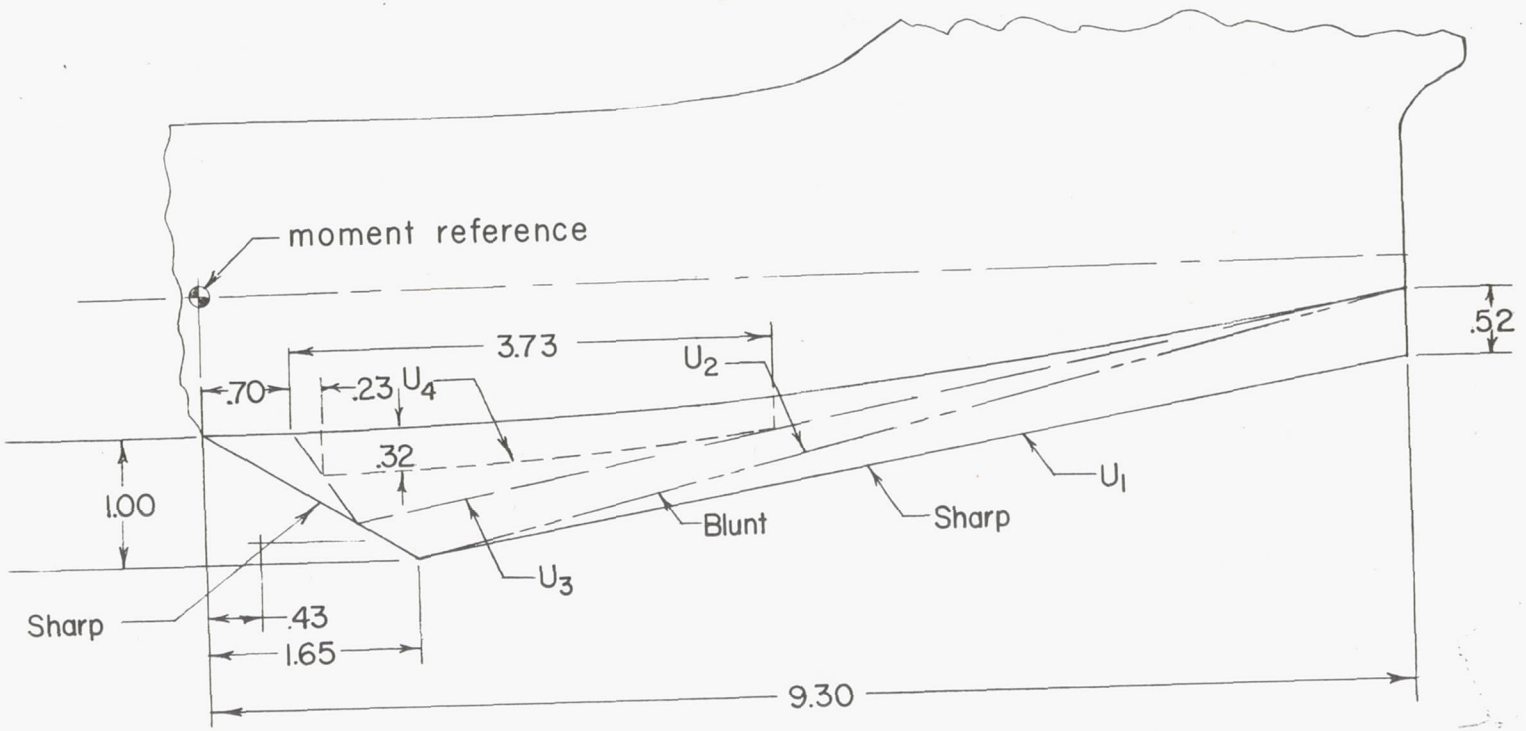

(c) Ventral-fin details.

Figure 2.- Concluded.

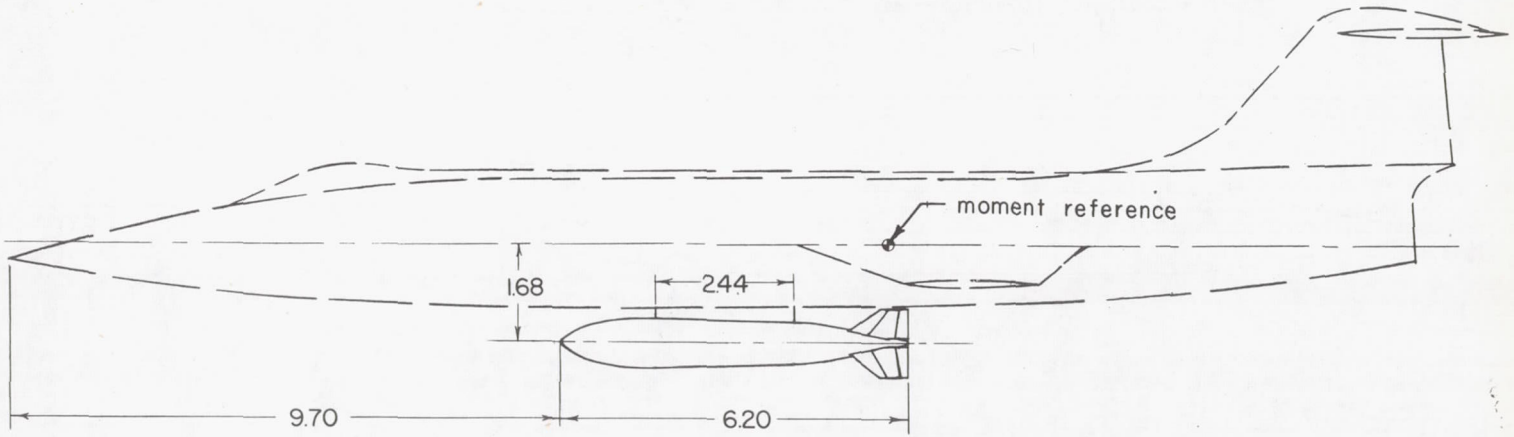

(a) Fuselage store (A_1).

Figure 3.- Details of store arrangements.

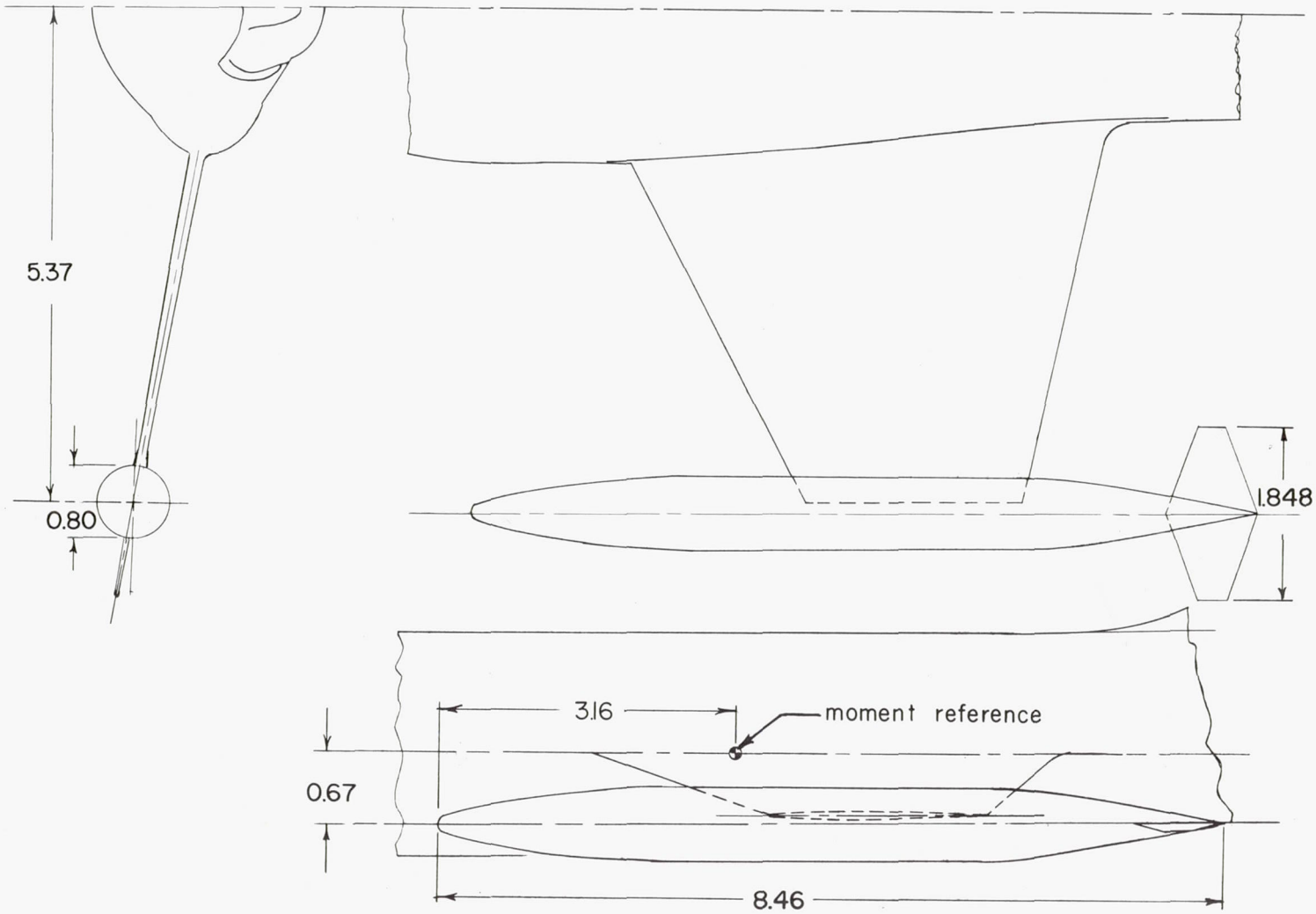

(b) Tip tanks (T_1).

Figure 3.- Continued.

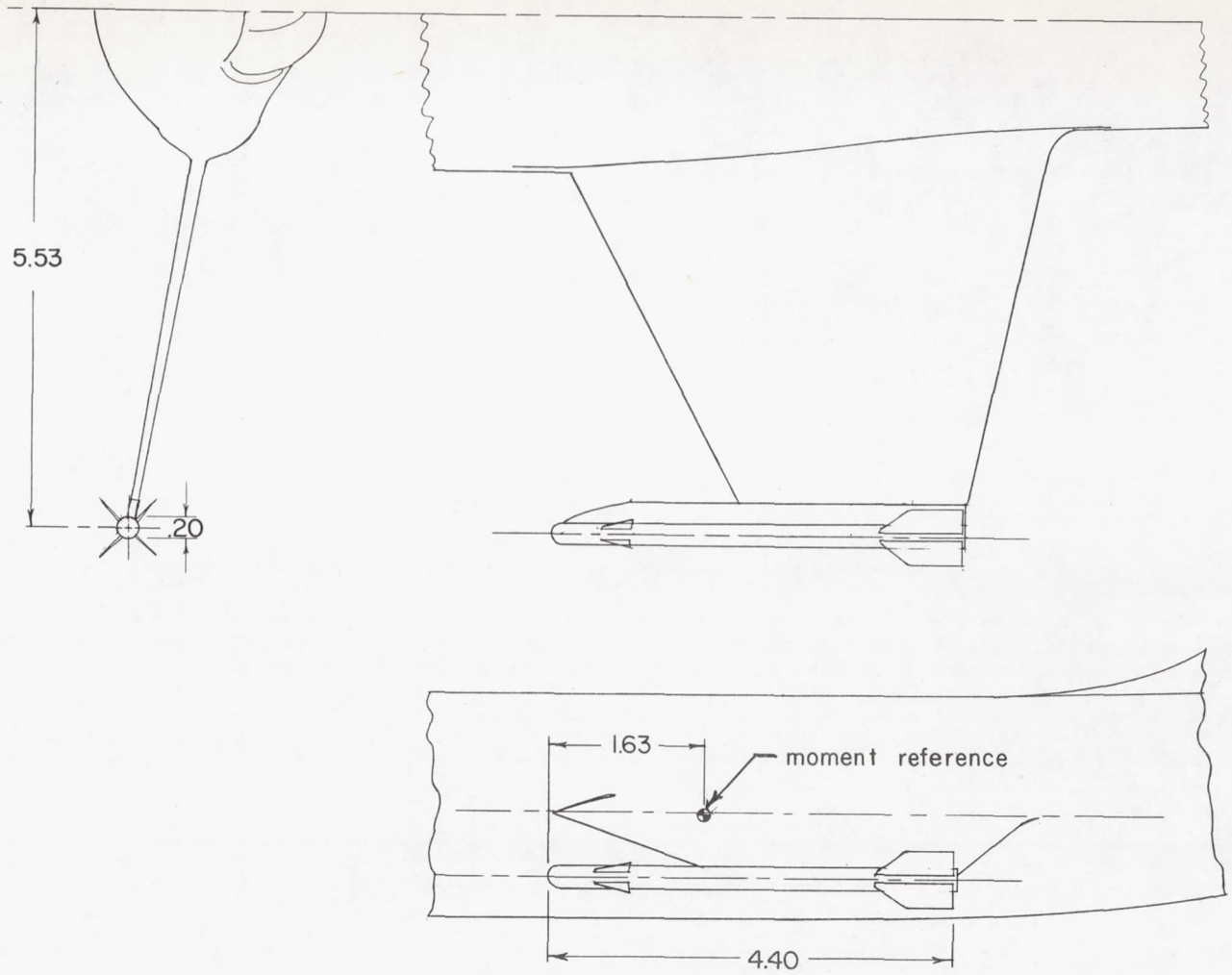

(c) Two tip-mounted Sidewinder missiles (M_9).

Figure 3.- Continued.

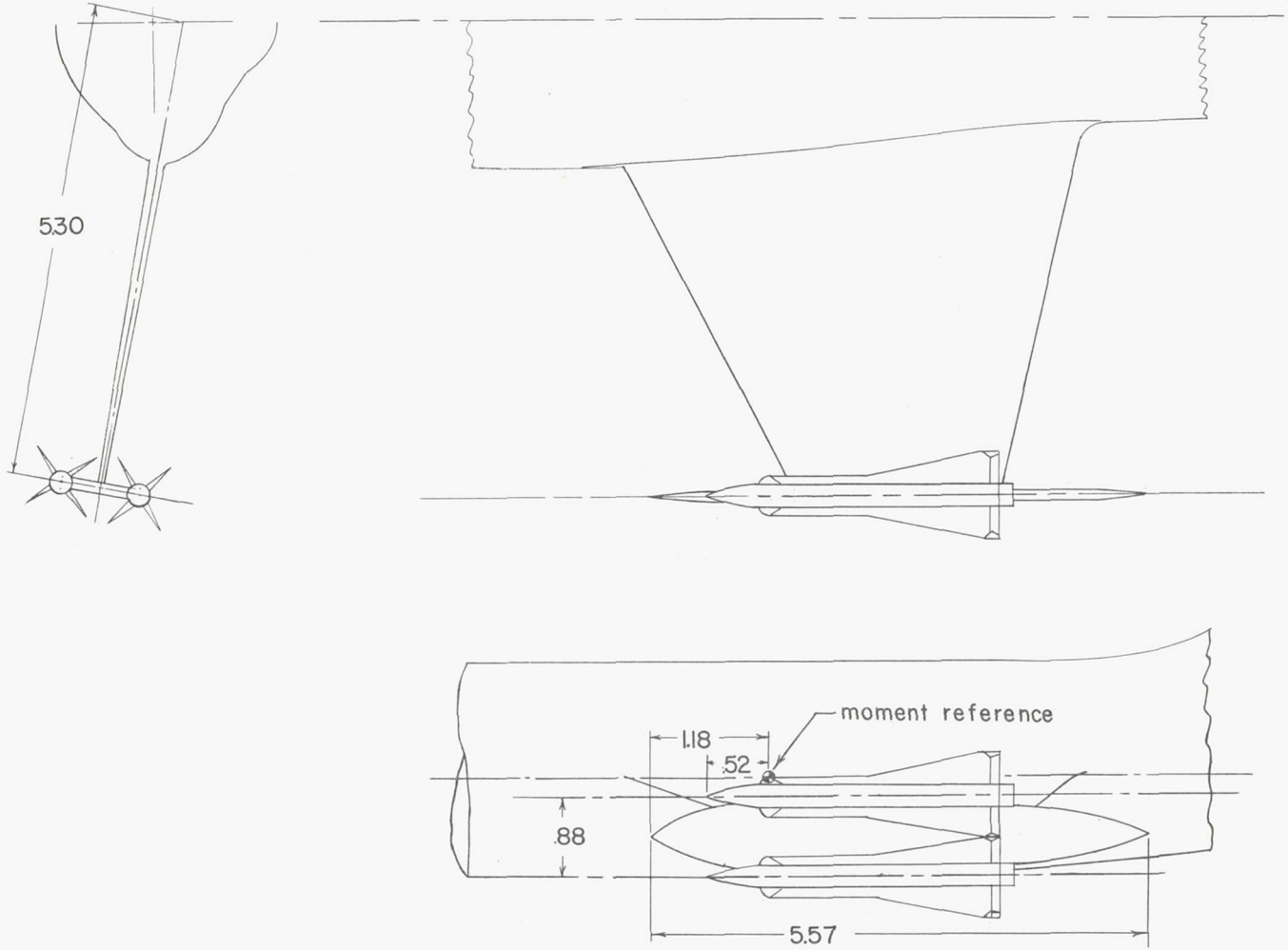

(d) Four tip-mounted Falcon missiles (M_1).

Figure 3.- Concluded.

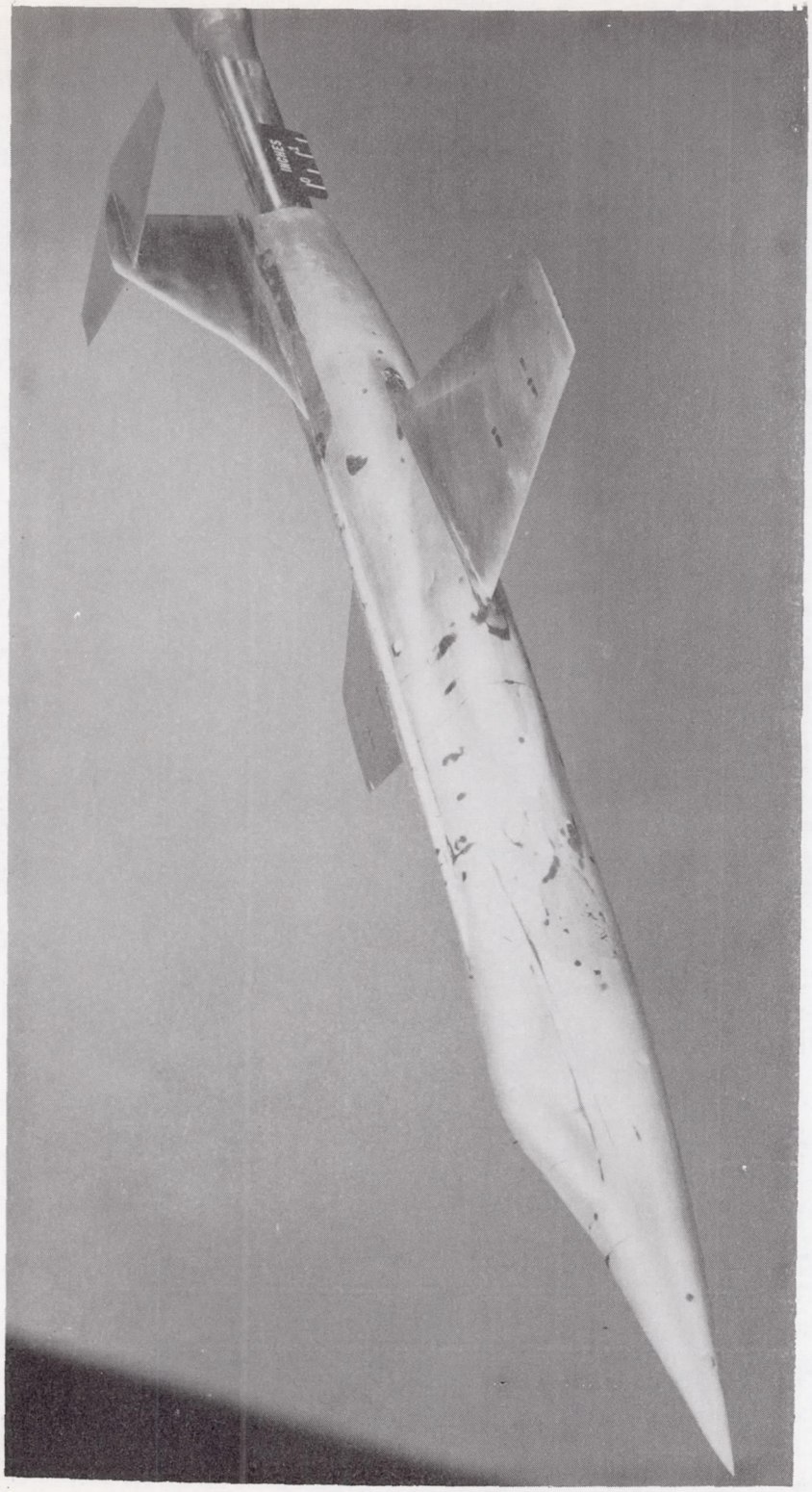

L-89750

(a) Basic model, BWV_2H.

Figure 4.- Photographs of model.

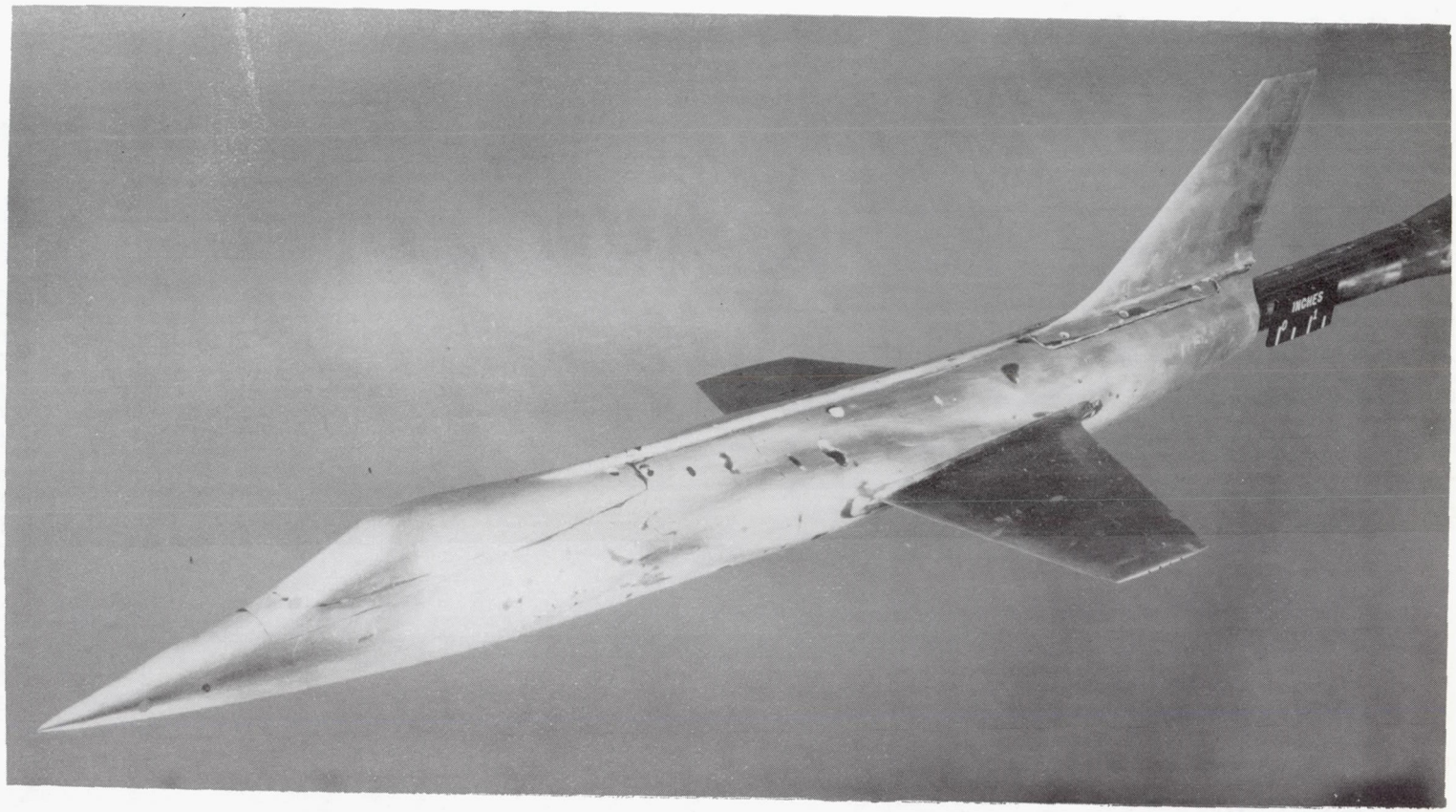

(b) Enlarged tail, BWV_3. L-89751

Figure 4.- Continued.

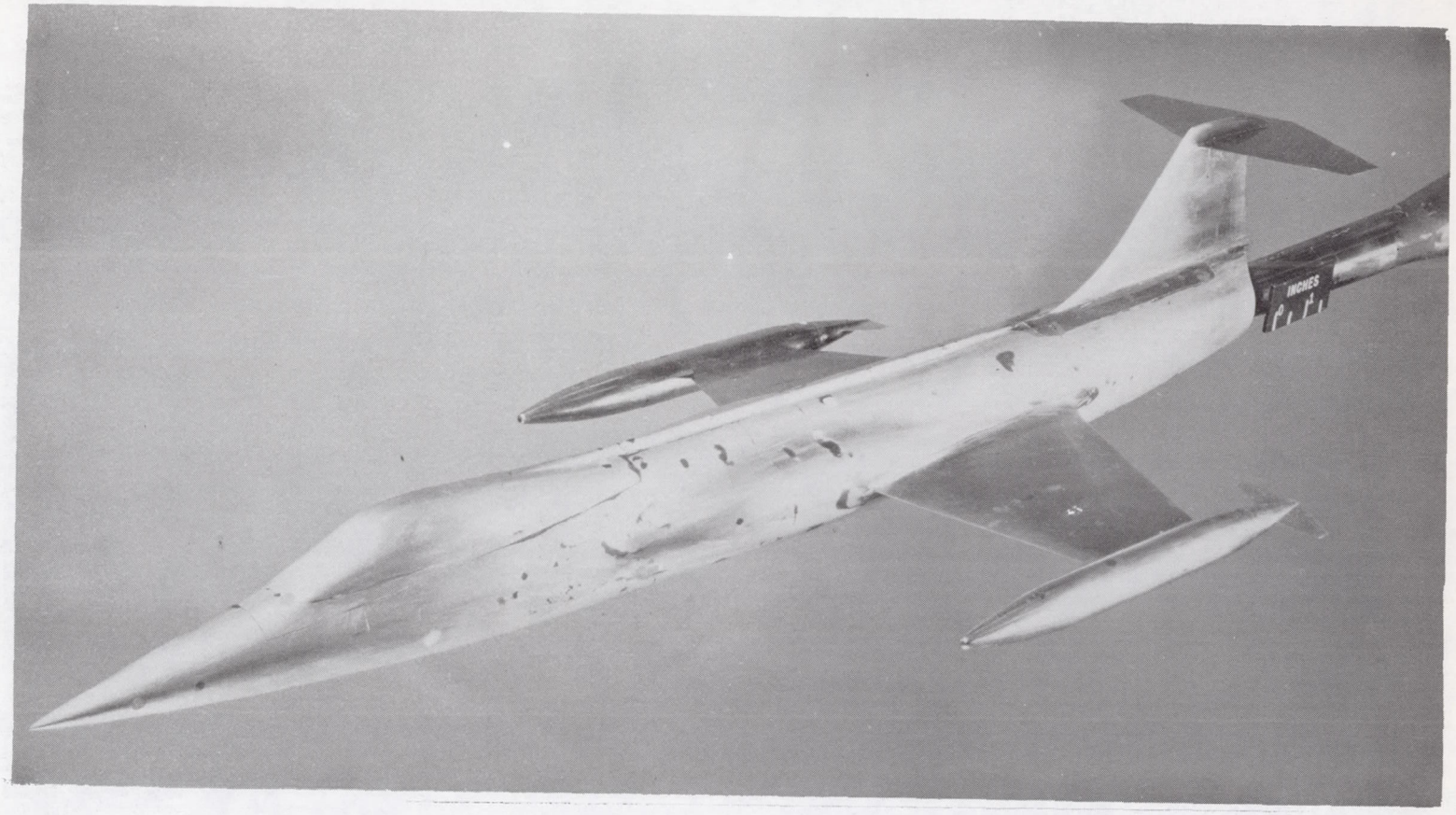

(c) Basic model with wing-tip tanks. L-89749

Figure 4.- Continued.

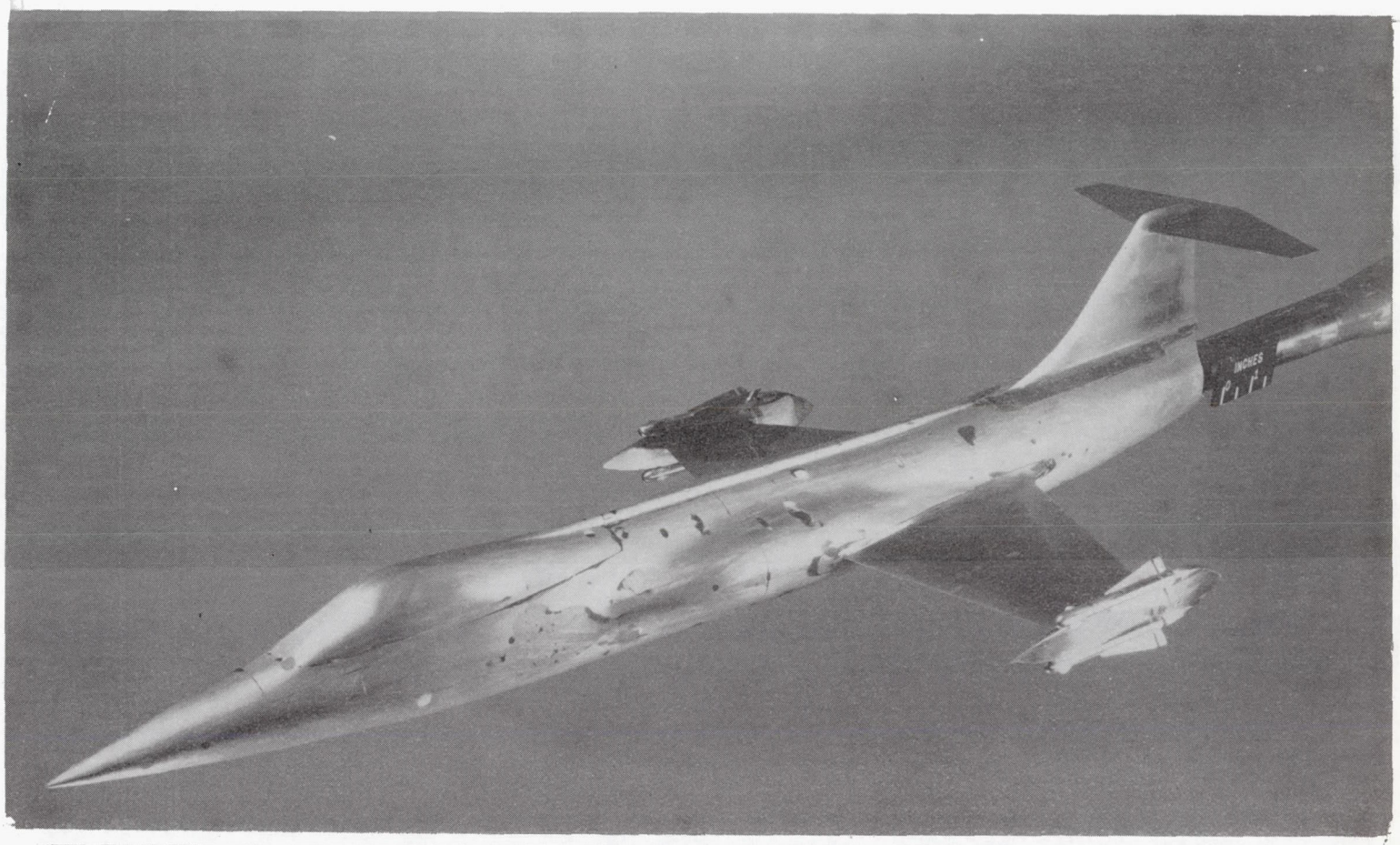

L-89748

(d) Basic model with four tip-mounted Falcon missiles.

Figure 4.- Concluded.

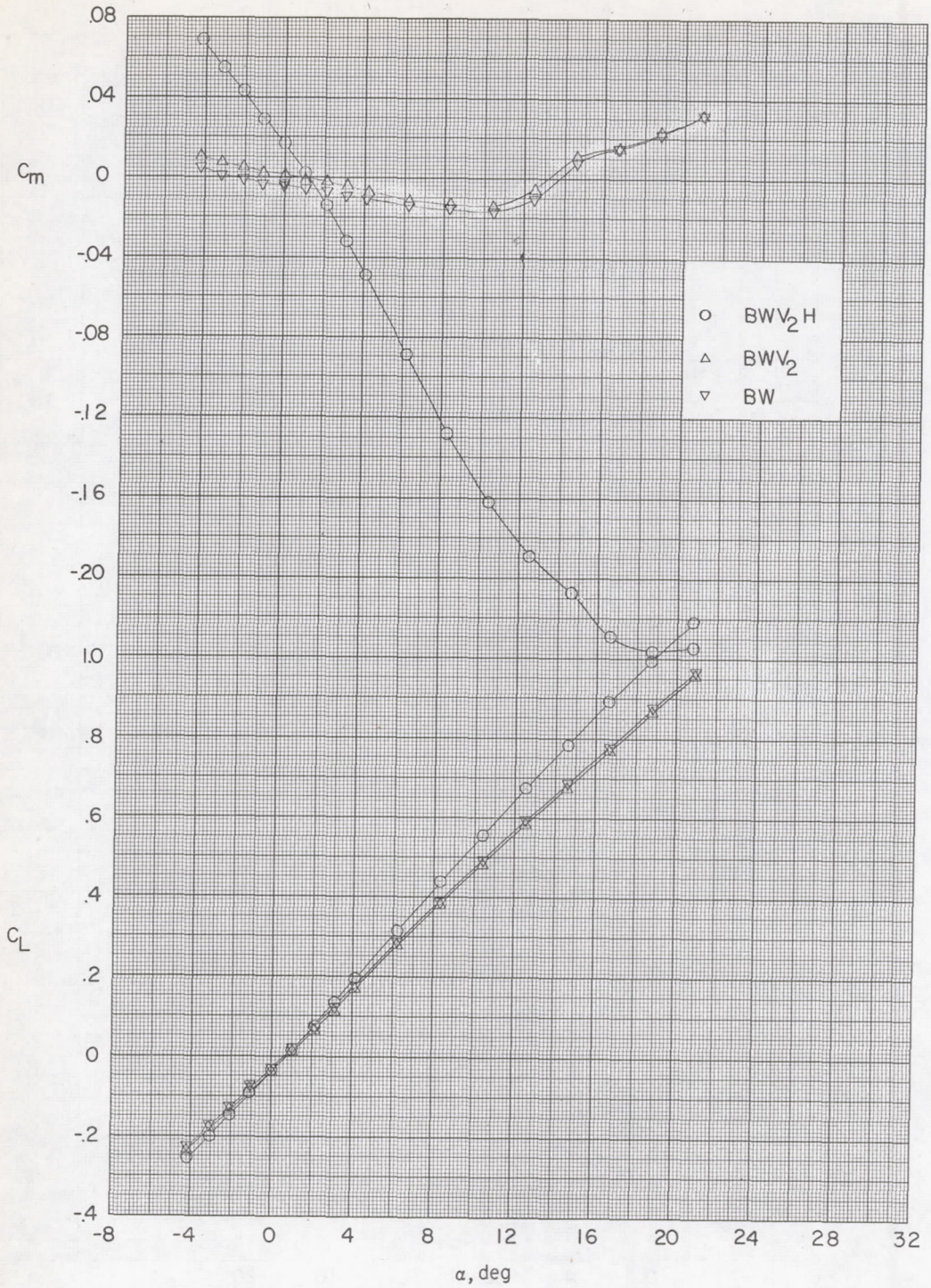

Figure 5.- Effect of component parts on the aerodynamic characteristics in pitch. M = 1.82.

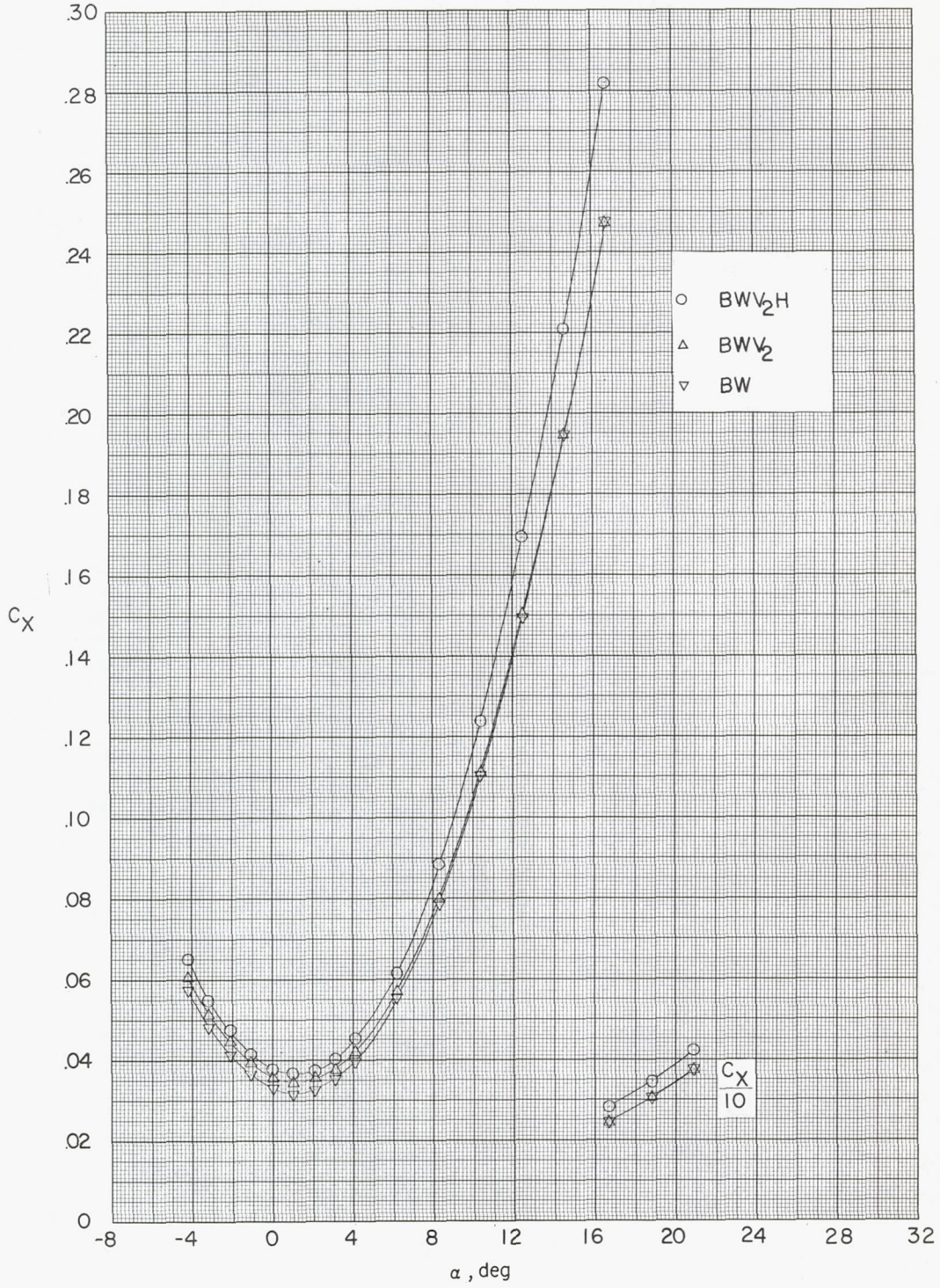

Figure 5.- Concluded.

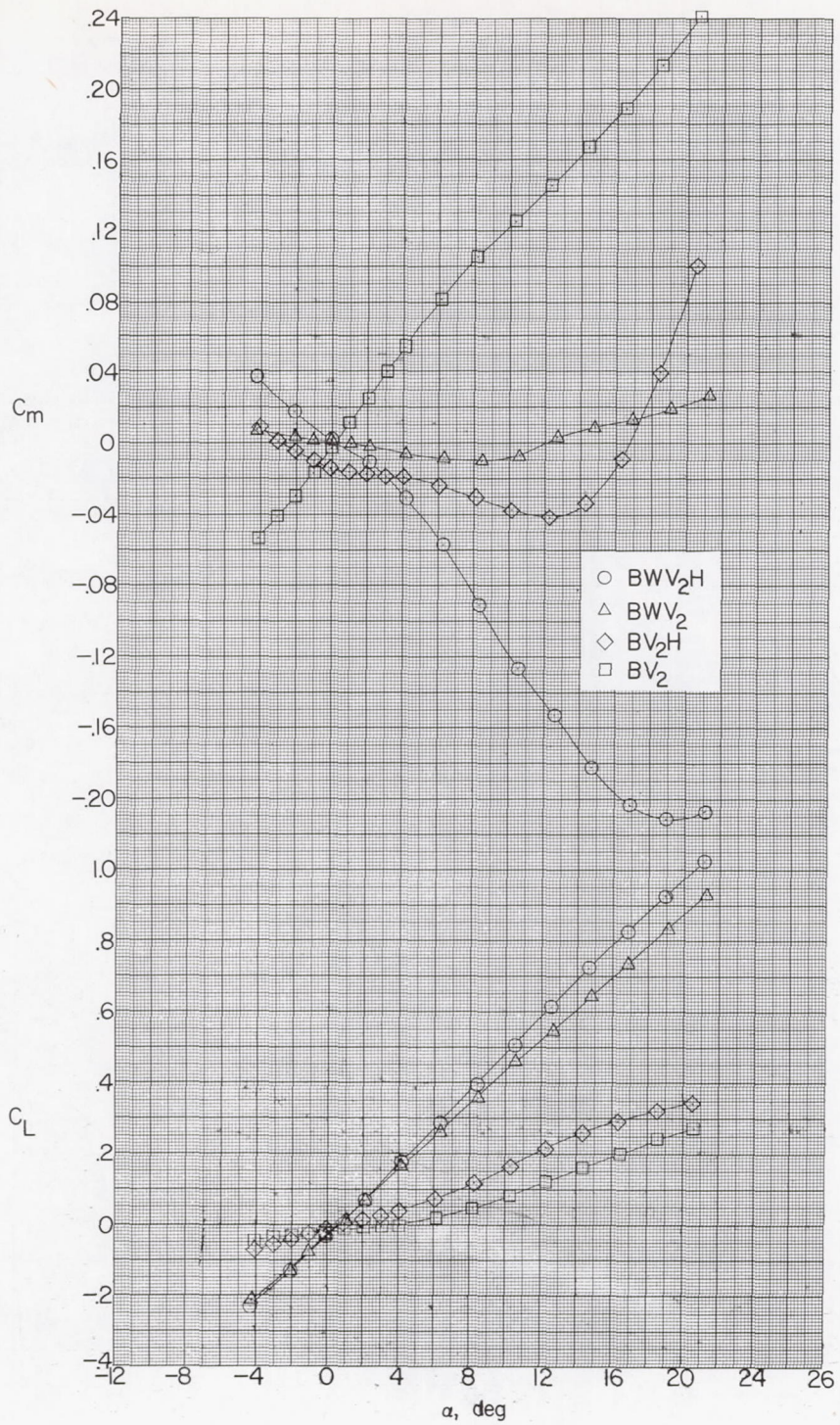

Figure 6.- Effect of component parts on the aerodynamic characteristics in pitch. M = 2.01.

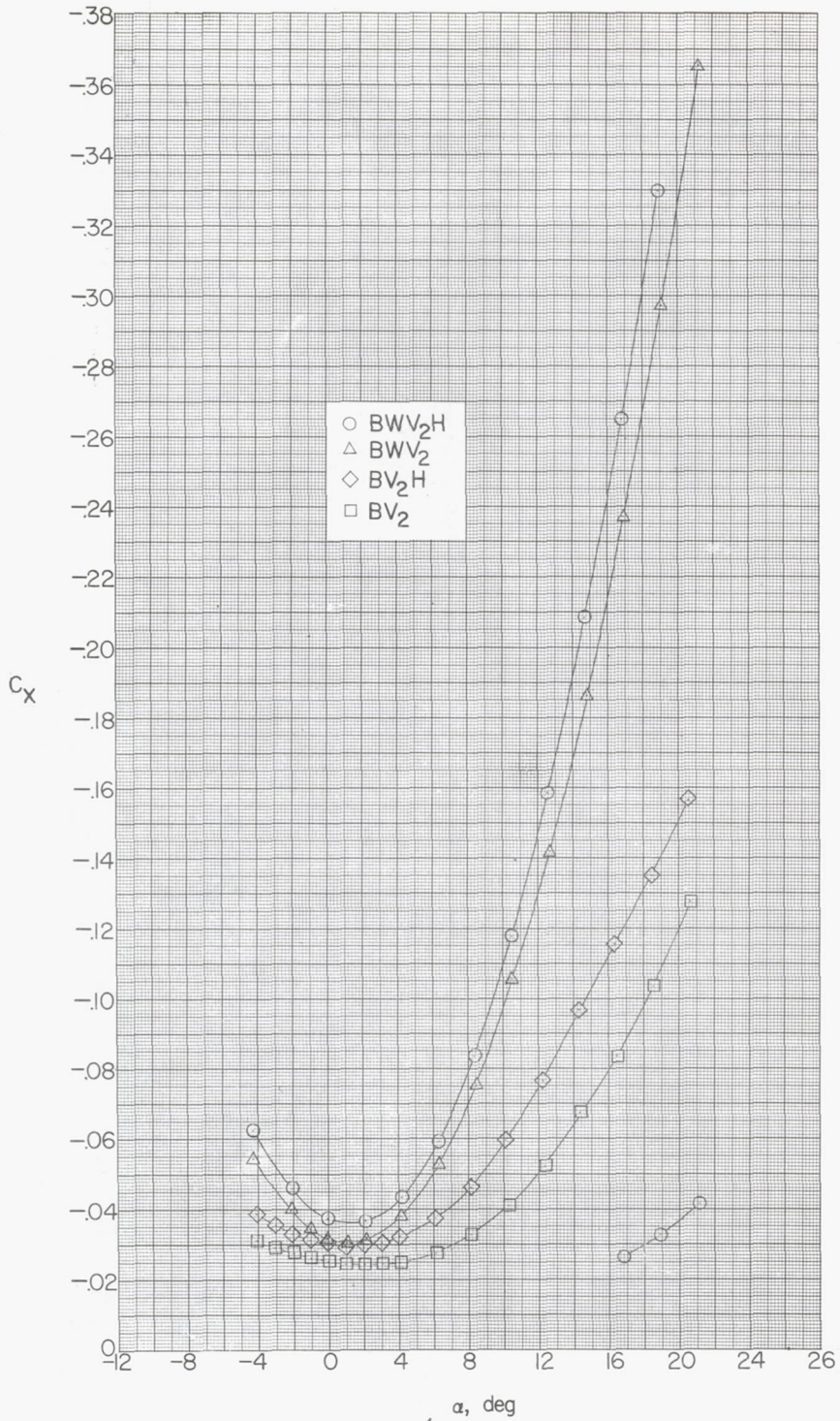

Figure 6.- Concluded.

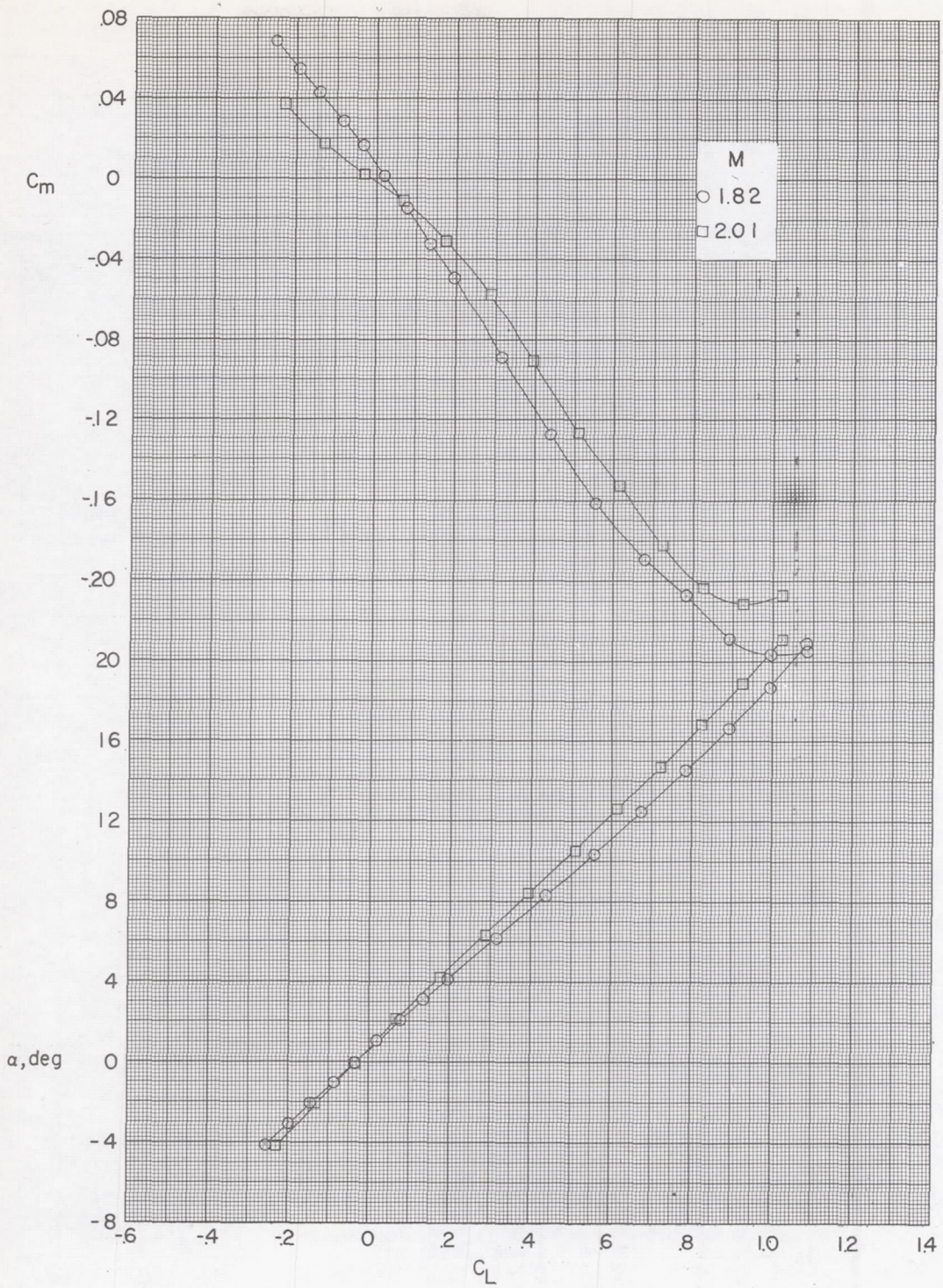

Figure 7.- Comparison of longitudinal stability characteristics of complete model (BWV_2H) at Mach numbers of 1.82 and 2.01.

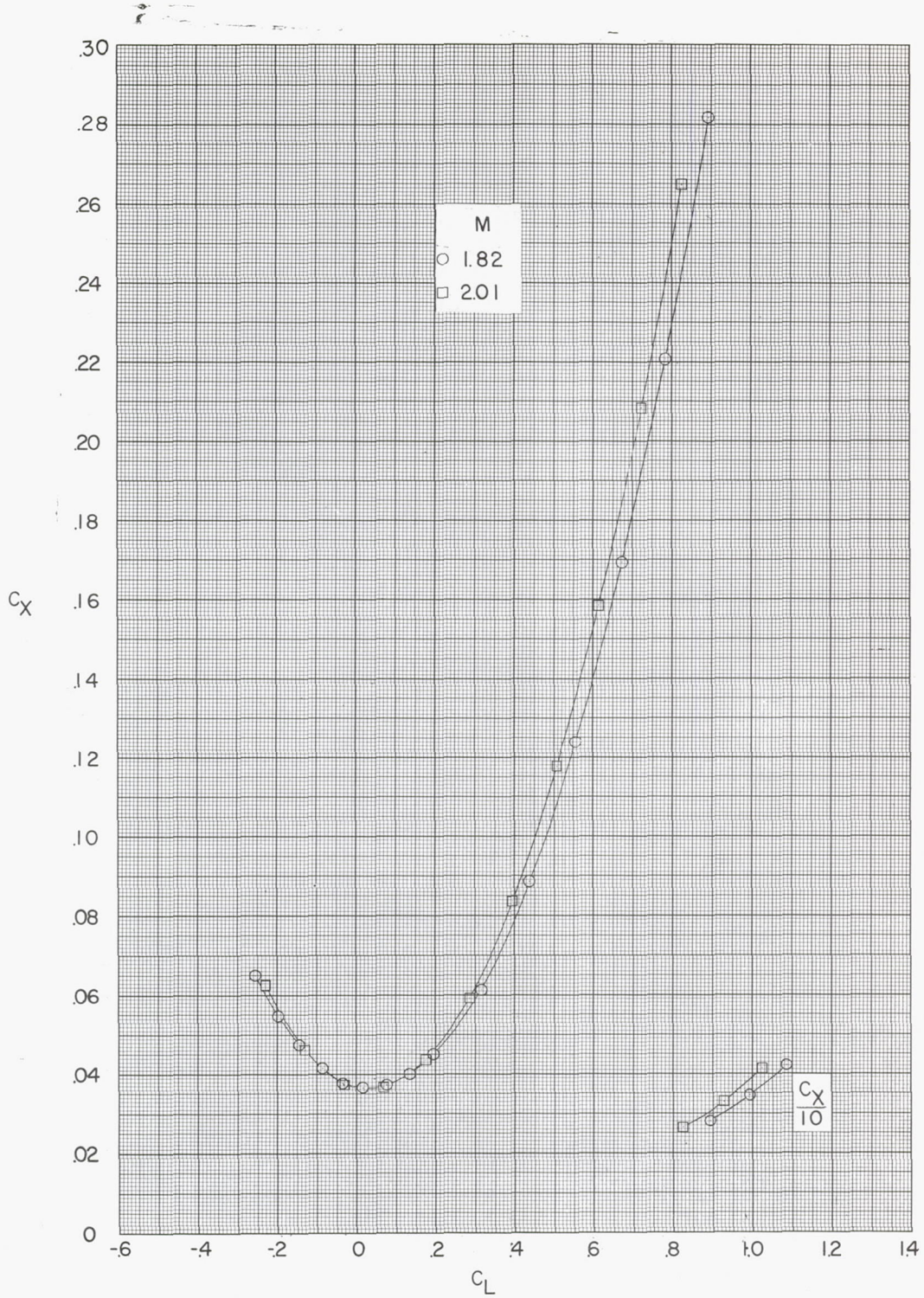

Figure 7.- Concluded.

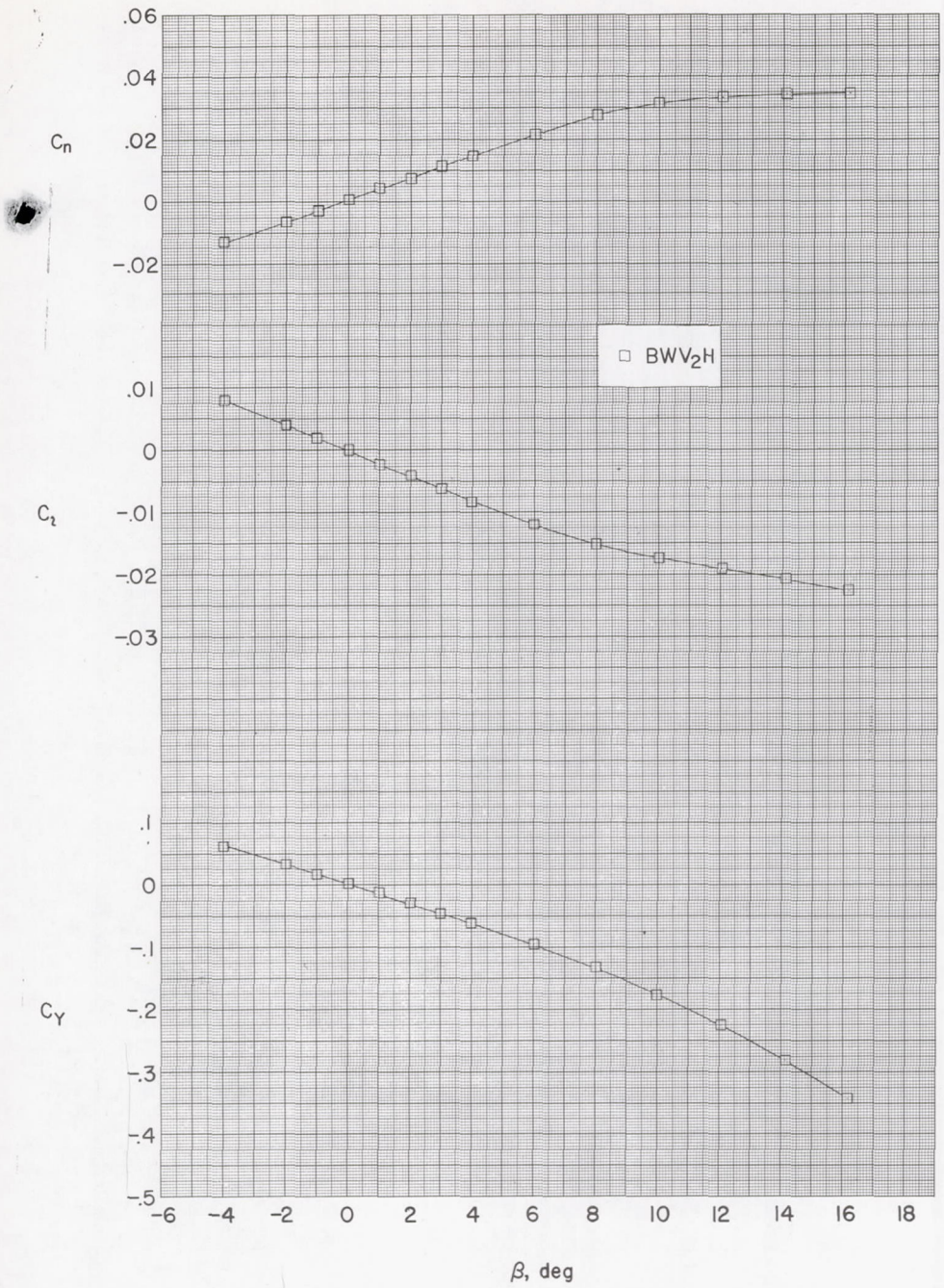

(a) $\alpha \approx 2.4^{\circ}$.

Figure 8.- Effect of component parts on the aerodynamic characteristics in sideslip at various angles of attack. M = 1.82.

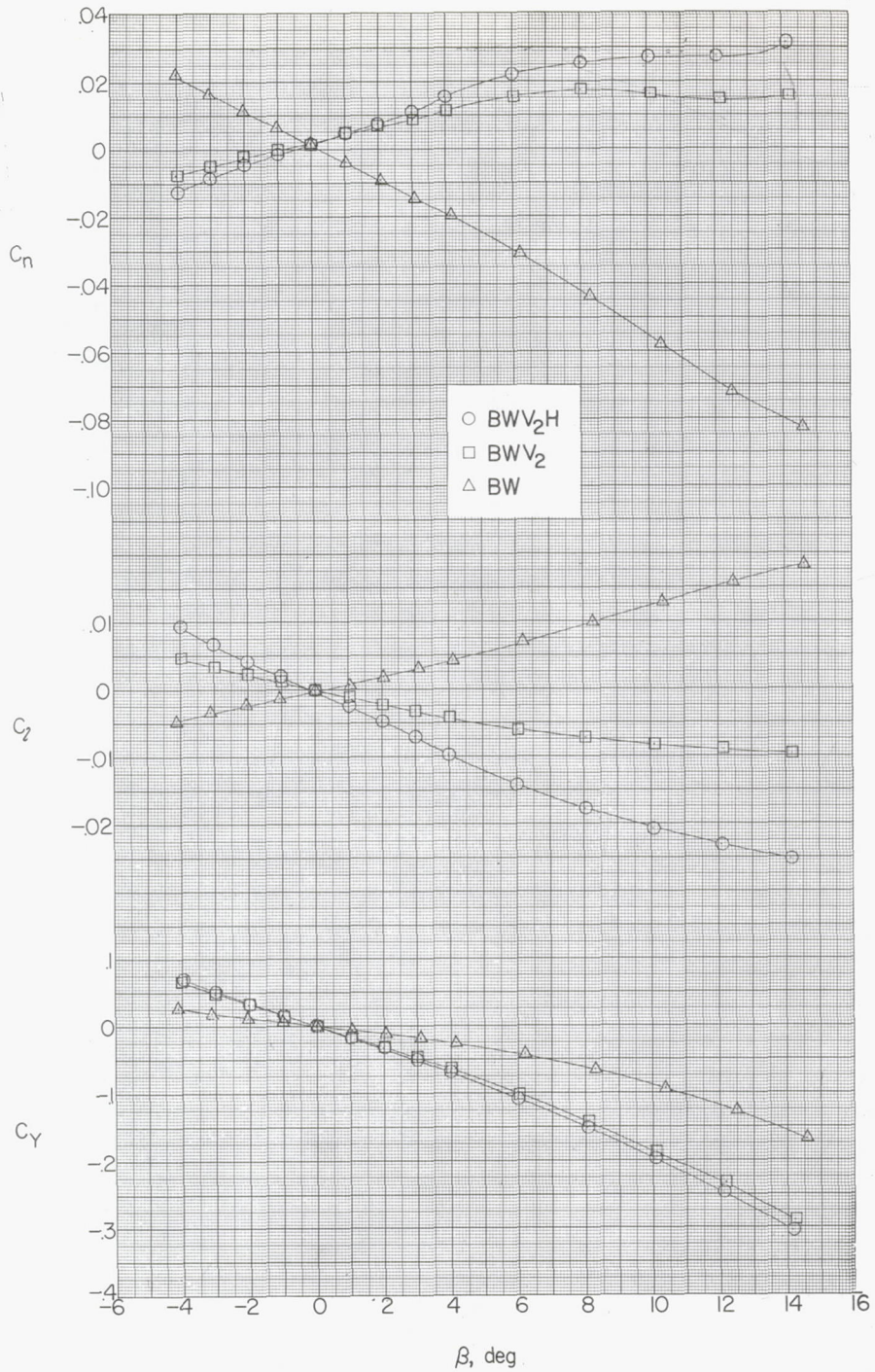

(b) $\alpha \approx 8^{\circ}$.

Figure 8.- Continued.

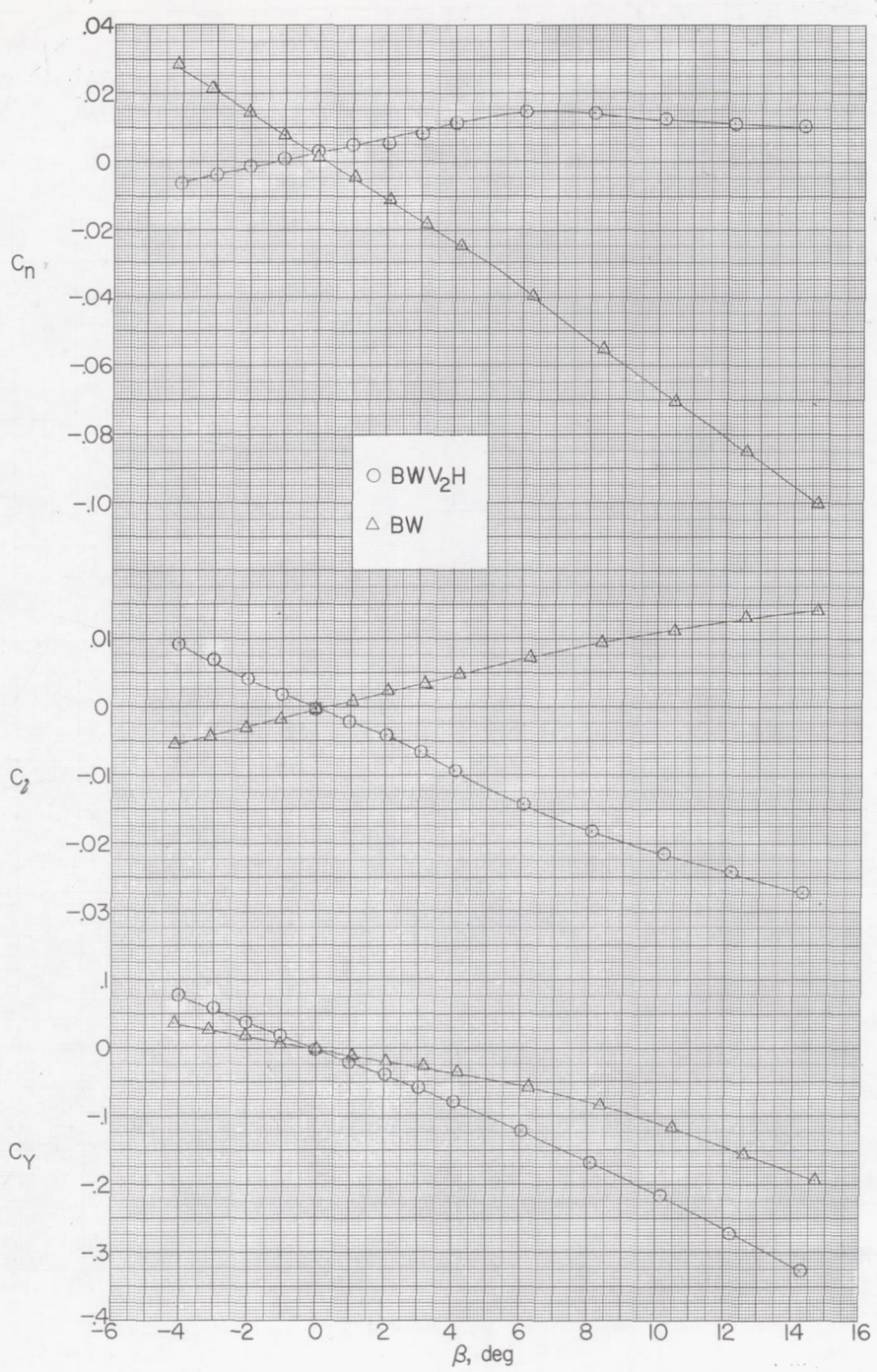

(c) $\alpha \approx 12.7^{\circ}$.

Figure 8.- Concluded.

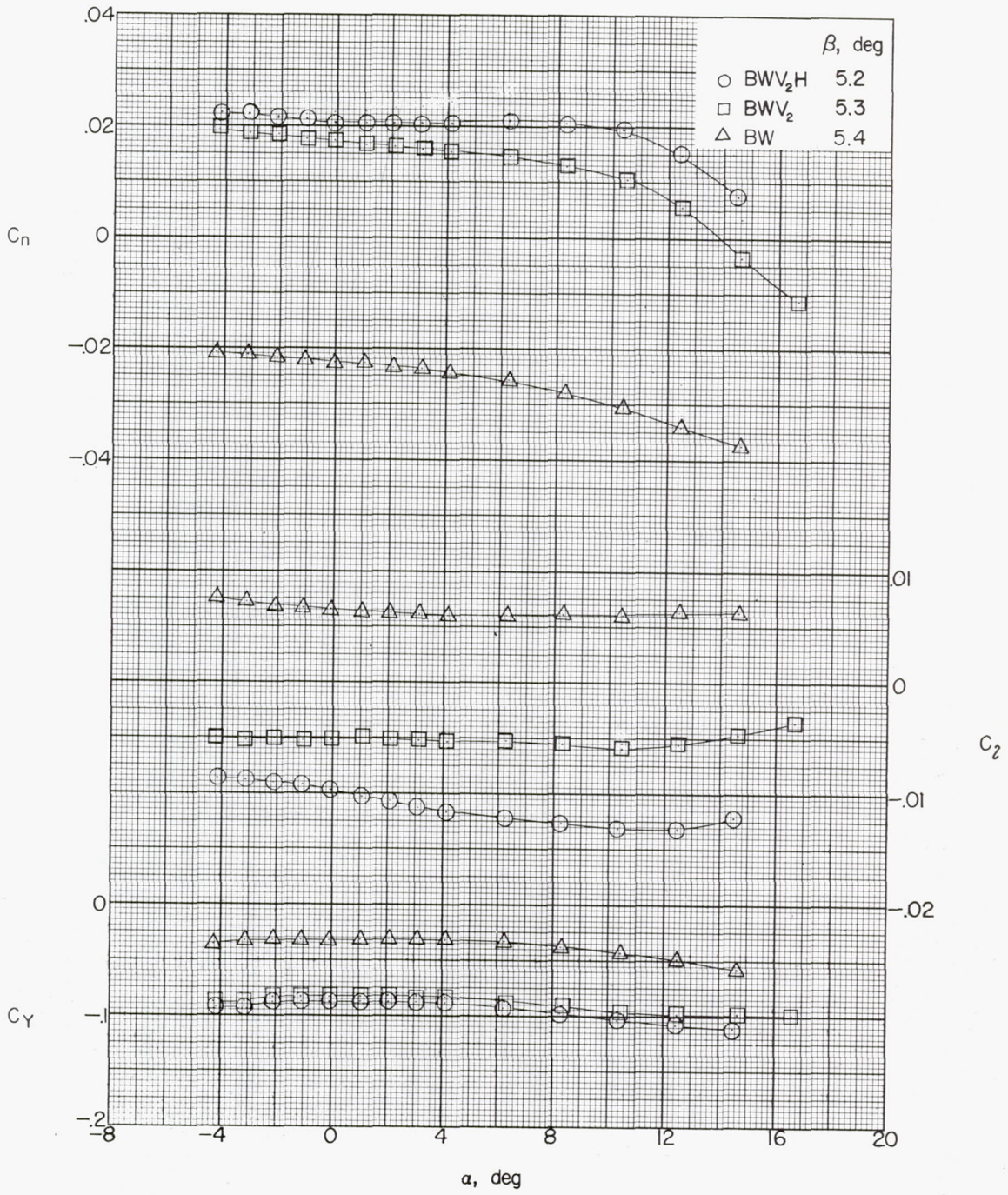

Figure 9.- Effect of component parts on the lateral and directional characteristics in pitch. M = 1.82.

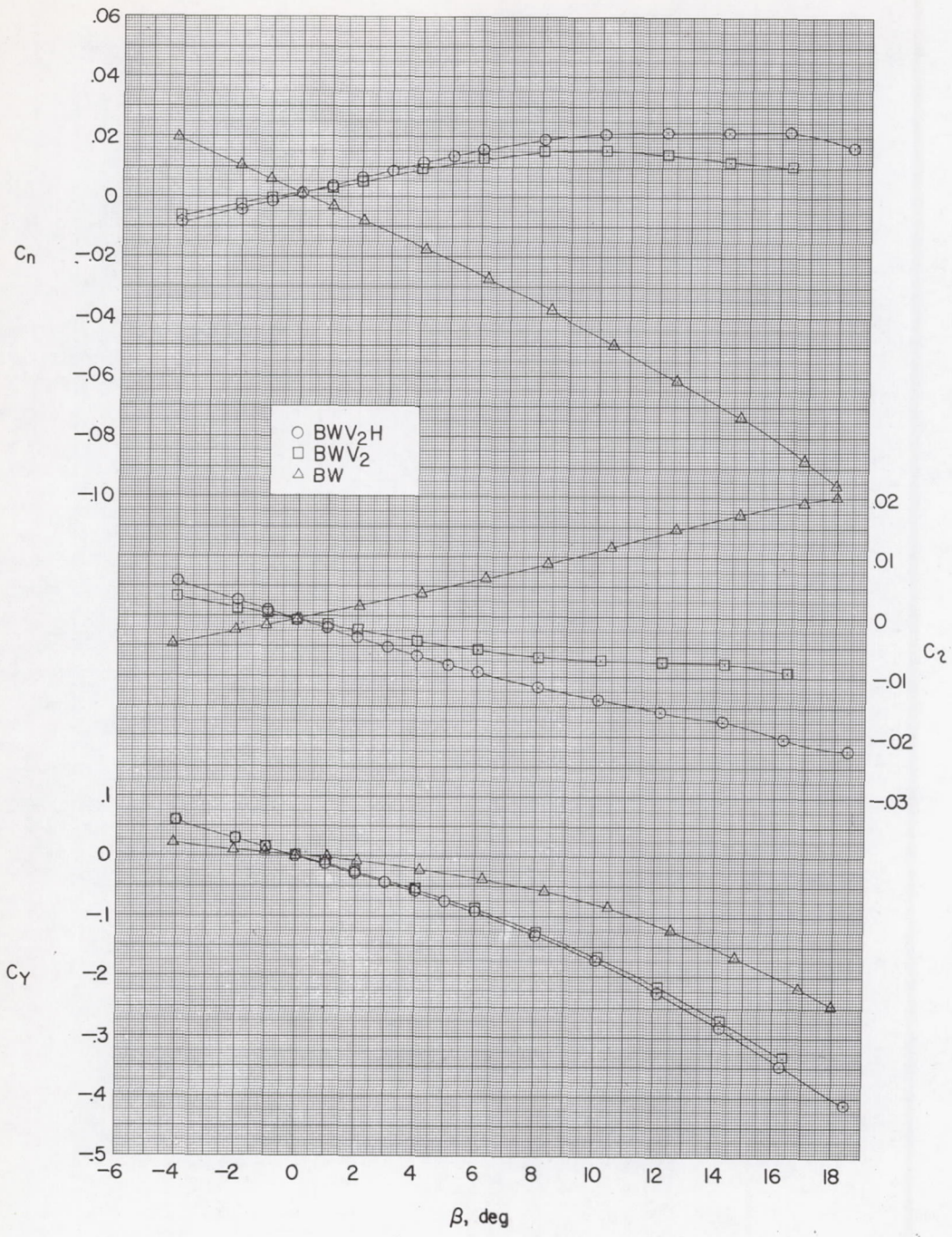

(a) $\alpha \approx 2.4^\circ$.

Figure 10.- Effect of component parts on the aerodynamic characteristics in sideslip at various angles of attack. M = 2.01.

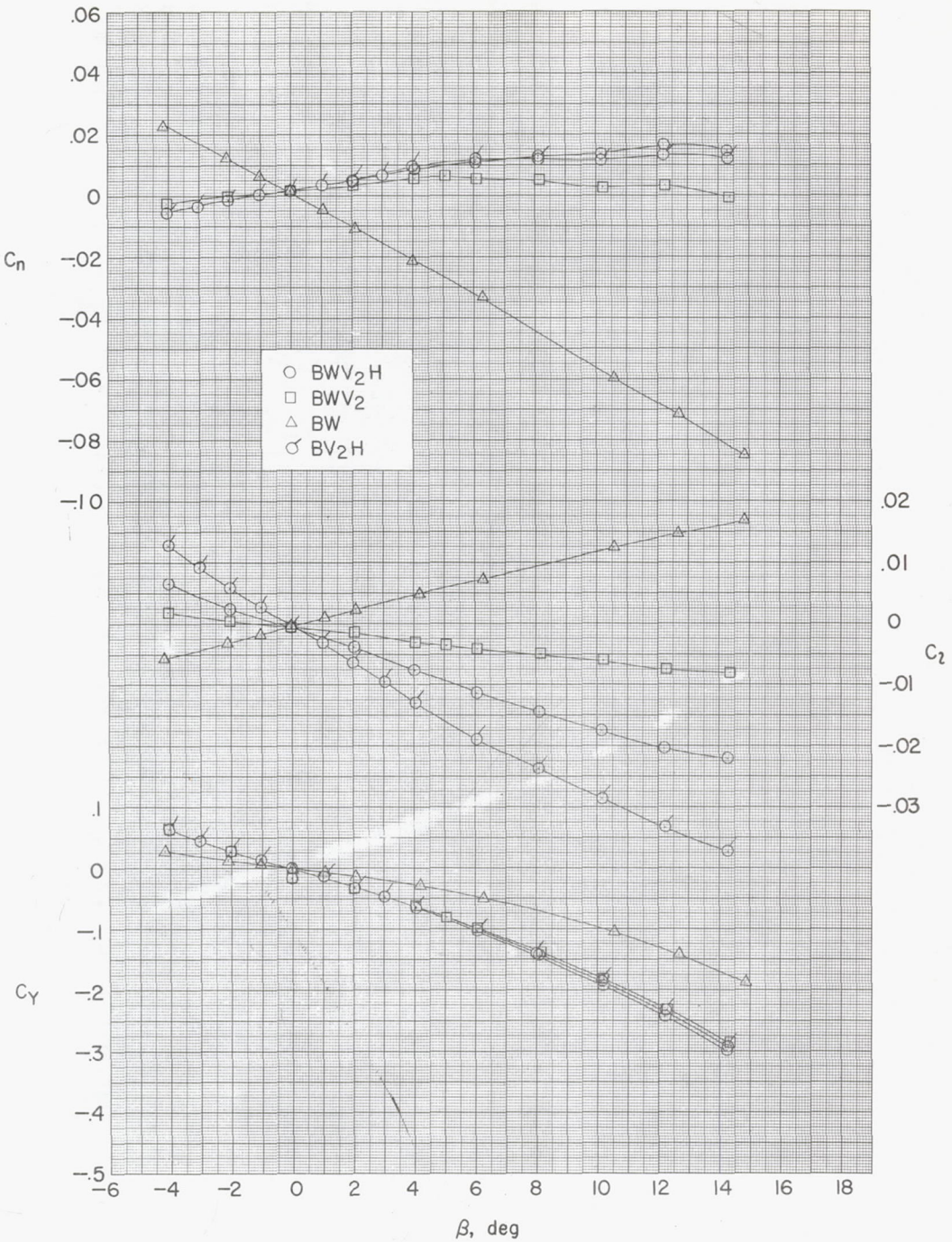

(b) $\alpha \approx 8^{\circ}$.

Figure 10.- Continued.

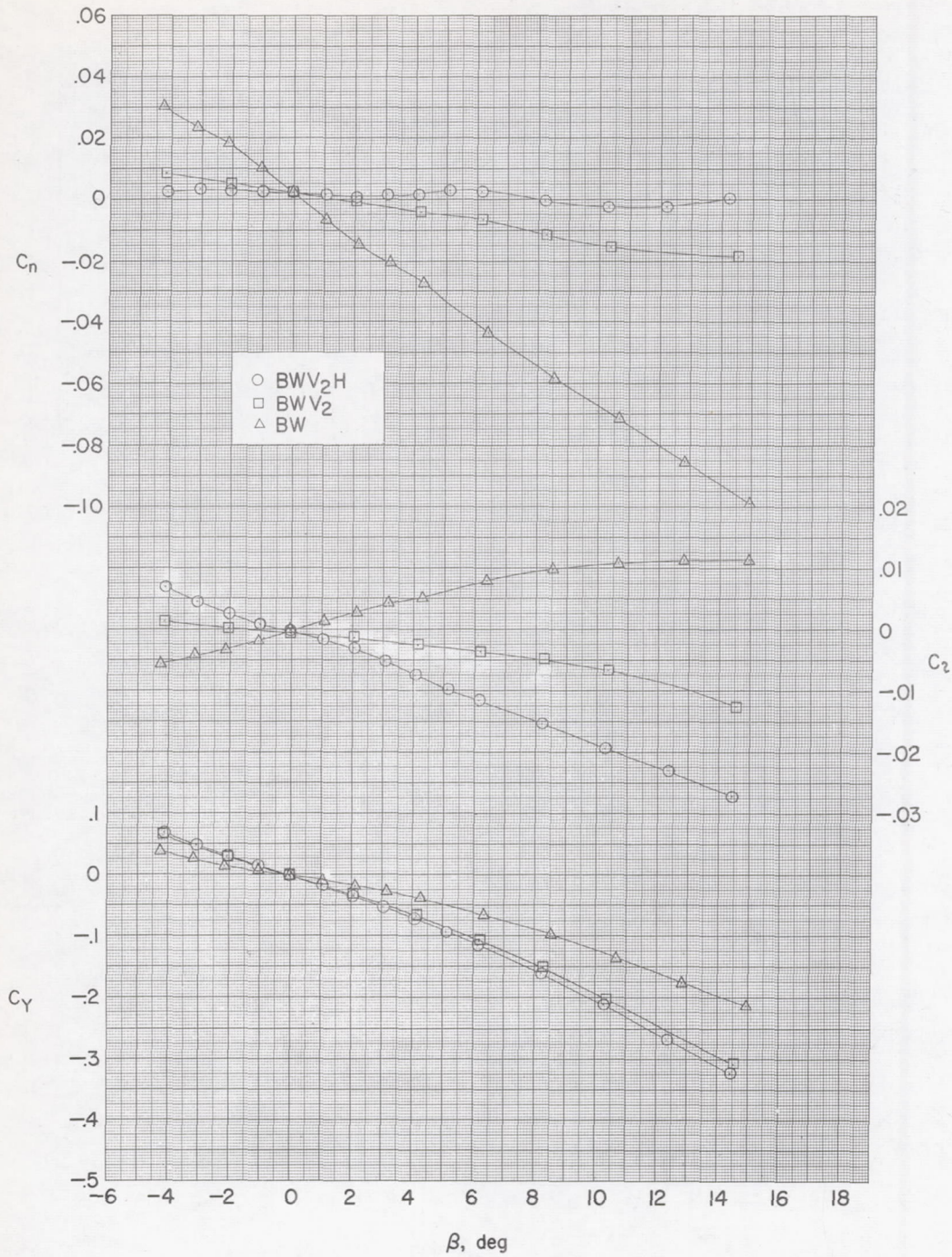

(c) $\alpha \approx 12.8^{\circ}$.

Figure 10.- Continued.

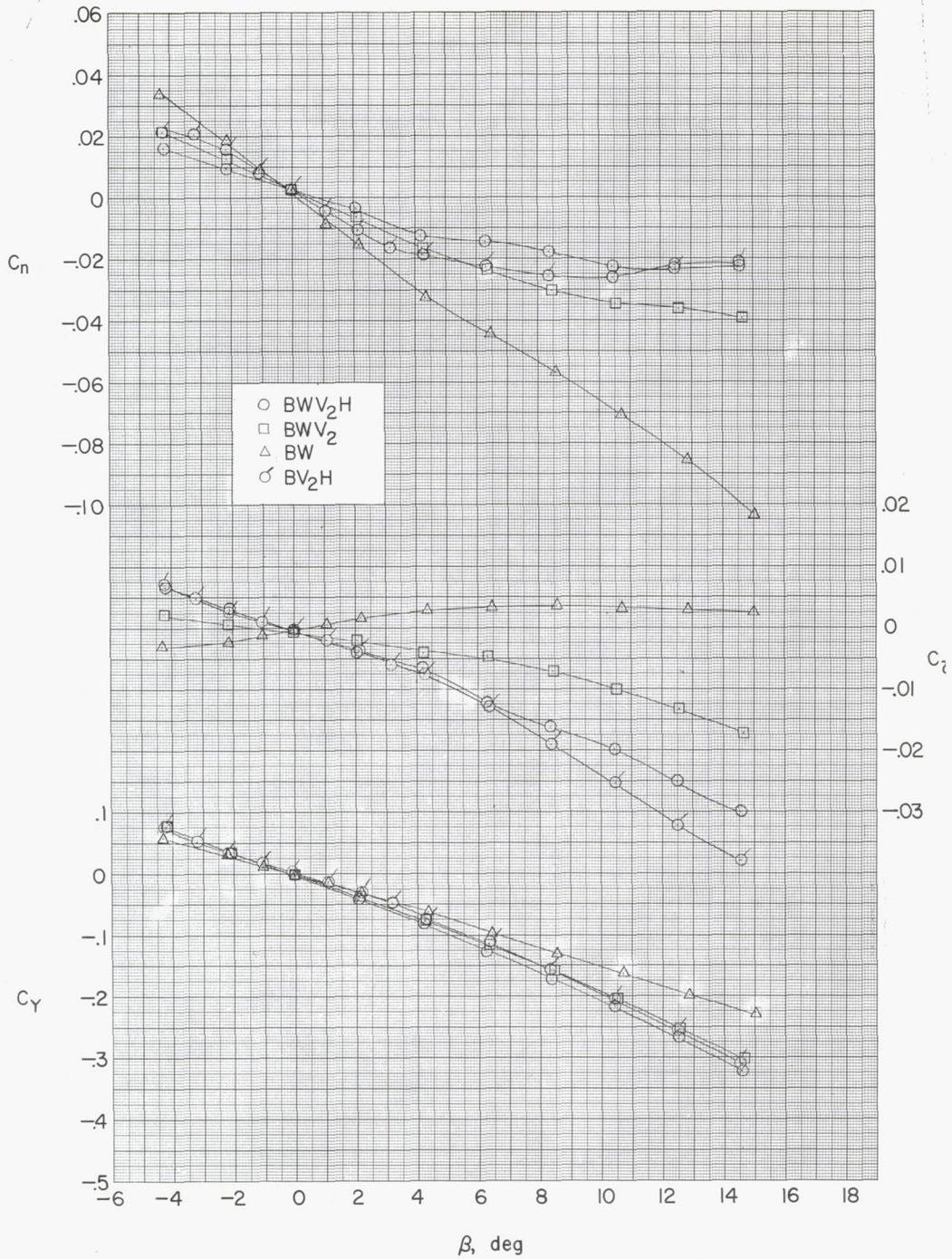

(d) $\alpha \approx 18.2^{\circ}$.

Figure 10.- Concluded.

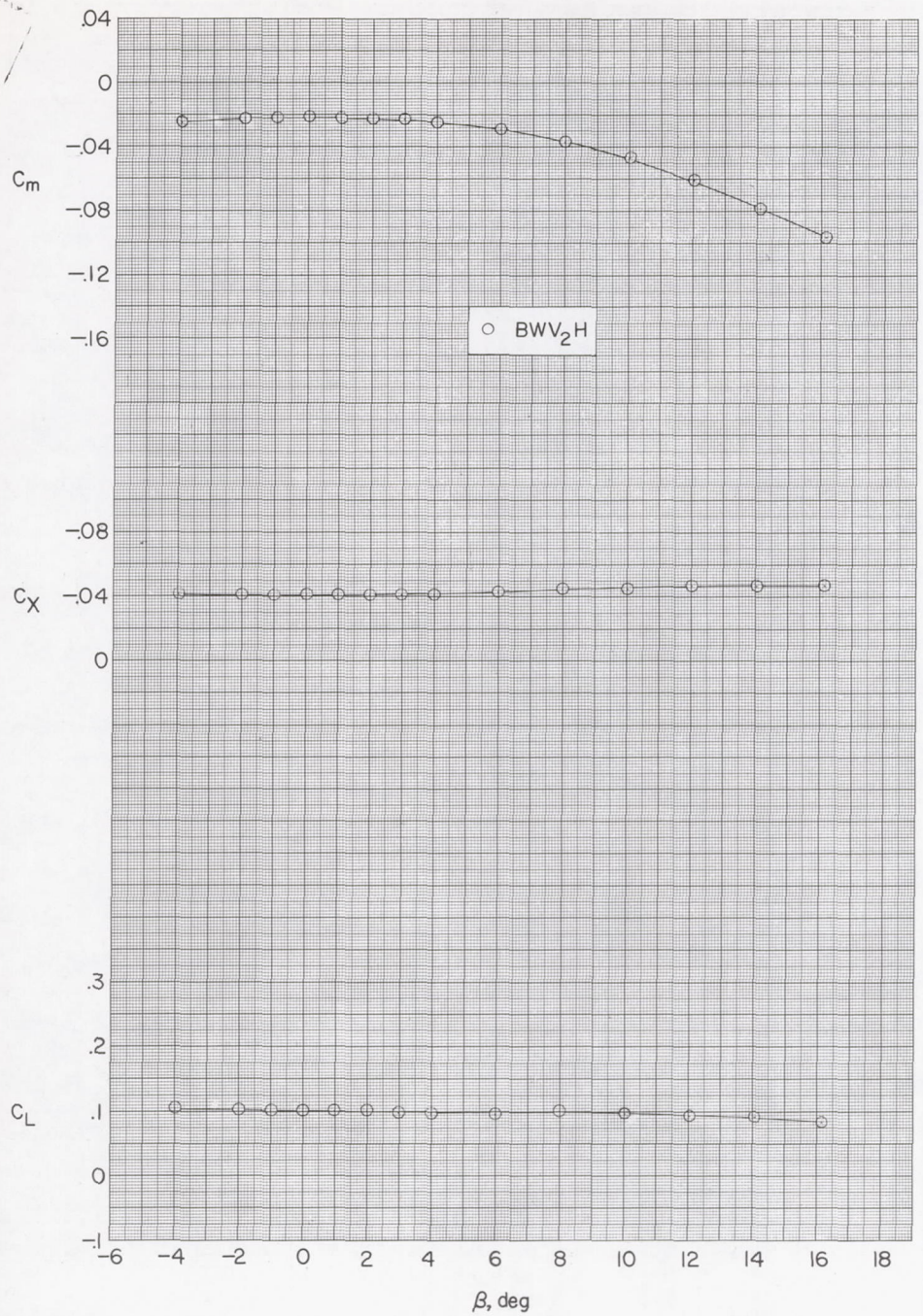

(a) $\alpha \approx 2.4^{\circ}$.

Figure 11.- Effect of component parts on longitudinal characteristics in sideslip at various angles of attack. M = 1.82.

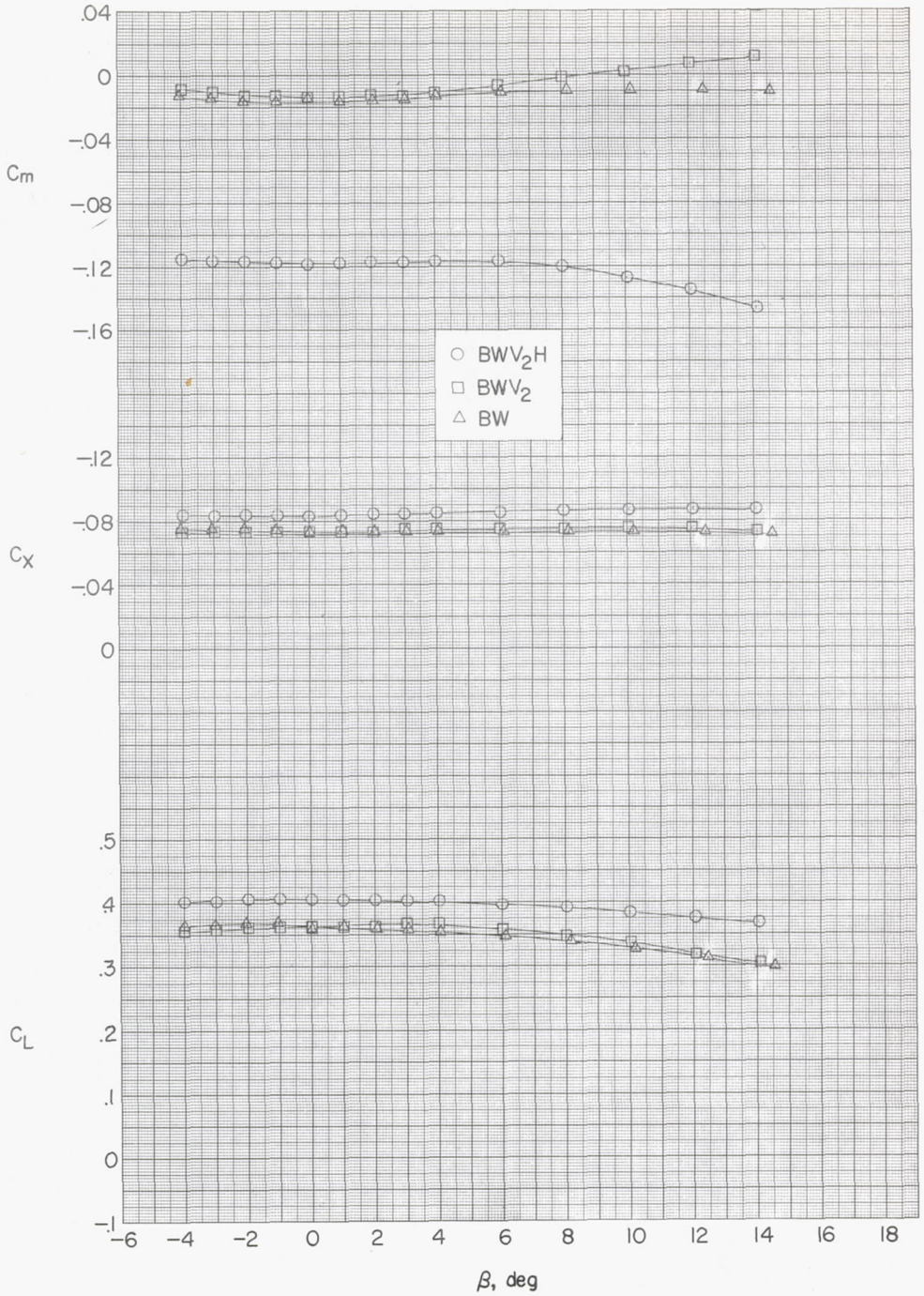

(b) $\alpha \approx 8^{\circ}$.

Figure 11.- Continued.

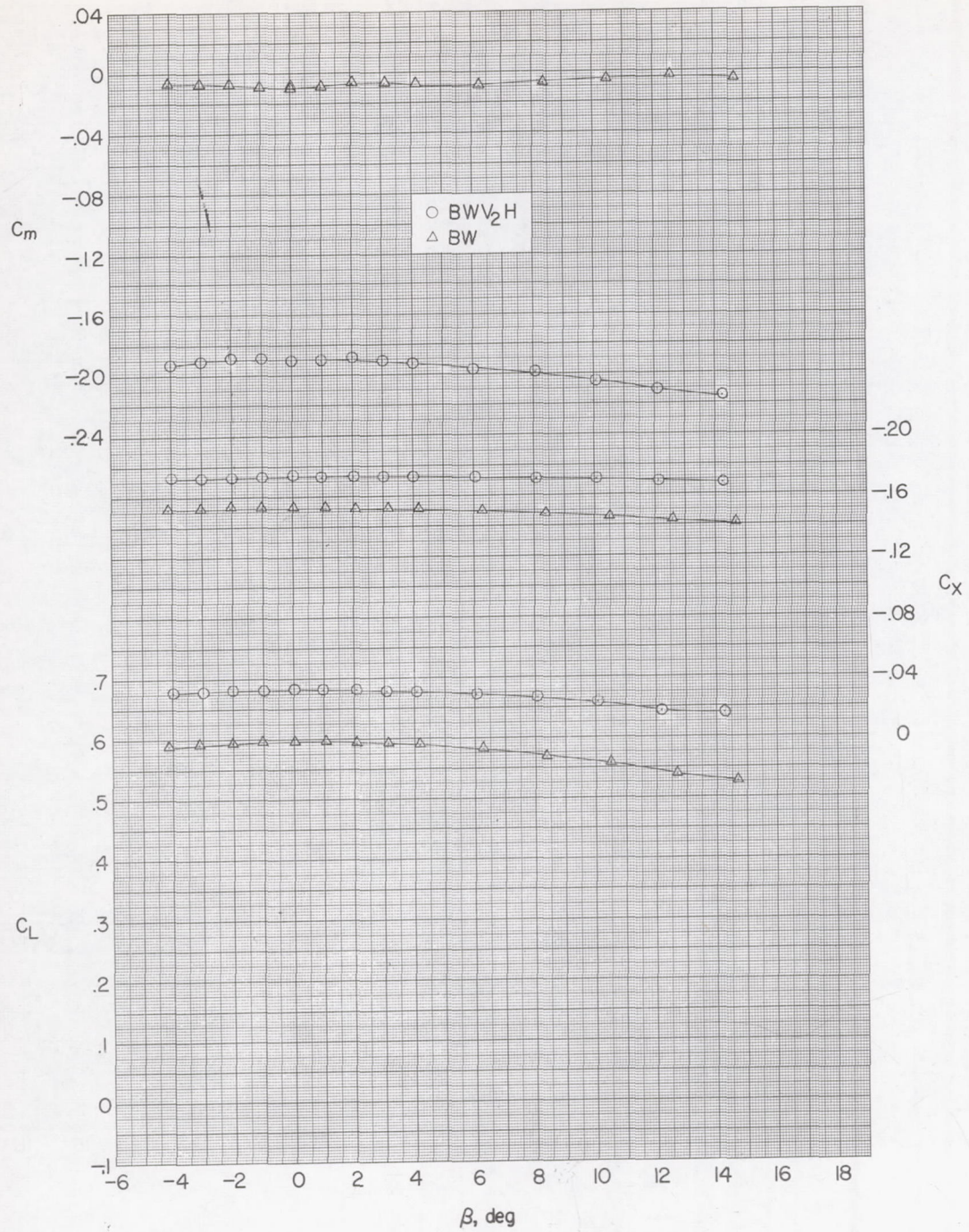

(c) $\alpha \approx 12.7^{\circ}$.

Figure 11.- Concluded.

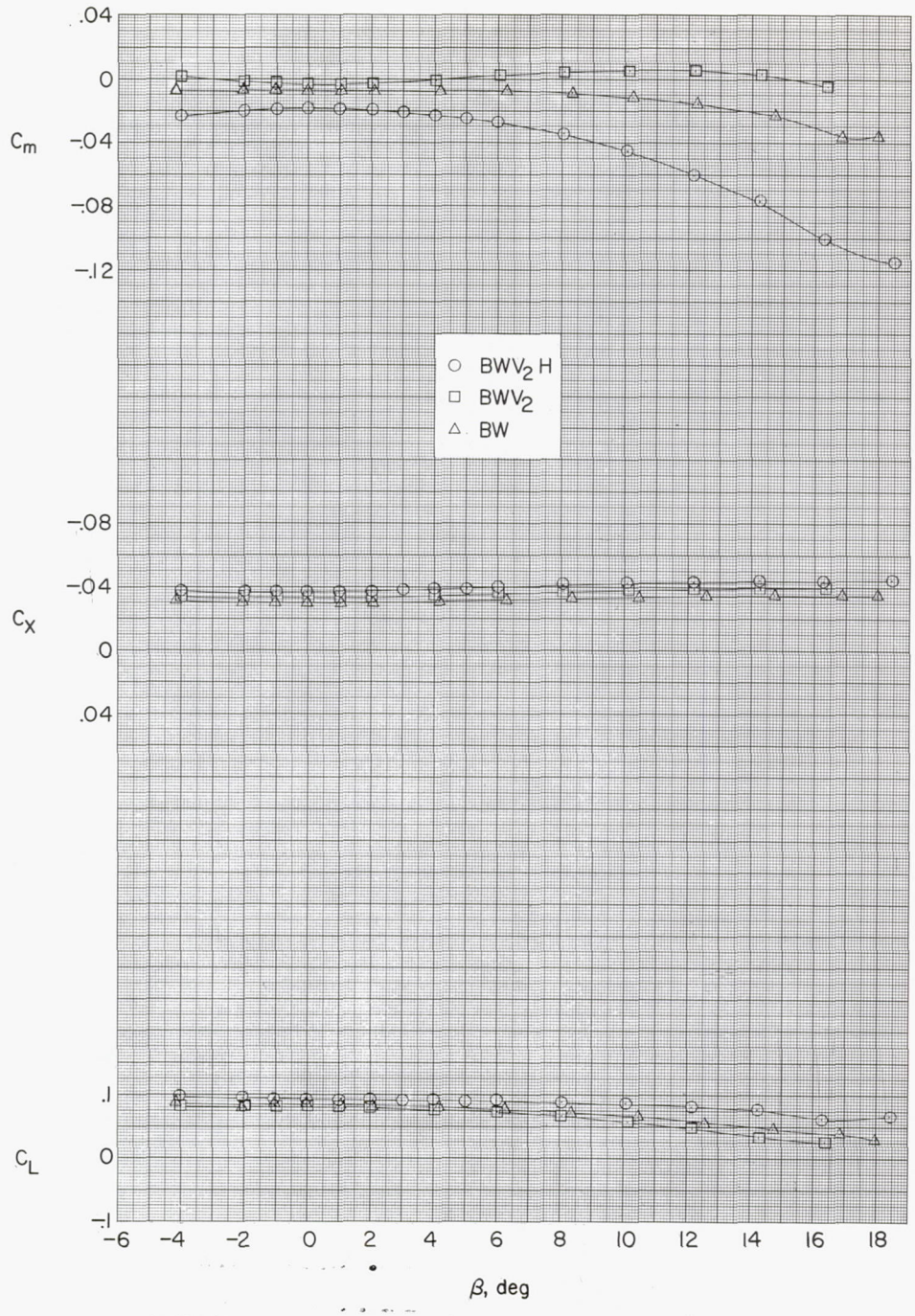

(a) $\alpha \approx 2.4^{\circ}$.

Figure 12.- Effect of component parts on longitudinal characteristics in sideslip at various angles of attack. M = 2.01.

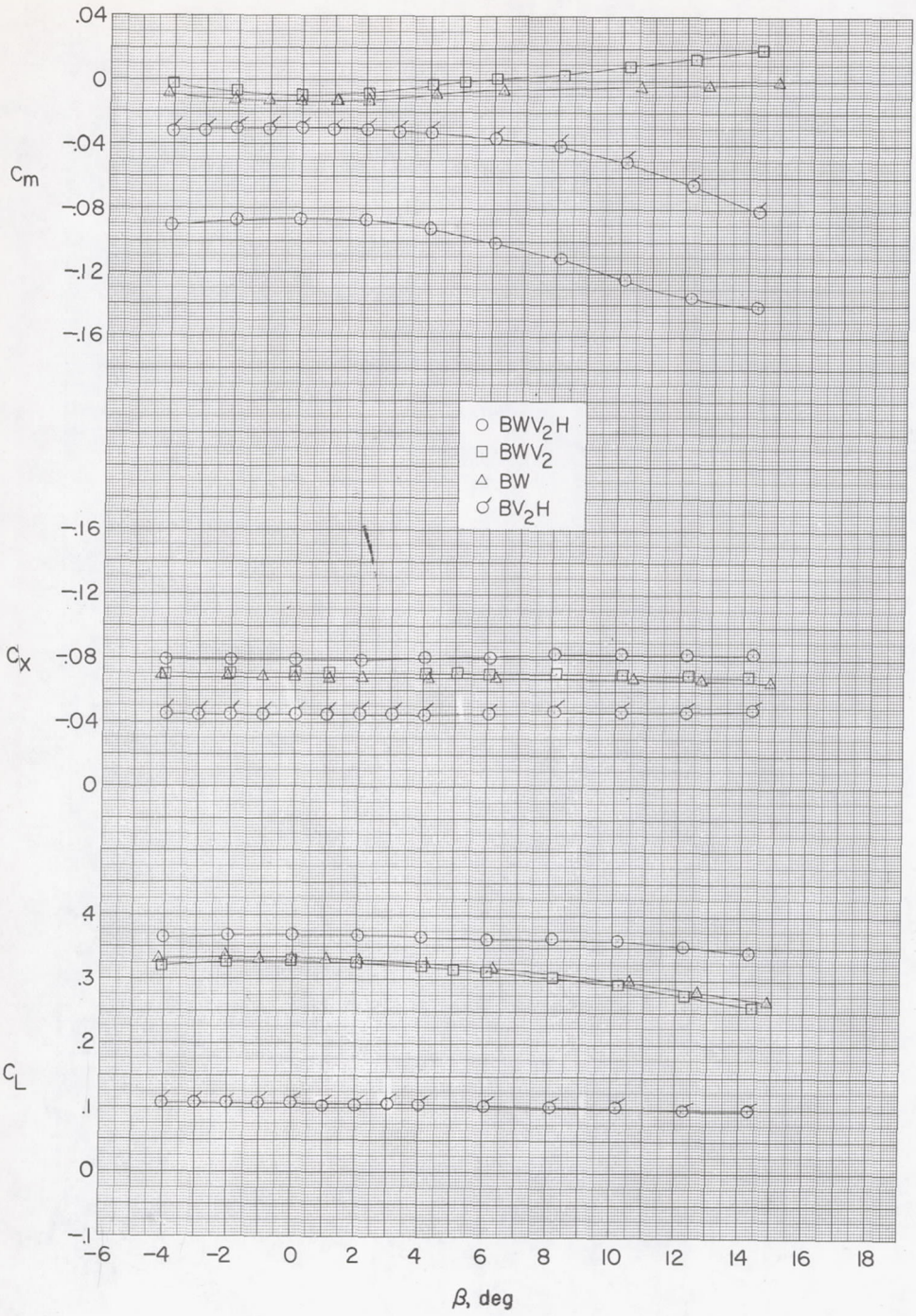

(b) $\alpha \approx 8^{\circ}$.

Figure 12.- Continued.

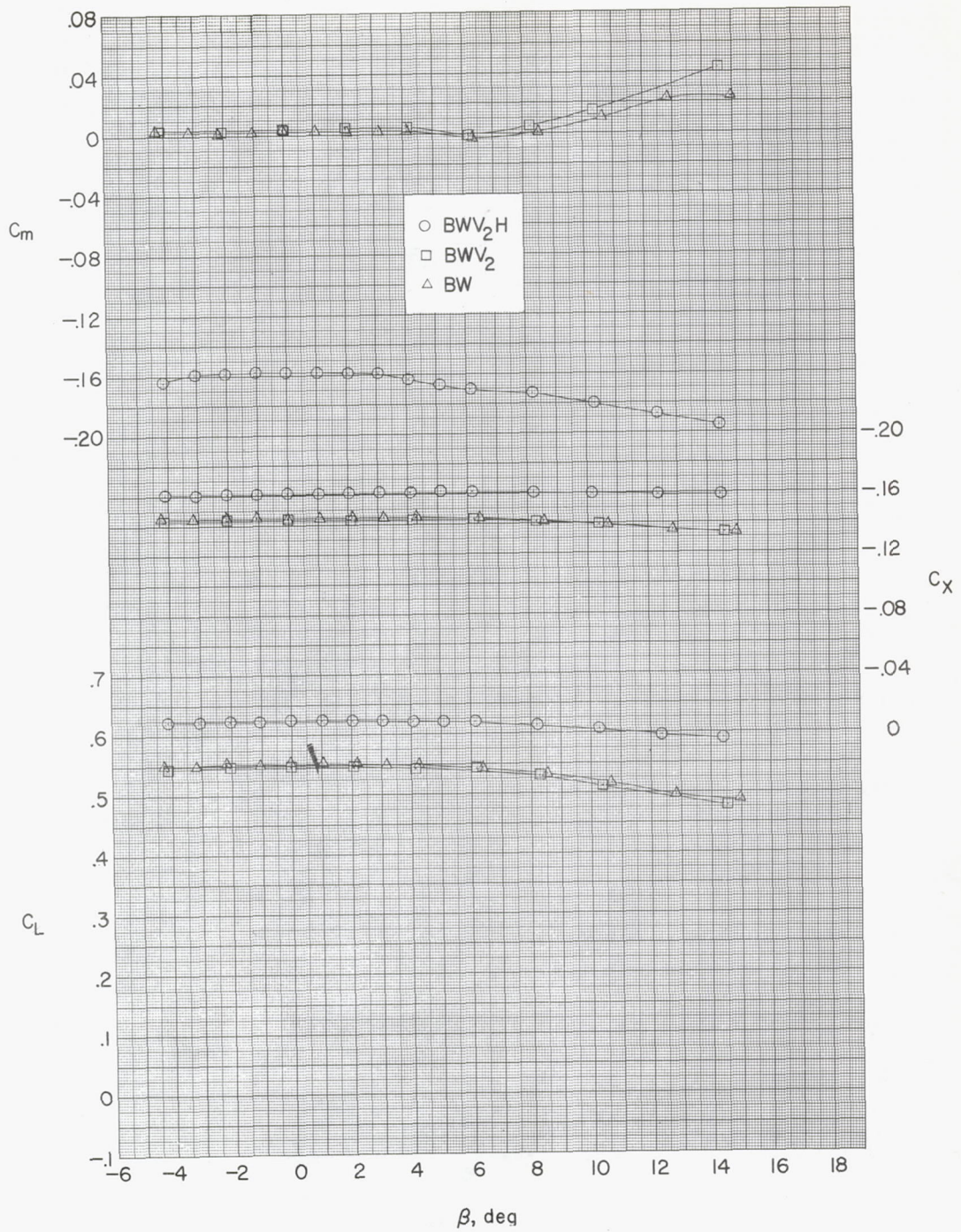

(c) $\alpha \approx 12.8^{\circ}$.

Figure 12.- Continued.

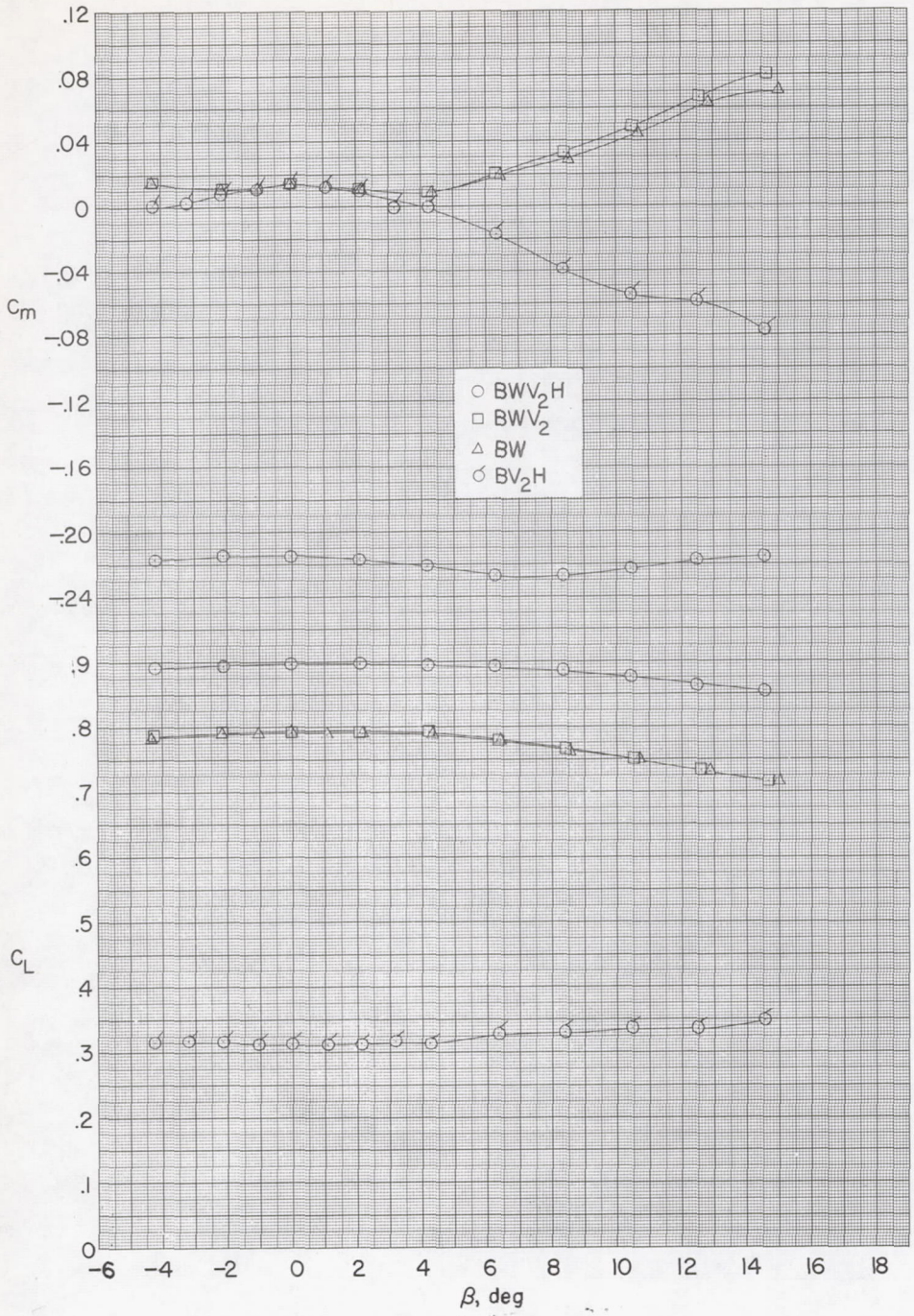

(d) $\alpha \approx 18.2^{\circ}$.

Figure 12.- Continued.

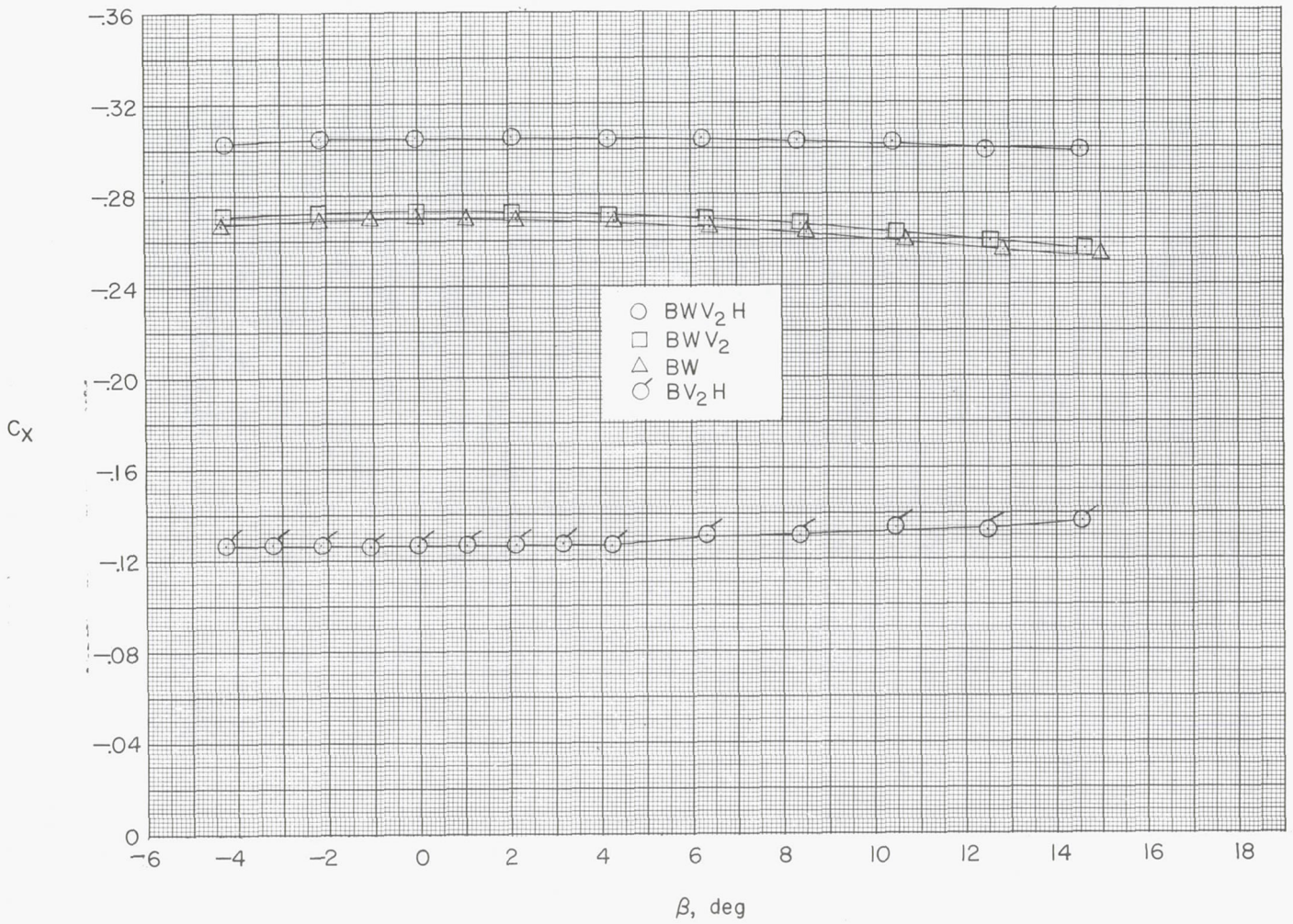

(d) Concluded.

Figure 12.- Concluded.

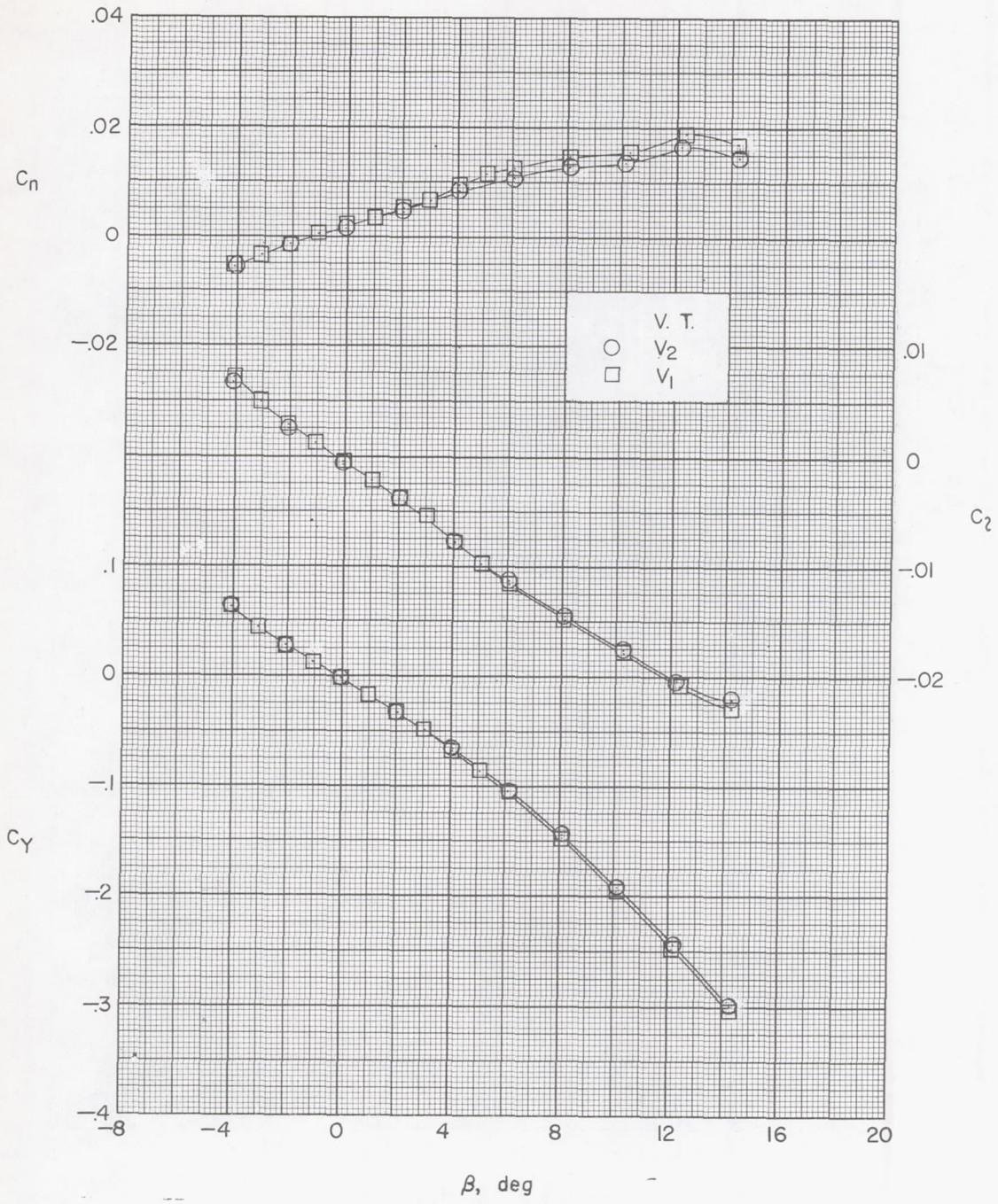

(a) $\alpha \approx 8^{\circ}$.

Figure 13.- Effect of vertical-tail section on the aerodynamic characteristics in sideslip at various angles of attack. Horizontal tail on; M = 2.01.

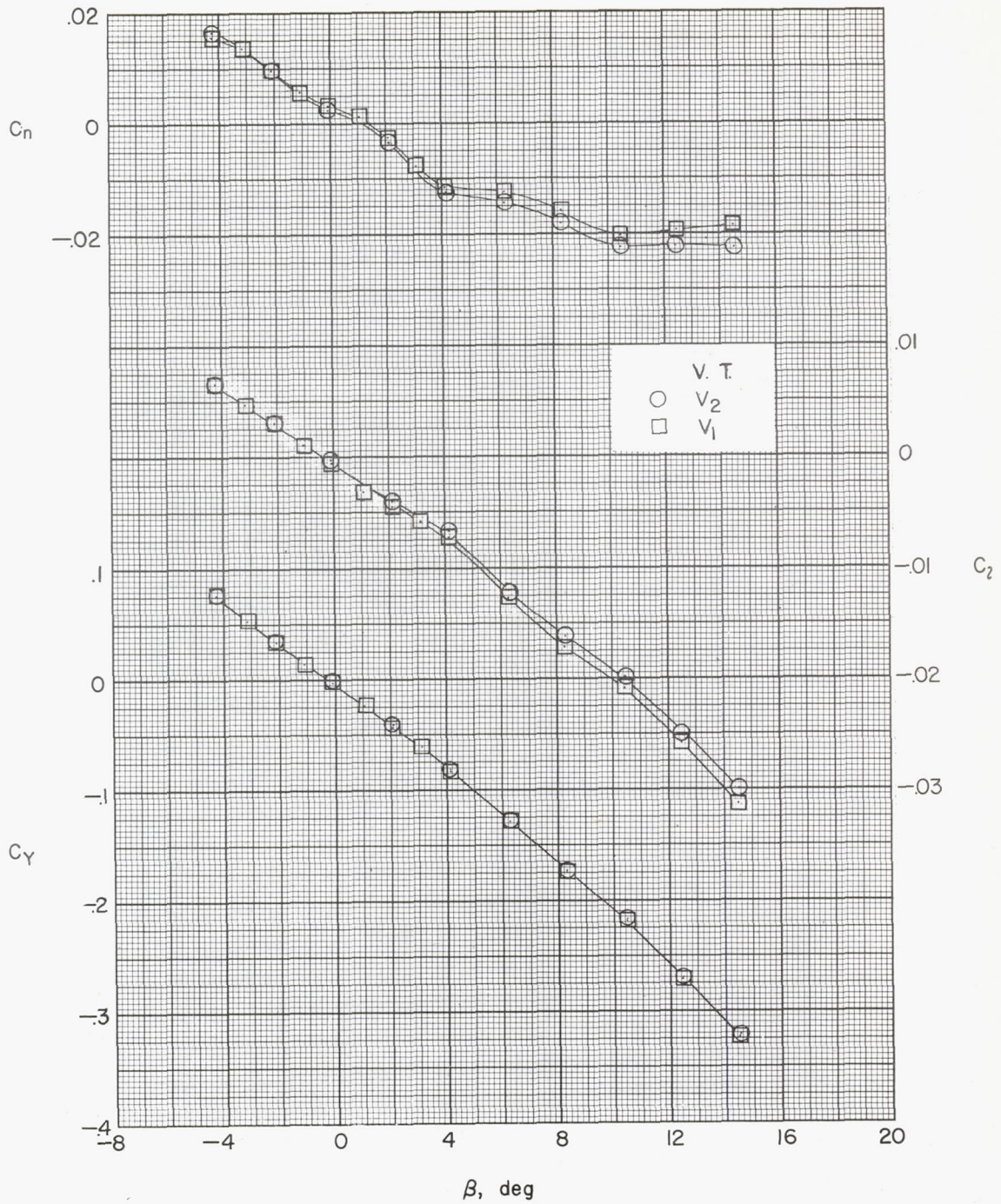

(b) $\alpha \approx 18.2^{\circ}$.

Figure 13.- Concluded.

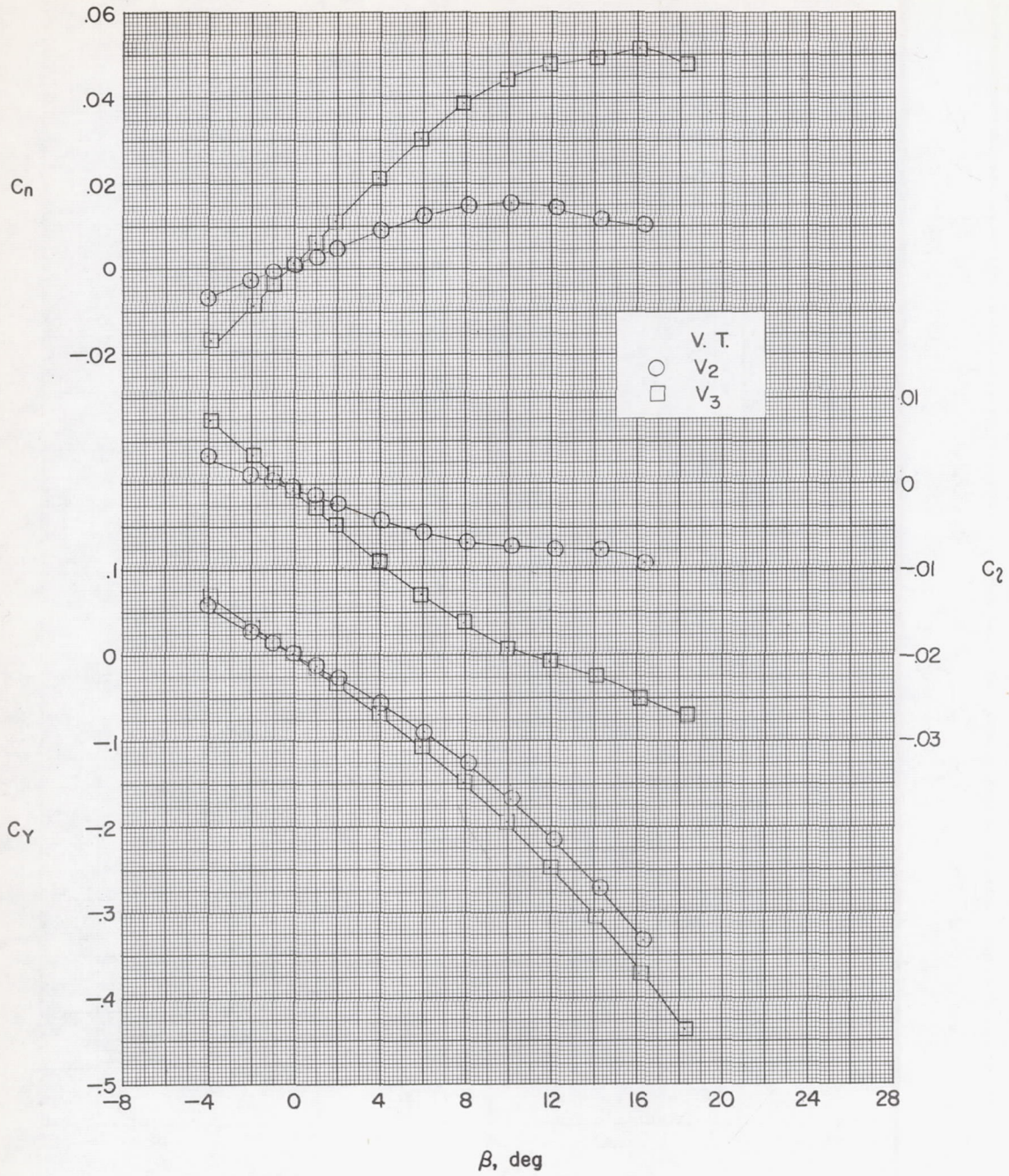

(a) $\alpha \approx 2.4^\circ$.

Figure 14.- Effect of vertical-tail plan form on the aerodynamic characteristics in sideslip at various angles of attack. Horizontal tail off; M = 2.01.

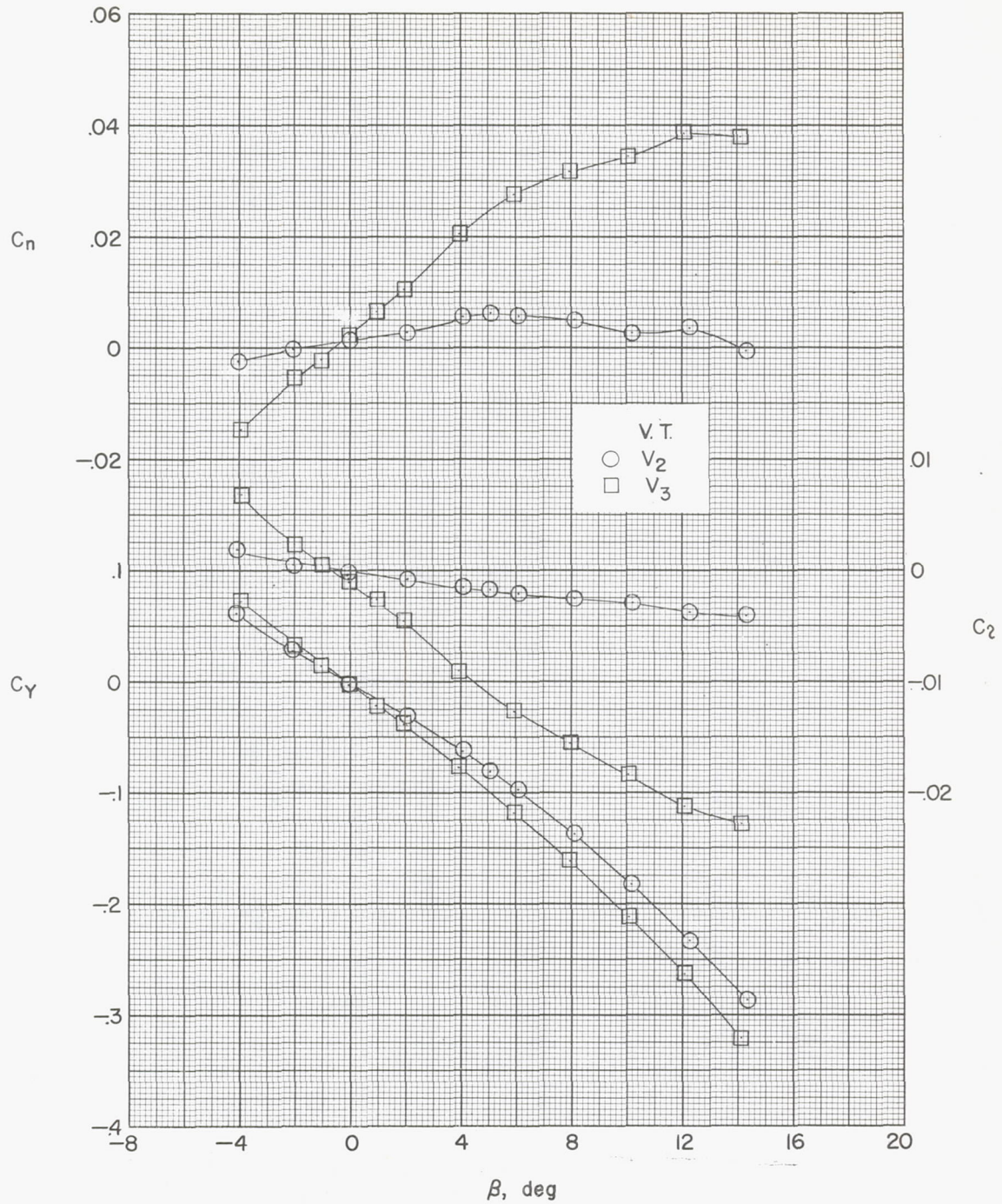

(b) $\alpha \approx 8^\circ$.

Figure 14.- Continued.

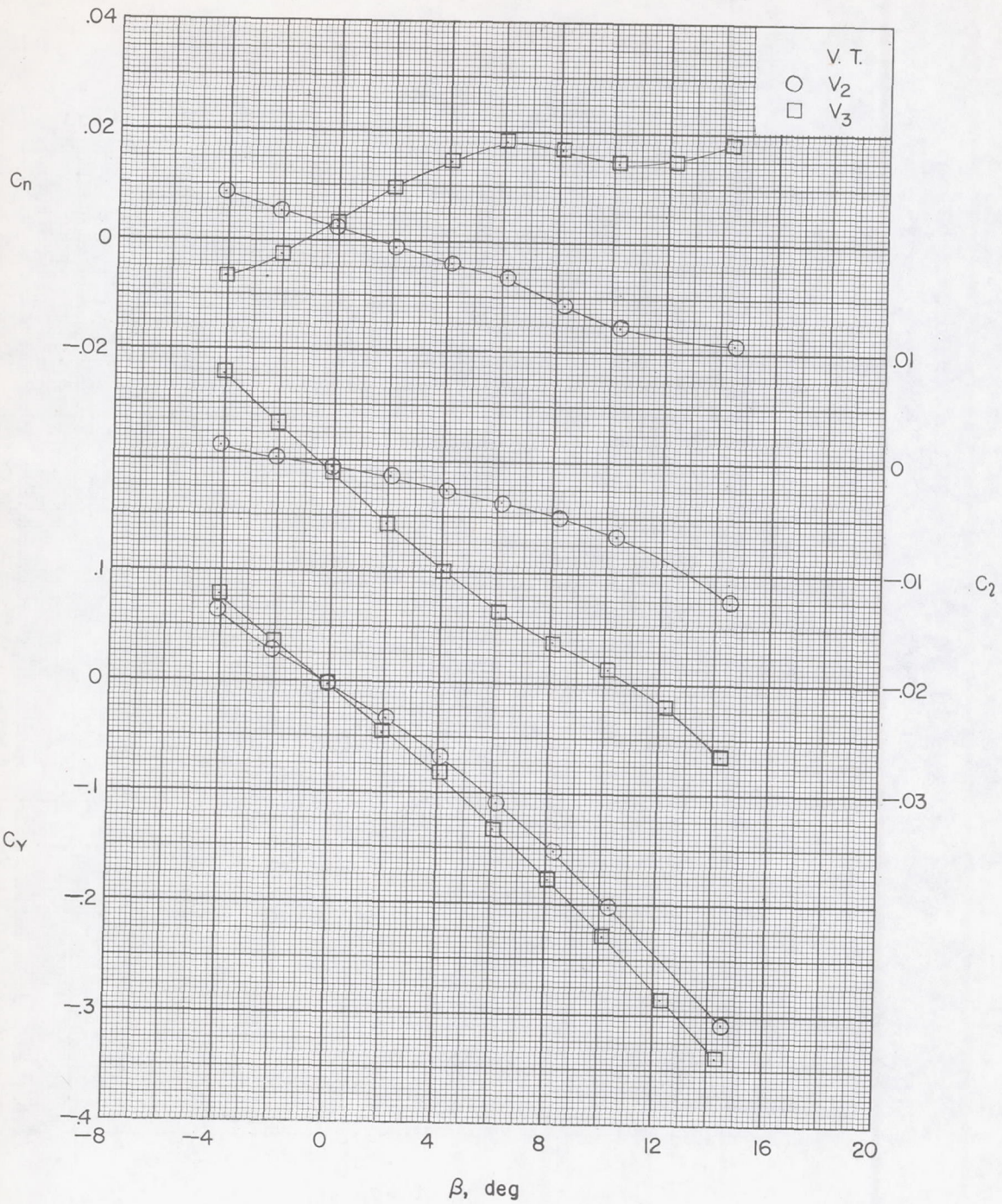

(c) $\alpha \approx 12.8^{\circ}$.

Figure 14.- Continued.

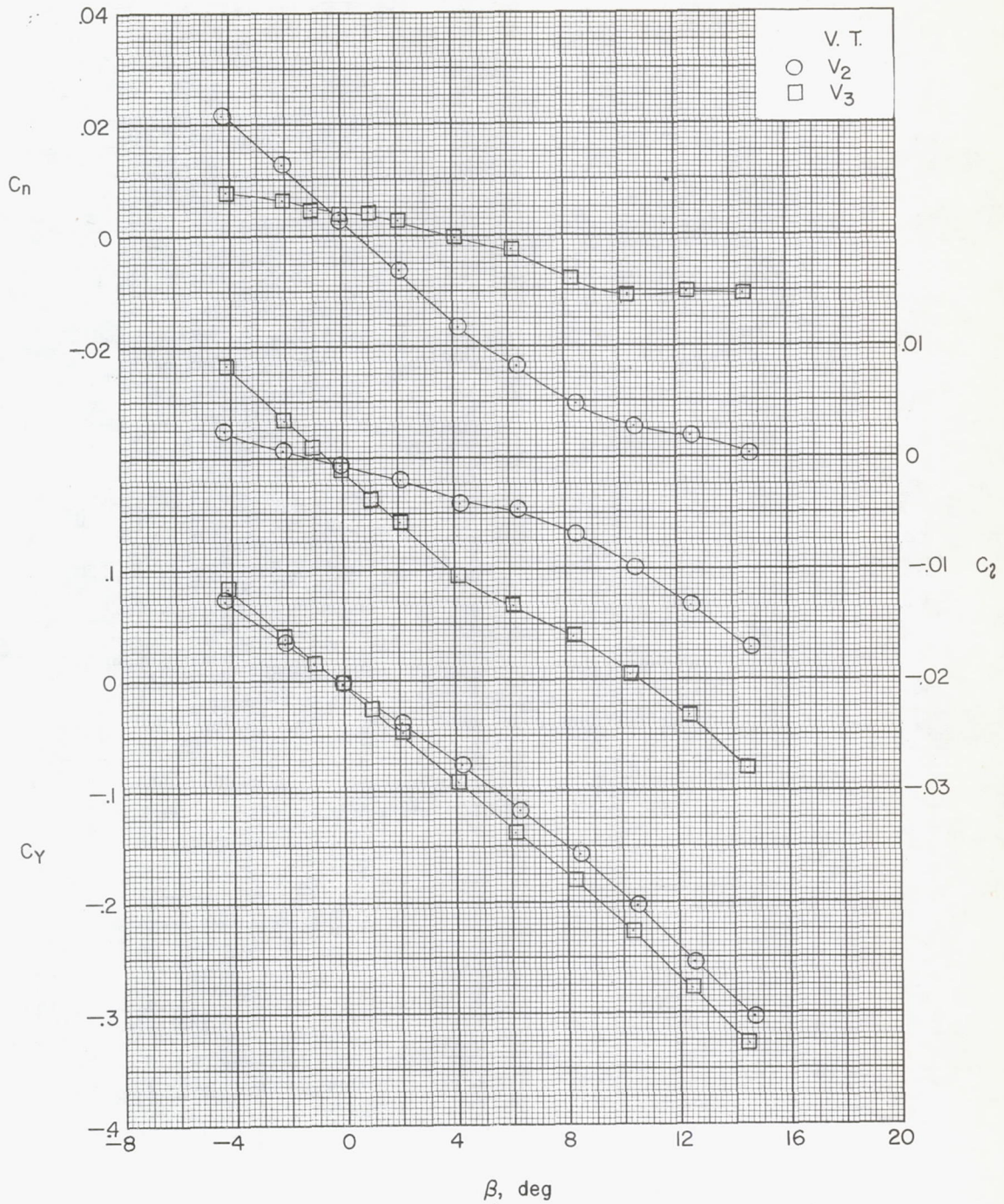

(d) $\alpha \approx 18.3^{\circ}$.

Figure 14.- Concluded.

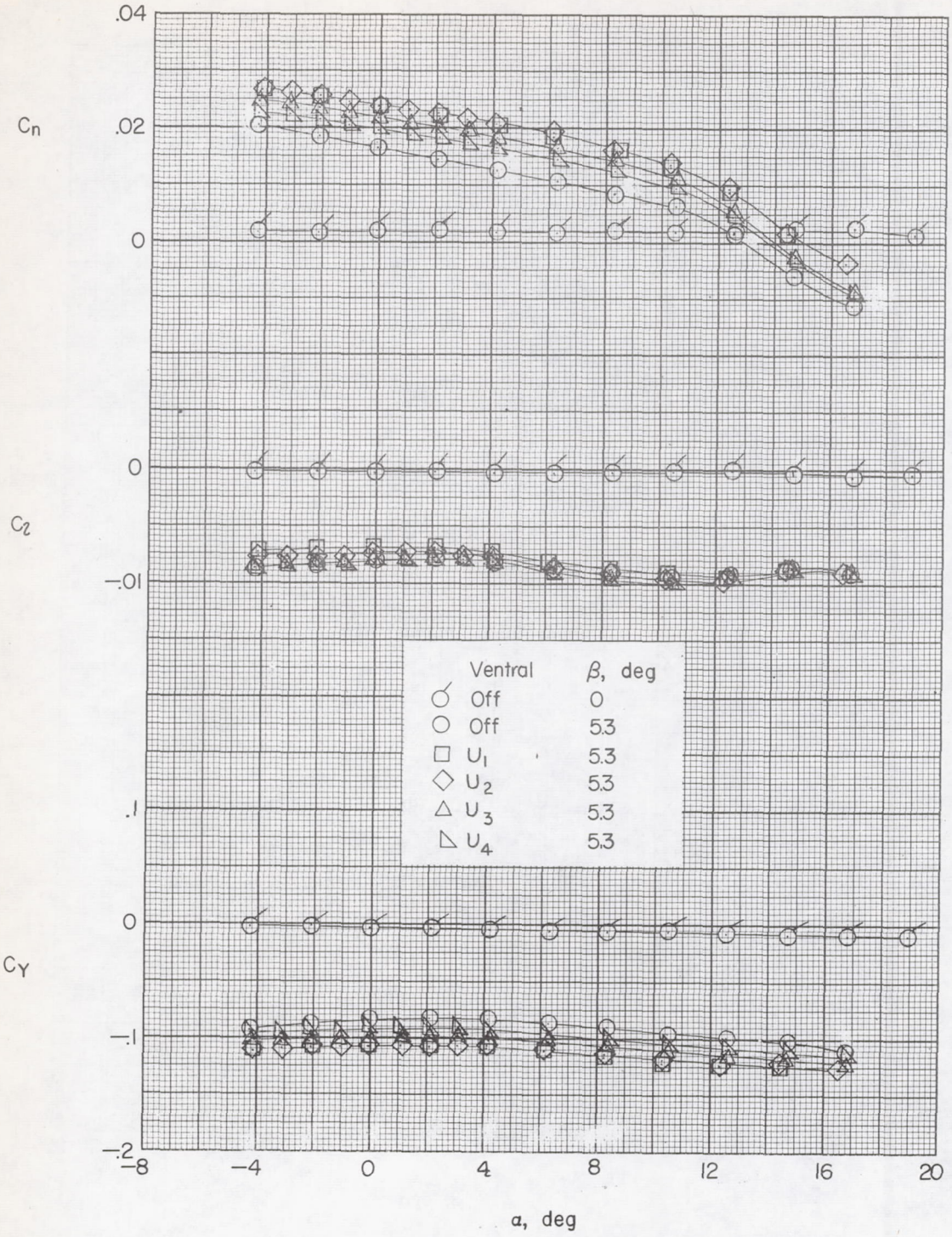

Figure 15.- Effect of ventral fins on the lateral and directional characteristics in pitch. M = 2.01.

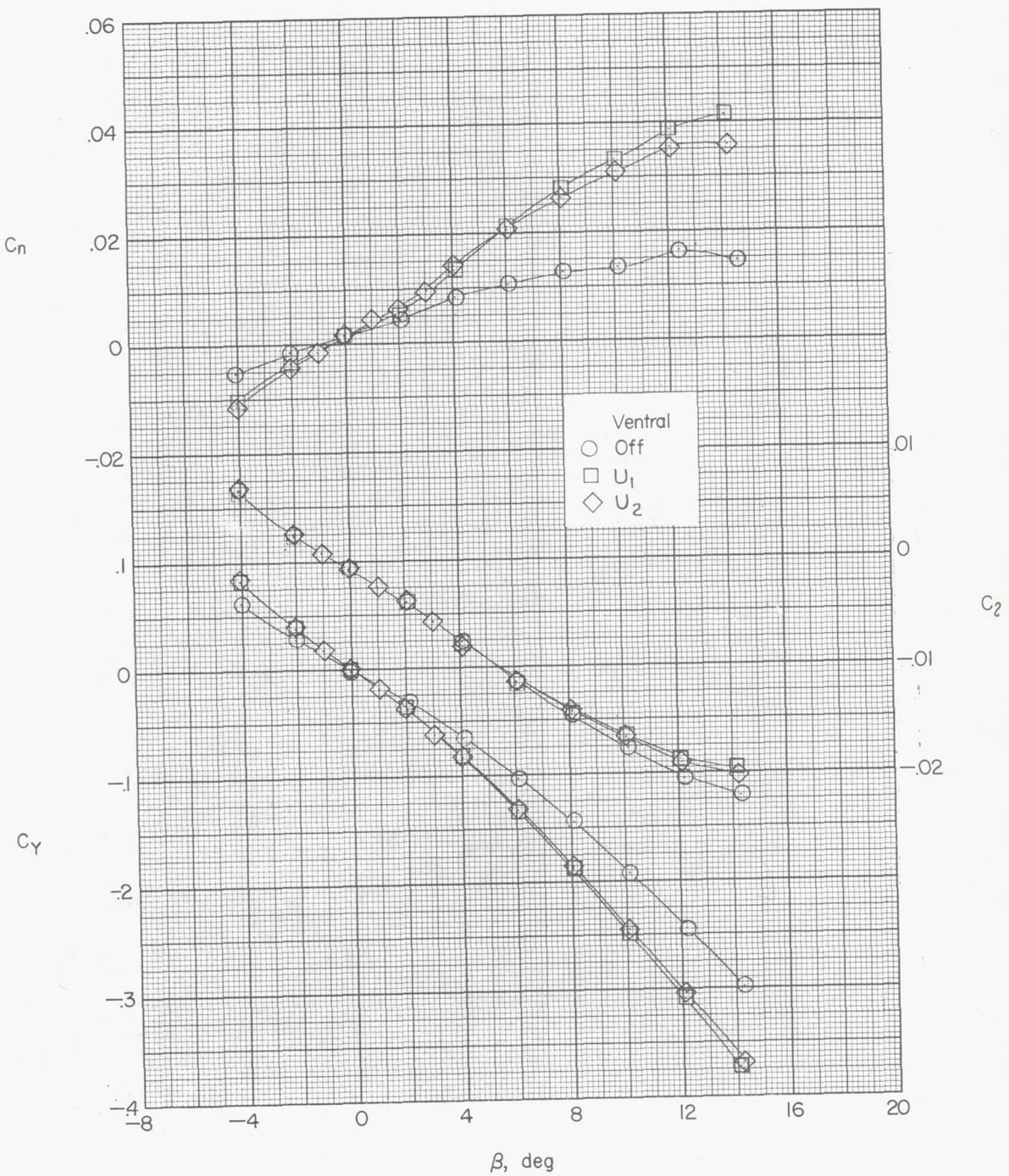

Figure 16.- Effect of ventral fins on the aerodynamic characteristics in sideslip. $\alpha \approx 8^{\circ}$; M = 2.01.

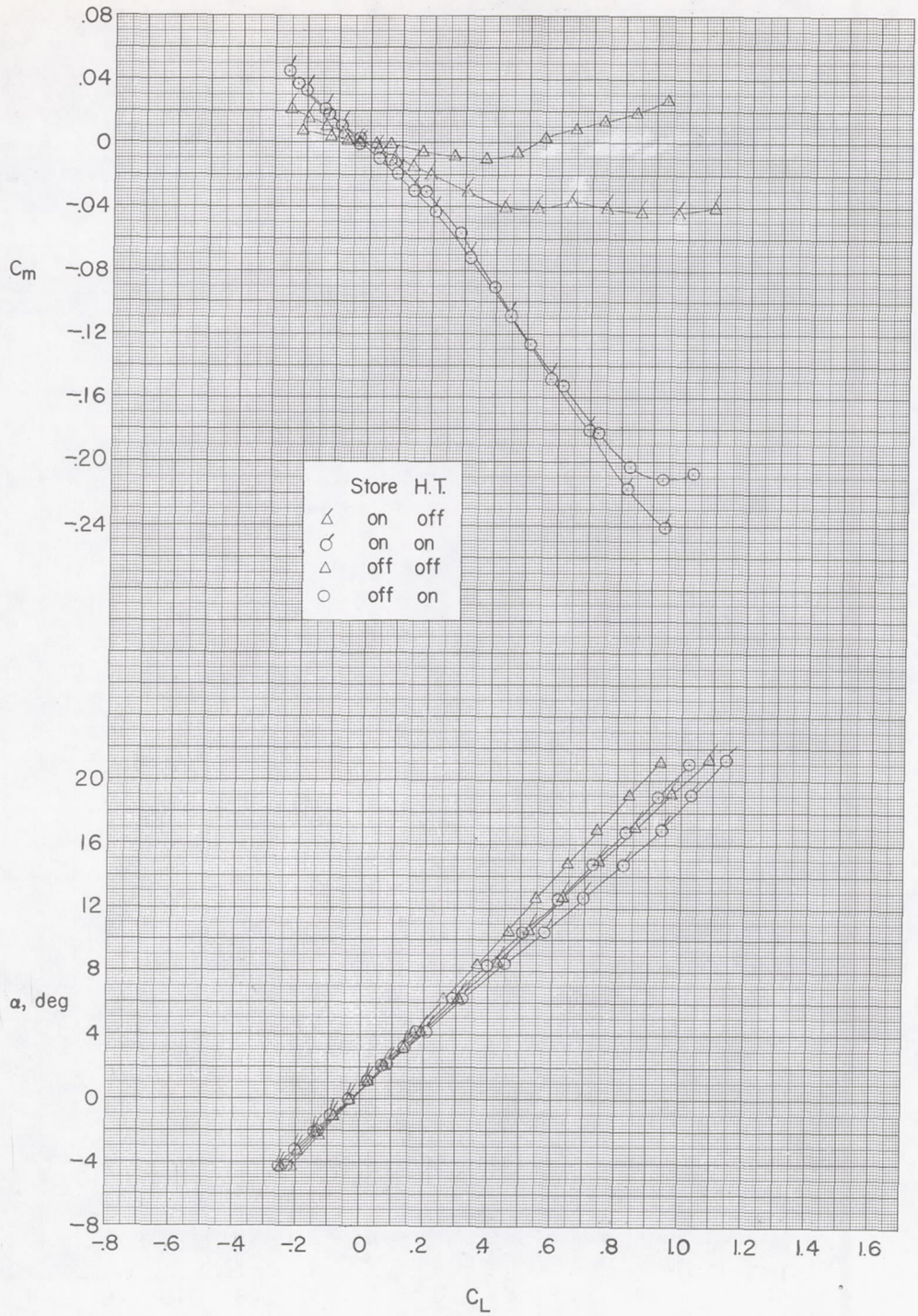

Figure 17.- Effect of tip-mounted tanks (T_1) on the aerodynamic characteristics in pitch. M = 2.01.

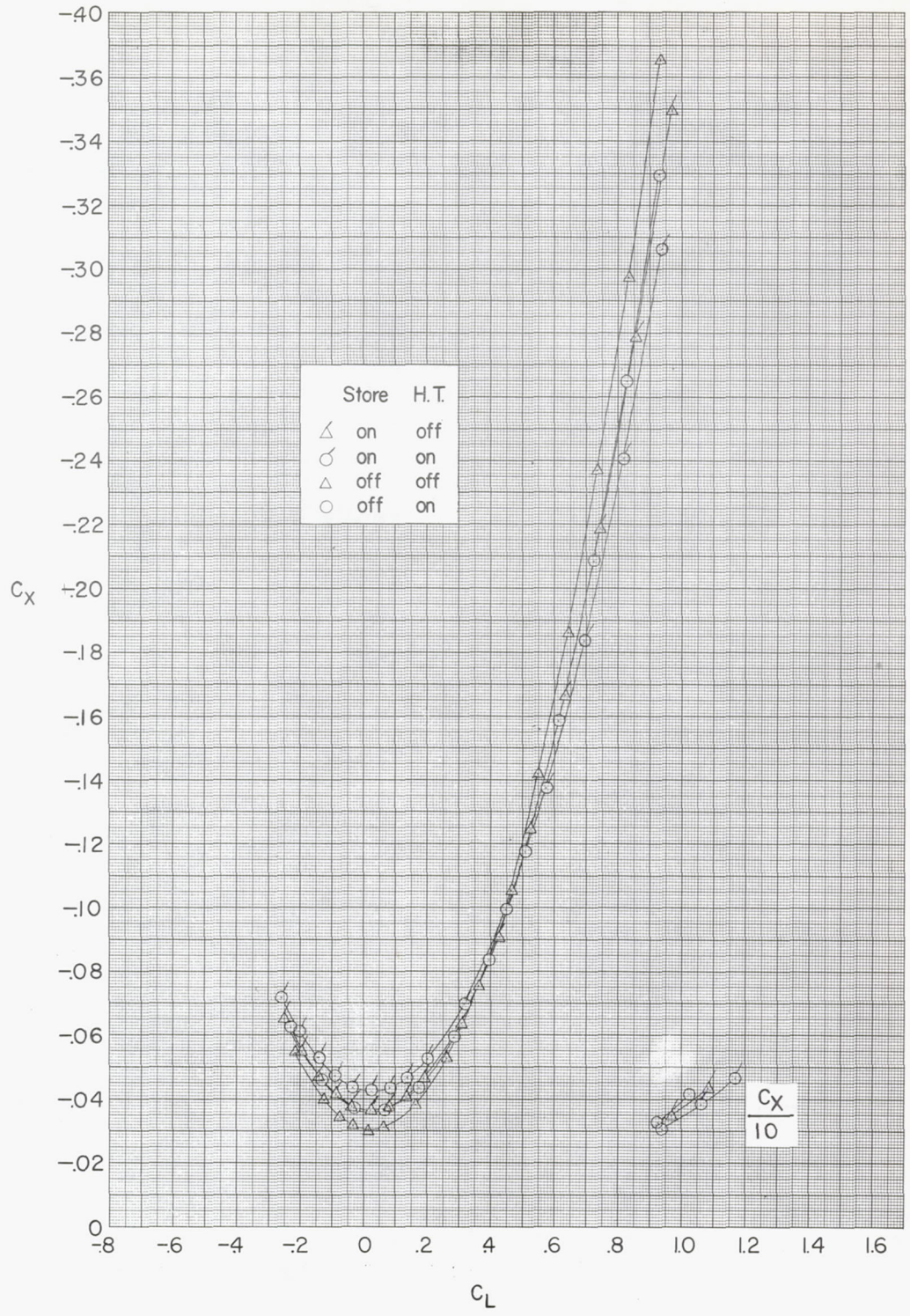

Figure 17.- Concluded.

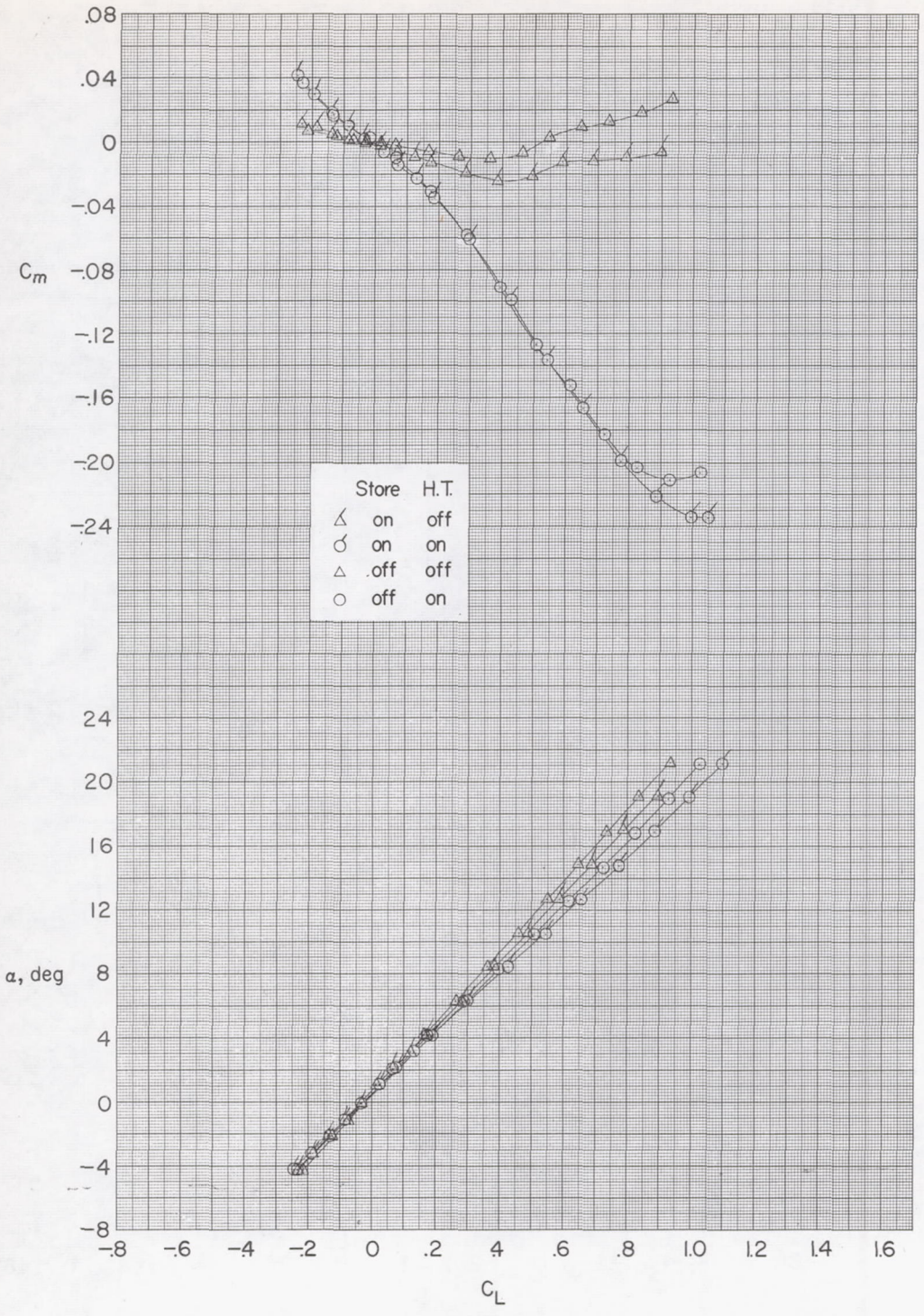

Figure 18.- Effect of two tip-mounted Sidewinder missiles (M_9) on the aerodynamic characteristics in pitch. M = 2.01.

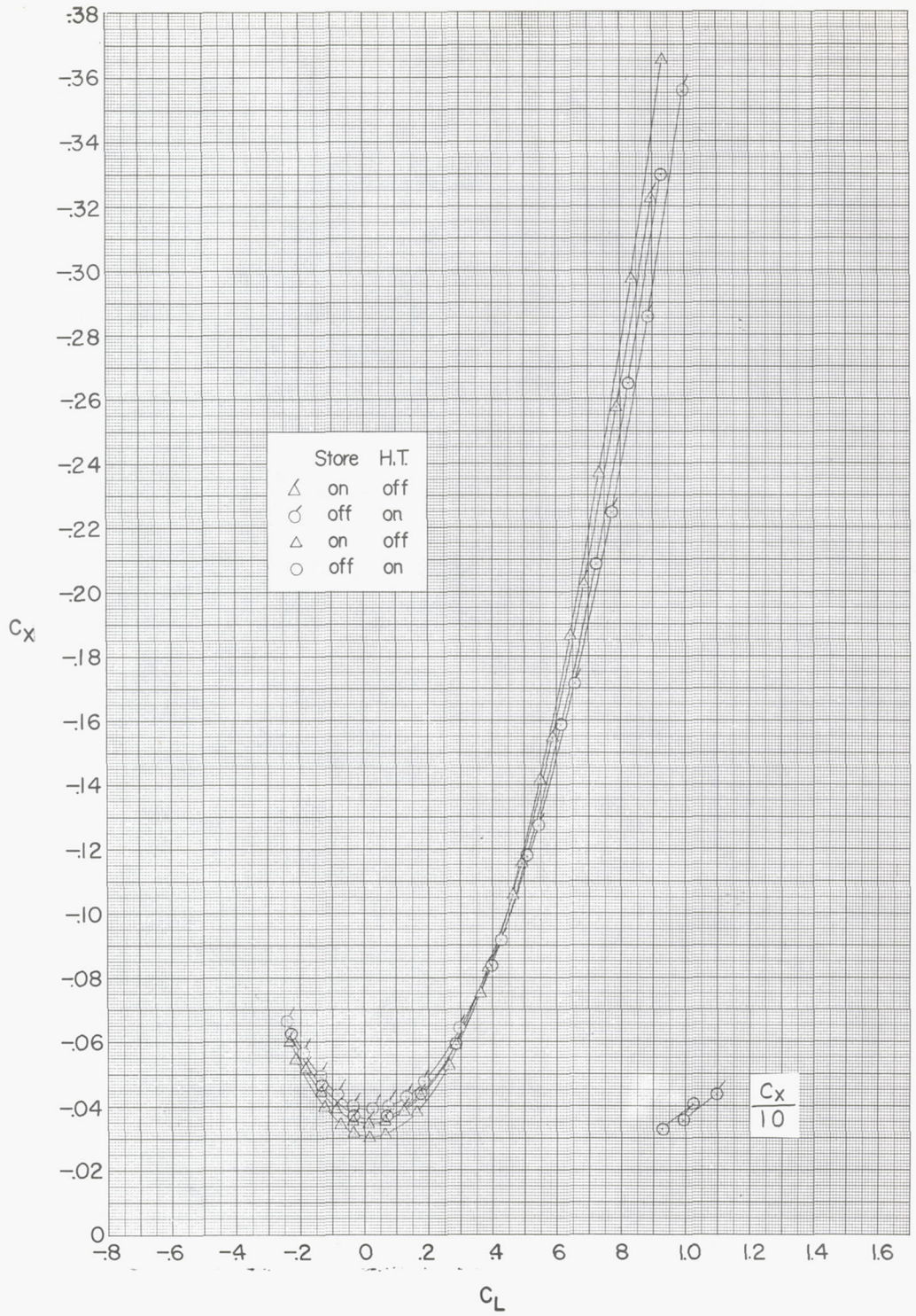

Figure 18.- Concluded.

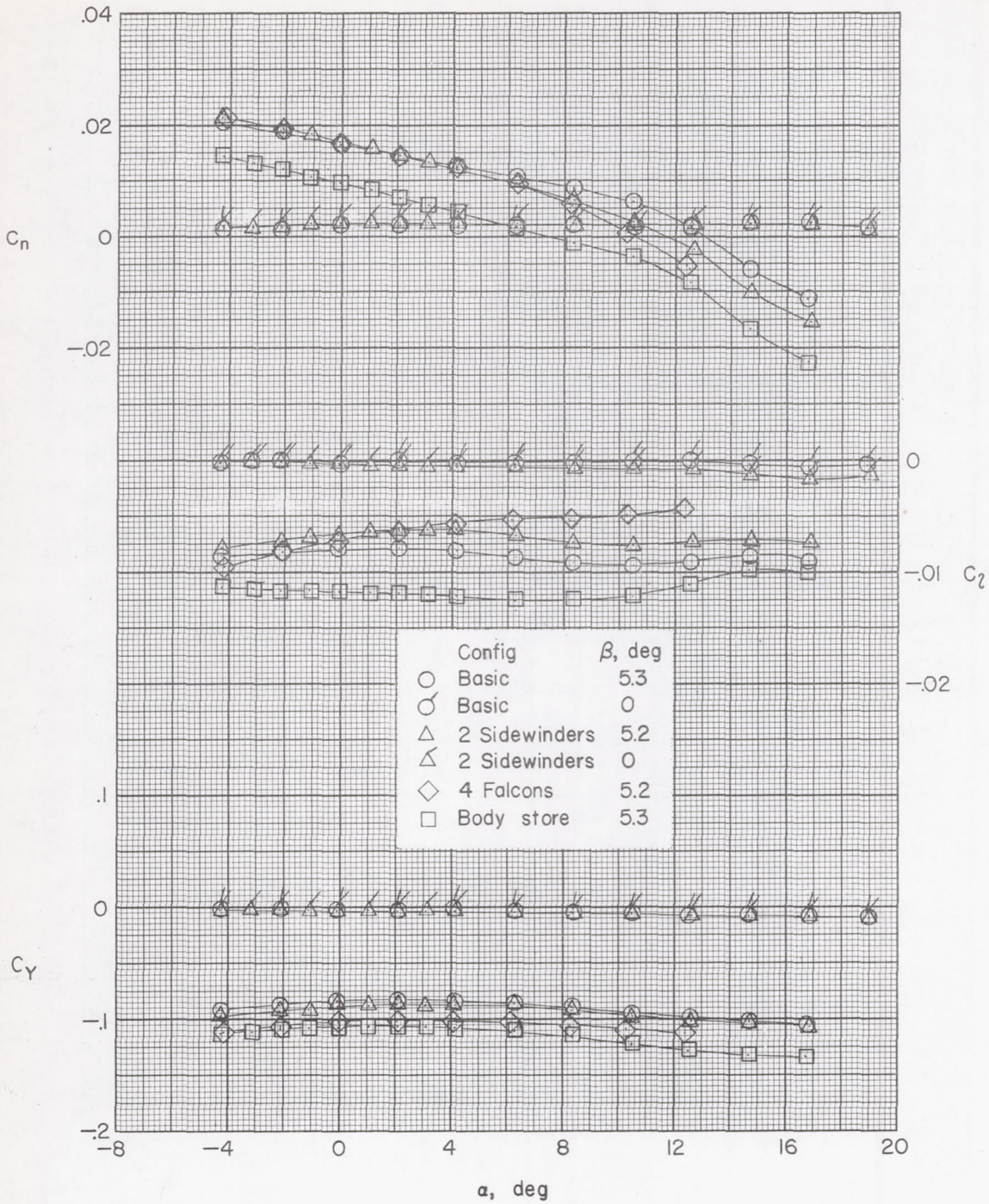

Figure 19.- Effects of various store arrangements on the lateral and directional characteristics in pitch. M = 2.01.

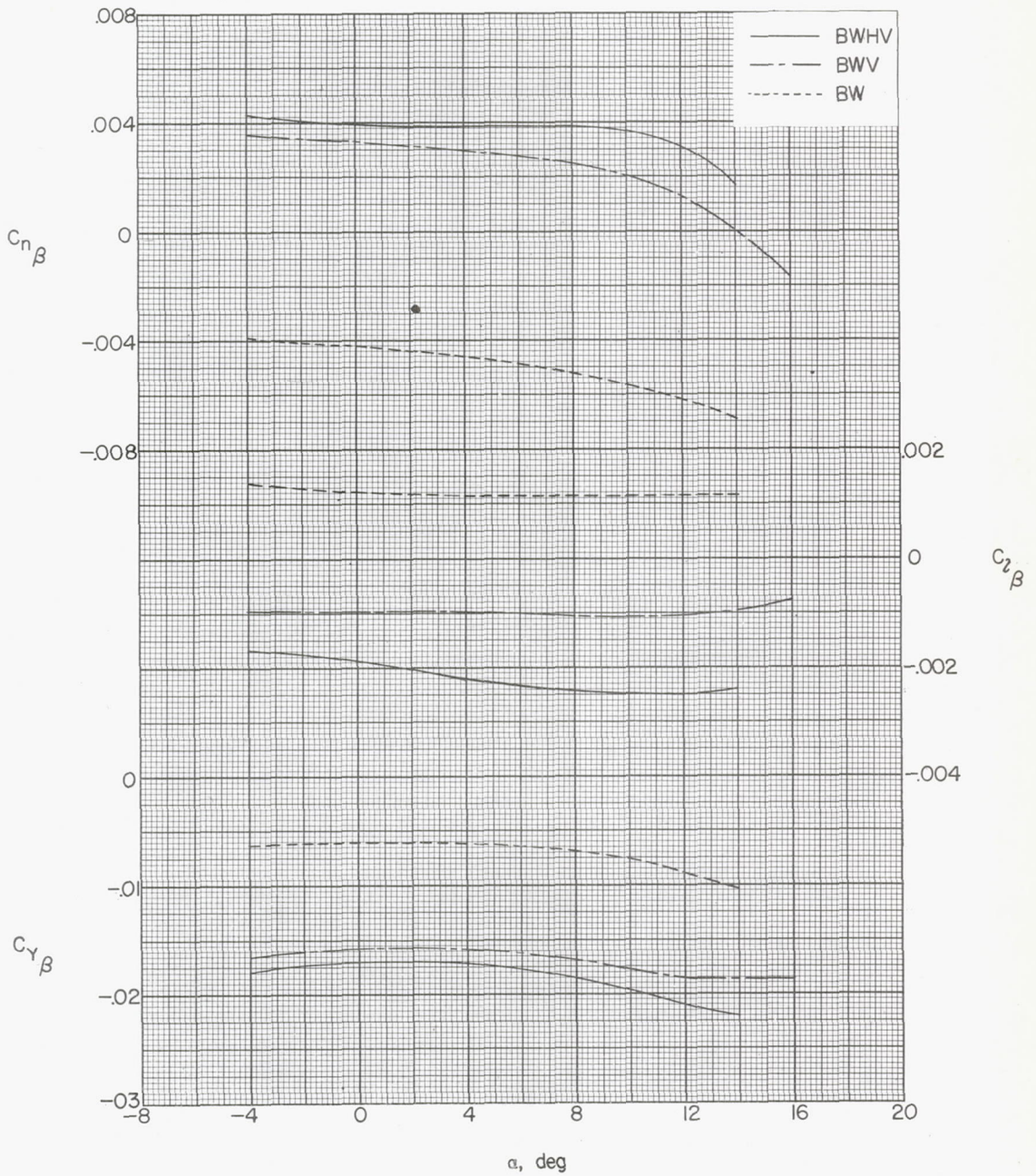

Figure 20.- Effects of component parts on sideslip derivatives. M = 1.82.

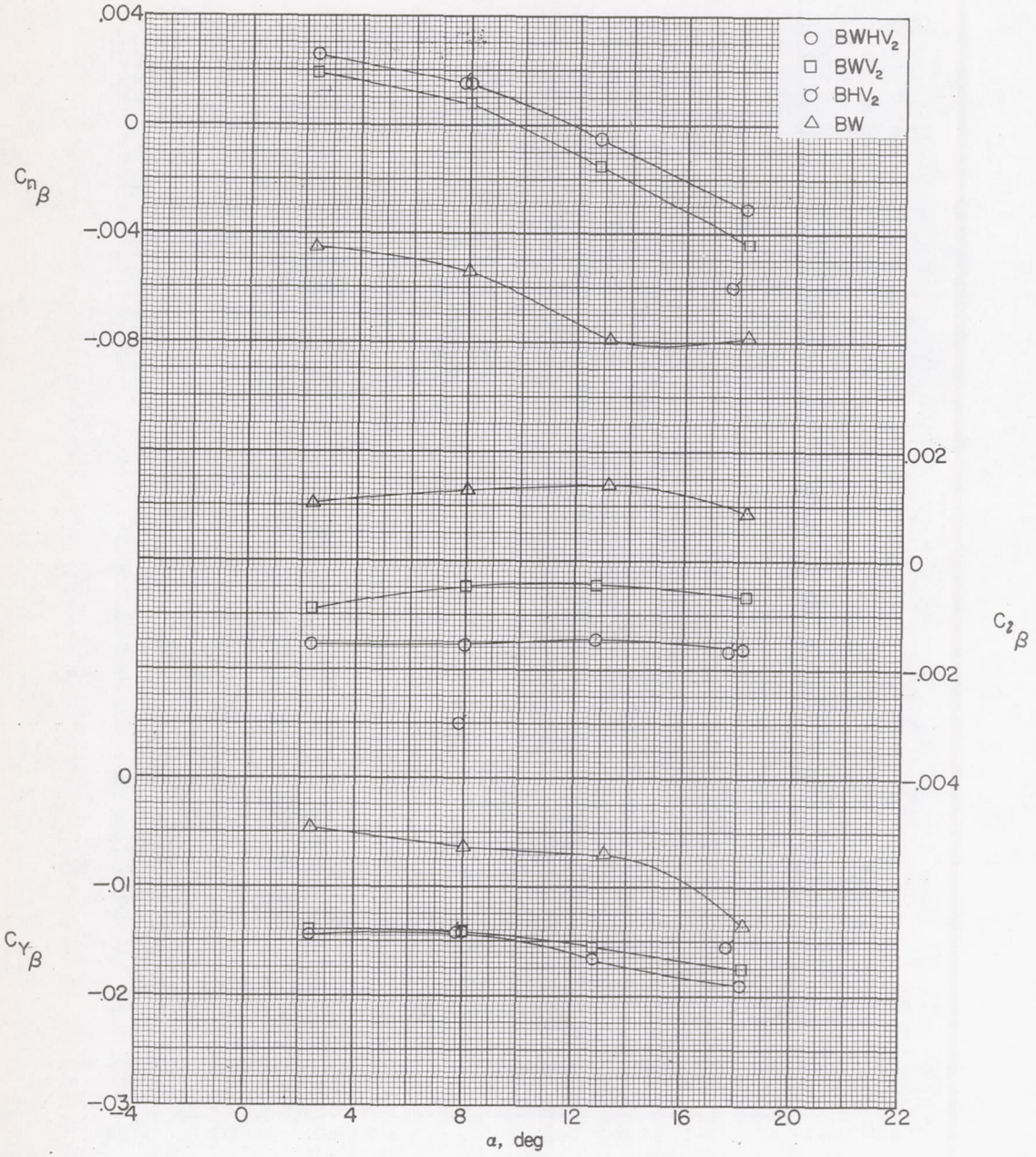

Figure 21.- Effects of component parts on sideslip derivatives. M = 2.01.

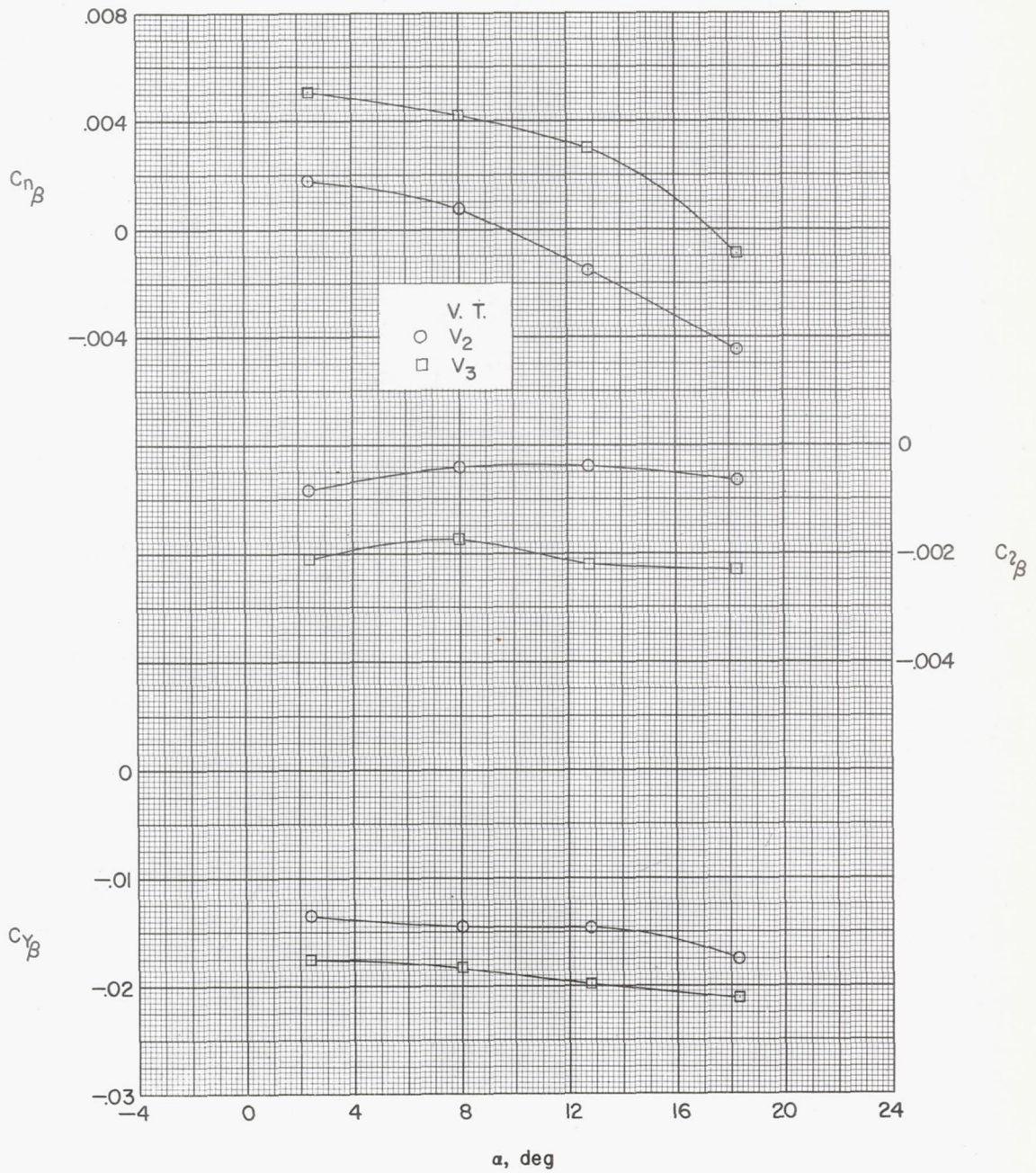

Figure 22.- Effects of vertical-tail plan form on sideslip derivatives. M = 2.01.

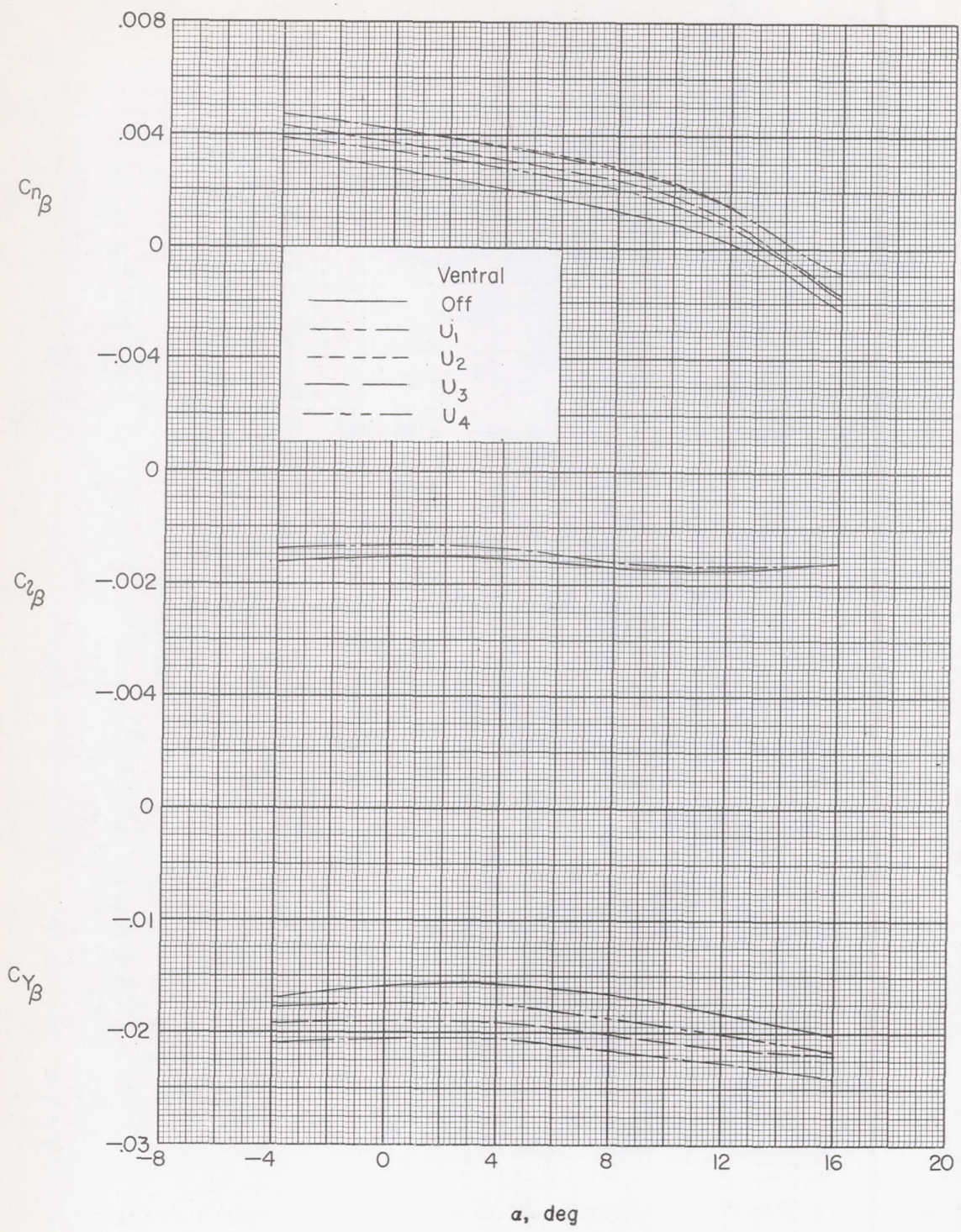

Figure 23.- Effects of ventral fins on sideslip derivatives. M = 2.01.

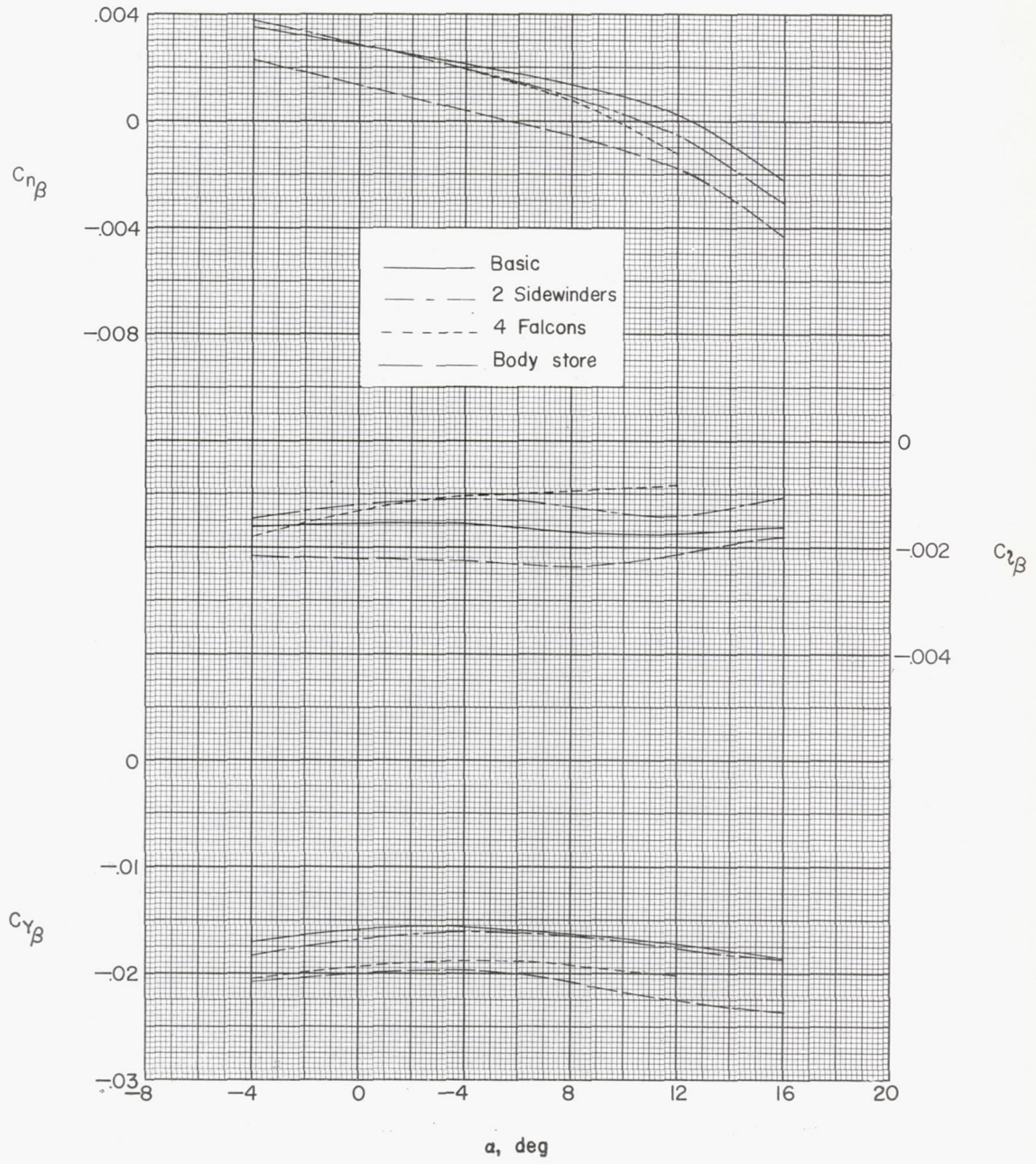

Figure 24.- Effects of external stores on sideslip derivatives. M = 2.01.